

University of Louisville

ThinkIR: The University of Louisville's Institutional Repository

Electronic Theses and Dissertations

5-2016

Characterization of the role of the *Burkholderia pseudomallei* type 3 secretion system using in vivo imaging.

Maria Gabriela Gutierrez
University of Louisville

Follow this and additional works at: <https://ir.library.louisville.edu/etd>

Part of the [Bacteriology Commons](#)

Recommended Citation

Gutierrez, Maria Gabriela, "Characterization of the role of the *Burkholderia pseudomallei* type 3 secretion system using in vivo imaging." (2016). *Electronic Theses and Dissertations*. Paper 2465.
<https://doi.org/10.18297/etd/2465>

This Doctoral Dissertation is brought to you for free and open access by ThinkIR: The University of Louisville's Institutional Repository. It has been accepted for inclusion in Electronic Theses and Dissertations by an authorized administrator of ThinkIR: The University of Louisville's Institutional Repository. This title appears here courtesy of the author, who has retained all other copyrights. For more information, please contact thinkir@louisville.edu.

CHARACTERIZATION OF THE ROLE OF THE *BURKHOLDERIA PSEUDOMALLEI*
TYPE 3 SECRETION SYSTEM USING *IN VIVO* IMAGING

By

Maria Gabriela Gutierrez

B.S., San Diego State University, 2011

M.S., University of Louisville, 2013

A Dissertation

Submitted to the Faculty of the

School of Medicine of the University of Louisville

In Partial Fulfillment of the Requirements

For the Degree of

Doctor of Philosophy in Microbiology and Immunology

Department of Microbiology and Immunology

Louisville, KY

May 2016

Copyright 2016 by Maria Gabriela Gutierrez

All rights reserved

CHARACTERIZATION OF THE ROLE OF THE *BURKHOLDERIA PSEUDOMALLEI*
TYPE 3 SECRETION SYSTEM USING *IN VIVO* IMAGING

By

Maria Gabriela Gutierrez

B.S., San Diego State University, 2011

M.S., University of Louisville, 2013

A Dissertation Approved on:

November 18th, 2015

By the Following Dissertation Committee:

Jonathan M. Warawa, Ph.D.

Yousef Abu-Kwaik, Ph.D.

Donald Demuth, Ph.D.

Jill Suttles, Ph.D.

Silvia M. Uriarte, Ph.D.

DEDICATION

I would like to dedicate this dissertation to my great grandmother Emperatriz, my grandmother Silvia, my mother Aleyda and to my daughter Reagan. Your tenacious spirits and unconditional love have been an inspiration to become a better person everyday.

ACKNOWLEDGEMENTS

First and foremost I would like to thank Dr. Jonathan M. Warawa for his mentorship, support, selflessness and personal sacrifice during the course of my studies in his laboratory.

I want to thank my Dissertation Committee Members for their support and guidance. Your tough love and advice was imperative for my success, and for this, I am forever grateful and indebted.

I would like to thank my mother Aleyda and stepfather Raymundo for their unconditional love and support. Without you, I would have not been able to complete my studies, so I am forever indebted to you.

Thank you Reagan for your love and support! Your kind words always gave me the strength and motivation to continue. Thank you for being such an awesome daughter, I could not imagine going through this journey without you.

Lastly, I want to thank my friends and family for supporting and motivating me to continue studying and always reminding me how blessed I am to live this amazing life.

ABSTRACT

CHARACTERIZATION OF THE *BURKHOLDERIA PSEUDOMALLEI* TYPE 3 SECRETION SYSTEM USING *IN VIVO* IMAGING

Maria Gabriela Gutierrez

November 18th, 2015

Melioidosis is a fatal infectious disease caused by the Tier 1 Select Agent *Burkholderia pseudomallei*. Hallmarks of melioidosis include pneumonic disease and prominent septicaemic spread. Both forms of disease are contingent upon the bacterium's intracellular life cycle and particularly on its ability to escape from host cell phagosomes. Upon encountering a host cell, *B. pseudomallei* is internalized into membrane-bound vacuoles from which the bacterium must rapidly escape to the cytoplasm in order to replicate and promote its survival. In the host cytoplasm, *B. pseudomallei* is capable of polymerizing actin for intracellular and intercellular motility and spread, lysing the host cell and perpetuating the cycle of infection. Commonly used intranasal and aerosol models to study respiratory melioidosis result in significant upper respiratory tract colonization, dramatically altering disease progression. Accordingly, we developed an improved lung-specific instillation approach to deliver bacteria directly into mice lungs, coupled with *in vivo* optical imaging and observed the development of

disease that closely resembles human melioidosis in mice. We found that in the absence of upper respiratory tract infection, a capsular polysaccharide (CPS) mutant is only 6.8-fold attenuated. This mutant is unable to spread to secondary sites of infection, consistent with the role of capsule in protecting the bacterium from host antimicrobial activity. Similarly, a type 3 secretion system cluster 3 (T3SS3) structural mutant is spread deficient, yet this mutant is attenuated 290-fold, strongly suggesting that T3SS3 is critical for respiratory melioidosis. Having a strong platform for studying the pathogenesis of *B. pseudomallei* in a mouse model of lung-specific melioidosis, we used transposon mutagenesis to comprehensively identify virulence factors required for *B. pseudomallei* lung colonization and spread to the liver and spleen. Notably, T3SS3, capsular polysaccharide and type 6 secretion system cluster 5 (T6SS5) were the major genetic loci required for respiratory melioidosis. A T6SS5 mutant is not attenuated by LD₅₀ estimations using our lung-specific melioidosis mouse model. Yet by competition analysis T6SS5, T3SS3 and CPS mutants were attenuated, substantiating the requirement of these factors for *B. pseudomallei* infection as previously reported. These results highlight the importance of competition analysis for studying the fitness of distinct virulence determinants. Importantly, T3SS3 was the only virulence determinant attenuated by both LD₅₀ analysis and competition studies, corroborating the critical requirement of this virulence system for respiratory melioidosis. *B. pseudomallei* is a facultative intracellular cytosolic bacterium and its ability to survive intracellularly is fundamental to mammalian host infection. Upon *B. pseudomallei* internalization into host cell vacuoles, the bacterium rapidly escapes this compartment by action of the T3SS3. The T3SS3 is required by *B. pseudomallei* for intracellular survival by

translocating protein effectors to the cytoplasm of host cells and mediating the rapid escape of the bacterium from phagosomes of these cells. We hypothesized that effectors act in concert to mediate *B. pseudomallei*'s rapid escape from phagosomes of host cells by manipulating host signaling pathways and promoting bacterial survival. Using a high-resolution, high-throughput *in vivo* imaging screening approach we profiled the contributions of five of the six *B. pseudomallei* putative type 3 effectors to the bacterium's rapid phagosome escape. Effector mutants exhibited distinct temporal differences in escape, with *bopA* inactivation resulting in the most pronounced delay in vacuolar rupture, strongly suggesting that BopA directly mediates escape of *B. pseudomallei* from endocytic vesicles. We confirmed that a previously identified BopA host target, the trafficking particle protein C8 (TRAPPC8), colocalized with *Burkholderia* containing vacuoles. Small interfering RNA knockdown of this protein strongly suggests that TRAPPC8 is required for vacuolar membrane stabilization. These findings substantiate the significant role of the T3SS3 and provide a paradigm to study *B. pseudomallei* natural infection processes and potential vaccine and therapeutic targets.

TABLE OF CONTENTS

DEDICATION	III
ACKNOWLEDGEMENTS	IV
ABSTRACT	V
LIST OF TABLES	XII
LIST OF FIGURES.....	XIII
CHAPTER I	1
<i>BURKHOLDERIA PSEUDOMALLEI</i> AND MELIOIDOSIS	1
1.1 IDENTIFICATION OF <i>BURKHOLDERIA PSEUDOMALLEI</i>	1
1.2 EPIDEMIOLOGY	3
1.3 CLINICAL MELIOIDOSIS	6
1.4 <i>BURKHOLDERIA PSEUDOMALLEI</i> GENETICS	9
1.5 <i>BURKHOLDERIA PSEUDOMALLEI</i> INTRACELLULAR LIFE CYCLE.....	11
1.6 <i>BURKHOLDERIA PSEUDOMALLEI</i> VIRULENCE DETERMINANTS	12
1.6.1 Type 3 Secretion Systems.....	13
1.6.2 Capsular Polysaccharide	20
1.6.3 Type 6 Secretion Systems.....	22
1.7 Specific Aims	28
CHAPTER II.....	30
MATERIAL AND METHODS	30
2.1 BACTERIAL STRAINS AND CULTURE.....	30
2.2 LUMINESCENT <i>BURKHOLDERIA PSEUDOMALLEI</i>	30

2.3 ETHICS STATEMENT	31
2.4 MOUSE RESPIRATORY INFECTIONS.....	31
2.5 BACTERIAL ENUMERATION AT KEY SITES OF INFECTION	32
2.6 TN-SEQ LIBRARY PREPARATION.....	32
2.7 TN-SEQ SCREEN	33
2.8 EARLY DISSEMINATION STUDIES.....	35
2.10 VIRULENCE ASSESSMENT OF A T6SS5 MUTANT IN RESPIRATORY MELIOIDOSIS.....	36
2.11 COMPETITION STUDIES.....	36
2.12 INFECTION OF CULTURED CELLS	37
2.13 CELL TRANSFECTION	38
2.15 IMMUNOFLUORESCENT STAINING AND CONFOCAL MICROSCOPY	38
2.16 STATISTICAL ANALYSES.....	39
CHAPTER III.....	42
TYPE 3 SECRETION SYSTEM CLUSTER 3 IS A CRITICAL VIRULENCE DETERMINANT FOR LUNG-SPECIFIC MELIOIDOSIS.....	42
3.1 INTRODUCTION	42
3.2 RESULTS	45
3.2.1 <i>Lung-specific delivery of Burkholderia pseudomallei impacts disease progression...</i>	45
3.2.2 <i>Respiratory melioidosis models exhibit similar disease kinetics</i>	46
3.2.3 <i>Sex difference influence host susceptibility to lung-specific melioidosis</i>	48
3.2.4 <i>Type 3 Secretion is more critical for respiratory melioidosis than capsule.....</i>	49
3.2.5 <i>Capsule and T3SS3 mutants are defective in spread from the lung.....</i>	50
3.3 DISCUSSION	52
CHAPTER IV	67

COMPREHENSIVE IDENTIFICATION OF VIRULENCE FACTORS REQUIRED FOR RESPIRATORY MELIOIDOSIS USING TN-SEQ MUTAGENESIS	67
4.1 INTRODUCTION	67
4.2 RESULTS	69
4.2.1 Lung-specific mouse infection with the Tn-Seq insertion library.....	69
4.2.3 <i>Burkholderia pseudomallei</i> early hepatic dissemination	71
4.2.4 Identification of virulence determinants required for <i>Burkholderia pseudomallei</i> <i>colonization of host lungs</i>	72
4.2.5 T6SS5 mutant is not attenuated in the IMIT model.....	74
4.2.6 A <i>Burkholderia pseudomallei</i> T6SS5 mutant is attenuated in competition studies	75
4.3 DISCUSSION	77
CHAPTER V.....	93
TYPE 3 SECRETION SYSTEM CLUSTER 3 EFFECTORS MEDIATE <i>BURKHOLDERIA</i> <i>PSEUDOMALLEI</i> 'S RAPID ESCAPE FROM HOST CELL PHAGOSOMES	93
5.1 INTRODUCTION	93
5.2.1 REAL-TIME GROWTH KINETICS OF BIOLUMINESCENT <i>BURKHOLDERIA PSEUDOMALLEI</i> IN CULTURED MACROPHAGES.....	96
5.2.2 A bioluminescent T3SS3 structural mutant exhibits a significant fitness defect during <i>infection of host cells</i>	97
5.2.3 T3SS3 effector proteins are required for full virulence of <i>Burkholderia pseudomallei</i> in <i>host cells</i>	98
5.2.5 <i>BopA</i> is associated with punctate structures in the cytoplasm of host cells.....	101
5.2.6 Contribution of host transport protein particle C8 to stabilizing the <i>Burkholderia</i> - <i>containing vacuole during infection of host cells</i>	102
5.3 DISCUSSION	103

CHAPTER VI	119
DISCUSSION AND FUTURE DIRECTIONS	119
6.1 IDENTIFICATION AND EFFICACY EVALUATION OF POTENTIAL <i>BURKHOLDERIA PSEUDOMALLEI</i> VACCINE AND THERAPEUTIC CANDIDATES USING INTUBATION-MEDIATED INTRATRACHEAL INSTILLATION	120
6.2 TN-SEQ SCREEN: A SOURCE OF NOVEL VIRULENCE DETERMINANTS	121
6.3 POTENTIAL ROLE OF BOPÉ IN APOPTOSIS INHIBITION THROUGH ACTIVATION OF THE RAB45 GTPASE	123
6.4 BAPC MAY MODIFY THE <i>BURKHOLDERIA PSEUDOMALLEI</i> CELL WALL DURING INFECTION OF HOST CELLS FACILITATING T3SS3 APPARATUS ASSEMBLY	124
6.5 INDUCTION OF PYROPTIC AND/OR APOPTIC CELL DEATH DURING <i>BURKHOLDERIA</i> <i>PSEUDOMALLEI</i> INFECTION OF HOST CELLS	126
REFERENCES.....	131
CURRICULUM VITAE	158

LIST OF TABLES

TABLE	PAGE
Table 1. Strains used in this study.....	40
Table 2. Plasmids used in this study.....	41
Table 3. Identification of prominent genetic loci required for pulmonary disease.....	92
Table 4. Type 3 secretion system cluster 3 putative secreted protein effectors.....	118

LIST OF FIGURES

FIGURE	PAGE
Figure 1. Worldwide distribution of <i>Burkholderia pseudomallei</i> endemicity.....	26
Figure 2. The <i>Burkholderia pseudomallei</i> intracellular life cycle.....	27
Figure 3. <i>In vivo</i> optical diagnostic imaging of respiratory melioidosis.....	59
Figure 4. Host response to lung-specific delivery of <i>Burkholderia pseudomallei</i>	60
Figure 5. Bacterial enumeration at moribund disease for respiratory melioidosis models.....	61
Figure 6. Male host response to lung-specific delivery of <i>Burkholderia pseudomallei</i> .	62
Figure 7. Host response to capsule and T3SS3 mutants of <i>Burkholderia pseudomallei</i>	63
Figure 8. Detection of dissemination of <i>Burkholderia pseudomallei</i> mutants by optical imaging.....	64
Figure 9. Bacterial enumeration of <i>Burkholderia pseudomallei</i> mutants in moribund respiratory disease.....	65
Figure 10. Detection of pulmonary growth rates of <i>B. pseudomallei</i> mutants <i>in vivo</i> ...	66
Figure 11. <i>In vivo</i> disease progression of <i>Burkholderia pseudomallei</i> Tn-seq transposon library.....	83

Figure 12. Gene size distribution of the <i>Burkholderia pseudomallei</i> genome and transposon insertion coverage.....	84
Figure 13. <i>Burkholderia pseudomallei</i> Tn-seq transposon library tissue burdens at key sites of infection.....	85
Figure 14. Analysis of variation within capsular polysaccharide operon genes required for lung colonization by Tn-seq.....	86
Figure 15. Proximity heat map of genes required for respiratory melioidosis.....	87
Figure 16. <i>In vivo</i> characterization of a T6SS mutant.....	88
Figure 17. <i>Burkholderia pseudomallei</i> major virulence determinants are attenuated in competition assays.....	90
Figure 18. Growth kinetics of <i>Burkholderia pseudomallei</i> parental strain in J774A.1 macrophages.....	108
Figure 19. Growth kinetics of the <i>Burkholderia pseudomallei</i> type 3 secretion system structural mutant JW280 Δ sctU _{Bp3} in J774A.1 macrophages.....	109
Figure 20. Growth kinetics of the <i>Burkholderia pseudomallei</i> type 3 secretion system effector protein mutants JW280 Δ bapA and JW280 Δ bapC in J774A.1 macrophages.	110
Figure 21. Growth kinetics of the <i>Burkholderia pseudomallei</i> type 3 secretion system effector protein mutants JW280 Δ bopA, JW280 Δ bopC and JW280 Δ bopE in J774A.1 macrophages.....	112
Figure 22. A BopA effector mutant exhibits delayed vacuolar escape in RAW264.7 macrophages.....	114
Figure 23. Ectopically expressed BopA is associated with punctate structures in the cytoplasm of HEK293 cells.....	115

Figure 24. TRAPPC8 knockdown promotes intracellular survival of <i>Burkholderia pseudomallei</i> 's in RAW264.7 macrophages.....	116
Figure 25. Model for BopA inhibition of TRAPPC8 function.....	117
Figure 26. Model of the potential functions of T3SS3 effectors BopA, BopE and BapC during <i>Burkholderia pseudomallei</i> infection of host cells.....	129

CHAPTER I

BURKHOLDERIA PSEUDOMALLEI AND MELIOIDOSIS

1.1 Identification of *Burkholderia pseudomallei*

Burkholderia pseudomallei, the causative agent of melioidosis, was first isolated by the pathologist Alfred Whitmore and his assistant C. S. Krishnaswami in April 1911 during a routine post-mortem examination of a morphine addict in the Laboratory of the Rangoon General Hospital in Rangoon, Burma [1]. Lung smears from the diseased man, identified the bacterium as a Gram-negative, non-motile organism that resembled *Burkholderia mallei*, the etiological agent of glanders, in both shape and size [1, 2]. Standard bacteriological examinations revealed that the organism isolated from the diseased lung yielded an abundant number of bacteria in broth culture after a three-day growth period [1, 2]. Curiously, this “rapid and luxuriant growth” in culture was unlike that of *B. mallei*, and male guinea pigs infected via intraperitoneal inoculation with the bacterium in question expired without inflammation of the testicles, a hallmark of glanders infection in male guinea pigs [1]. Expansion of bacteria isolated from the guinea pig bore a motile bacillus, leading Whitmore to hypothesize that the organism isolated from both the human and guinea pig lungs was motile in early cultures but lost

its motility within a few days [1]. The striking similarities between the human and animal cases prompted the investigation of additional post-mortem examinations conducted within the past few months. The bacterium was isolated in 38 separate incidents and examinations revealed patches of lung consolidation in the majority of victims. These patches became the hallmark of the unknown bacillus' pathology [1]. Thereupon, Whitmore characterized the bacterium as rod-shaped, Gram-negative, non acid-fast, displaying bipolar staining by Leishman's stain [1]. In broth culture, the bacillus was capable of rapid, abundant growth under aerobic and anaerobic conditions with formation of a thin white surface layer or pellicle and a thick bacterial aggregate undermost after extended periods of growth [1, 2]. Further, bacilli in young cultures expressed motility of a "serpentine character," which was later lost [1]. In agar, young bacterial colonies appeared moist and translucent, thickening into cream-colored colonies and shifting to wrinkled, pink-hued colonies after extended periods of growth [1, 2]. Characterization of the unknown organism led Whitmore to propose the name of *Bacillus pseudomallei* for the deadly bacterium [1].

In 1913 and 1917, investigations by A.T. Stanton and William Fletcher into several human infections and what was thought to be a distemper outbreak in mice at the Institute for Medical Research in Kuala Lumpur, Malaysia, isolated the same bacterium [2]. The cause of these outbreaks was again mistakenly concluded to be *B. mallei*, as clinical manifestations of *B. pseudomallei* pathology closely resembled those seen in glanders patients. Yet in 1917, Stanton concluded that the illness of animals and man in Kuala Lumpur was caused by *B. pseudomallei* [2]. In 1921, Stanton and Fletcher wrote an account of their experiences with the malady and proposed to rename the organism

Bacterium whitmori in honor of Whitmore, who first isolated and characterized the bacillus [2]. Further, the physicians proposed the name Melioidosis for the illness, for ancient Greek physicians referred to maladies that resembled (“eidos”) distemper of asses as “melis” [2, 3]. But since its discovery the bacterium has been reclassified into numerous genera, *Malleomyces* in 1939 [4], *Pseudomonas* in 1957 [5] and finally *Burkholderia* in 1992, when Yabuuchi et al. proposed the transfer of seven bacterial species to the new *Burkholderia* genus based on 16S rRNA sequences, DNA-DNA homology, cellular lipid and fatty acid composition and phenotypic characteristics [6].

1.2 Epidemiology

Burkholderia pseudomallei is an environmental free-living organism commonly found in the soil and stagnant water in endemic areas [7]. Scant human cases in Burma, Kuala Lumpur and Singapore marked the discovery of *B. pseudomallei*, the causative agent of melioidosis [1, 2, 8]. Years after the initial discovery of melioidosis, Krishnaswami and Knapp reported that *B. pseudomallei* had been isolated in approximately 5% of post-mortem bacteriological examinations conducted at Rangoon General Hospital [8]. Environmental surveys conducted in Malaysia, Singapore and Thailand revealed *B. pseudomallei*'s expansive prevalence in soil and water sources in the region [8]. In Java, Indonesia awareness of melioidosis led to an increase in case reports in humans and wild animals [8]. Around the same time, China, Hong Kong, Korea, the Philippines and Sri Lanka also began to report endemic cases of melioidosis [8]. And in Vietnam, the first case of melioidosis was confirmed in 1925 [8].

Importantly, the Vietnam War brought great notoriety to the disease in the region. Interest in melioidosis arose in the United States and Europe, as a result of military service men fighting in Southeast Asia becoming ill with the malady during and after the conflict [9]. It was estimated that approximately 225,000 American service members were exposed to *B. pseudomallei* during the war, based on seroconversion studies [10]. Around the same time in Thailand, increased awareness also shed light into the prevalence of the disease in the region, with a 29.1% *B. pseudomallei* seroconversion rate in healthy Thais reported in 1962 [8]. It has been estimated that one in five children under the age of 14 fall ill to melioidosis with a 51% mortality rate [11]. Alarming, current studies estimate that a large number of healthy individuals in the region have antibodies against *B. pseudomallei* by the age of 4 years and that the bacterium is responsible for up to 20% of community acquired septicaemia with an associated 50% mortality rate in the region [3, 11-13].

In northern Australia, the mortality rate associated with melioidosis is significant at approximately 20% [3, 10]. Striking figures from several studies showed that males are at great occupational risk as 69% of melioidosis patients were males involved in farming activities [10]. Approximately 39% of patients suffered from diabetes mellitus and 81% of all infections were contracted during the wet season [10]. Diabetes mellitus represents the highest pre-existing risk factor associated with melioidosis patients [13]. Surprisingly, the lack of pre-existing risk factors prior to infection with the bacillus was the sole “strongly predictive of survival” [10]. To date, *B. pseudomallei* infection is the “most common cause of fatal community-acquired septicaemic pneumonia in northern Australia” [3].

In Central and South America, sporadic cases of melioidosis have been reported more recently in El Salvador, Panama, Ecuador and Brazil [8, 14]. In Brazil, numerous outbreaks of melioidosis have been reported and the bacterium has been isolated from river water and mud, strongly suggesting that *B. pseudomallei* may be endemic to eastern coastal regions of the country [14]. Yet, unavailability of adequate diagnostic methods and the lack of familiarity with the disease in Latin American countries may lead to melioidosis being under-diagnosed in this region. In North America, the etiology of most melioidosis cases reported can be traced back to recreational or occupational travel to melioidosis endemic regions [14, 15]. In the United States, only five melioidosis cases have been reported with no history of travel to endemic regions, yet multi-locus sequence typing traced back the origins of three of these strains to Southeast Asia [16]. In addition, a great number of melioidosis cases were reported in veterans of the Vietnam War, which presented with acute febrile illness years after arriving back in the United States following the armed conflict [14]. Surprisingly, the longest disease-free interval recorded was 62 years for a veteran of the Pacific War [14]. In 2014, two cases of *B. pseudomallei* infection were reported in domesticated animals imported from Central America to the United States, thus the bacterium is also capable of persisting in animals years after initial infection [17]. Melioidosis is believed to be under-diagnosed in Central and South America, where incidence of the disease is mainly observed in rural and remote communities. Accordingly, improvements of rapid diagnostic methods and increased clinical awareness may be imperative for accurate identification, treatment and prevention of *B. pseudomallei* in this region [14].

Finally, melioidosis incidence not only in Southeast Asia and northern Australia,

but endemic pockets in the Middle East, Africa and Central and South America resolved that *B. pseudomallei* is likely native to the world's tropical and subtropical regions located between 20° N and 20° S of the Equator (Figure 1), however the increase of animal and plant exports from endemic regions to other parts of world, strongly suggests that exposure of the bacterium to other parts of the world may be on the rise [3, 9, 18].

1.3 Clinical Melioidosis

Infection with *B. pseudomallei* is primarily acquired through percutaneous inoculation via skin abrasions during occupational or recreational exposure to the bacterium, inhalation of organisms in aerosolized dust or water predominantly during heavy rain periods and ingestion [7, 10, 19]. The incubation period of melioidosis is approximately 1-21 days, with a mean incubation period of just 9 days [10]. Factors influencing the morbidity and mortality associated with *B. pseudomallei* infection include: host risk factors such as diabetes mellitus, alcoholism and renal disease, infectious dose, route of infection and virulence associated with the infecting *B. pseudomallei* strain [10]. In Australia, a vast majority (~85%) of reported melioidosis cases were acute in nature; with symptoms lasting less than 2 months and 11% of cases were chronic, with symptoms exceeding 2 months [10].

During infection, *B. pseudomallei* can be isolated from the blood, sputum, urine and superficial lesions of patients for diagnosis of culture-confirmed melioidosis [2]. The bacillus spreads through the blood stream very early in infection, which is supported by the septicaemic nature of melioidosis in guinea pigs [2]. Lung infection seems to be an

early event in the course of the disease [2], with autopsy results of fatal melioidosis cases showing patches of pale and caseous lung consolidation as a hallmark of the disease [1, 2, 20]. Further, *B. pseudomallei* is capable of causing focal lesions in every organ of the body with exception of the gastrointestinal tract and lymphatic system [9, 20]. Infection of the liver and kidneys with presentation of small caseous and necrotic patches of haemorrhagic zones and enlarged and softening of the spleen are also considered hallmarks of melioidosis [1, 2]. Transmission of melioidosis from person to person is unusual, only one case of perinatal transmission and one case of sexual transmission have been documented [3] and infection from animals to humans have never been reported [9].

Melioidosis manifestations take a vast array of forms and diagnosis may be impossible in early stages [2]. Accordingly, the malady has been termed “the great mimicker” [11]. Stanton and Fletcher likened melioidosis manifestations to those seen in malaria, enteric fever or tuberculosis, cholera, syphilis, plague, typhoid fever, mycosis, delirium, acute rheumatism and amoebic abscesses of the liver [2, 9]. Clinical presentations can range from asymptomatic seroconversion, acute or chronic pneumonia, genitourinary infection, osteomyelitis, localized skin, hepatic and spleen abscesses, neurological complications and fulminant septicaemic disease, which is the deadliest form of the illness [11, 13]. A recent report correlated the route of *B. pseudomallei* infection with presentations of bacteremia or pneumonic disease [21], finding that percutaneous inoculation is negatively associated with bacteremia, ingestion is associated with bacteremia and inhalation of the bacterium is associated with pneumonic disease [21]. Although, the primary route of inoculation with the bacterium in endemic areas occurs through percutaneous exposure, a shift to inhalational infection as the predominant

route of inoculation may occur during the rain season, as evidenced by the increase in incidence of melioidosis cases [16, 22, 23]. Yet, pneumonic disease remains the most common disease presentation in studies of melioidosis patients, with up to 90% mortality associated with septic shock from acute melioidosis pneumonia [16].

Antibiotic treatment of melioidosis is extremely limited due to the bacillus' intrinsic resistance to many classes of antibiotics commonly used to treat bacterial infections such as macrolides, beta-lactams, aminoglycosides and polymyxins [9, 13]. *B. pseudomallei* encodes for multidrug efflux systems on chromosome 2 given that the bacterium does not carry any plasmids [11], suggesting that antibiotic resistance promotes the bacterium's environmental survival and that these drug resistance determinants have not been recently acquired nosocomially, as is common for other multidrug resistant pathogens.

Melioidosis treatment for culture-confirmed cases includes a lengthy biphasic course of antibiotic therapy, divided into an acute phase and an eradication phase of treatment [16, 24]. In the acute phase of treatment, the recommended therapy is continuous infusion or intravenous administration of the β -lactam ceftazidime for approximately 7-28 days with the goal of bacteremia eradication [24, 25]. Alternate treatment of severe melioidosis patients with meropenem, showed that this antibiotic may be more efficient for the treatment of severe melioidosis, but comparative studies between the efficacy of ceftazidime and the latter are not available [26]. In the eradication phase, patients are treated with oral trimethoprim-sulfamethoxazole for approximately 12 to 20 weeks, with the goal of eradicating surviving *B. pseudomallei* and avoiding recrudescence of the bacillus [24, 27]. However, relapse after apparent

clearance of the bacillus is common. Accordingly, melioidosis was termed the “time bomb disease” for its ability to recrudesce many years post latency, with 62 years being the longest reported quiescence period after initial infection [8, 10]. Nevertheless, approximately 25% of patients with intermittent melioidosis are newly infected with a different *B. pseudomallei* strain rather than relapsing from initial infections [13, 24, 28].

For individuals who may be at risk of occupational exposure to *B. pseudomallei*, such as laboratory workers, the recommended post exposure prophylaxis include oral trimethoprim-sulfamethoxazole as the primary antibiotic cocktail of choice if the patient has no documented allergies to either drug and the infectious *B. pseudomallei* strain is susceptible to the antibiotics [29]. In cases of documented allergies or antibiotic resistance, doxycycline or amoxicillin-clavulanic acid may be administered, but doxycycline treatment alone is associated with higher relapse rates of infection and treatment failure, and amoxicillin-clavulanic acid has been shown to be more efficient in the treatment of naturally acquired melioidosis [29].

1.4 *Burkholderia pseudomallei* genetics

B. pseudomallei's remarkable genomic plasticity facilitates its ability to inhabit diverse niches, as horizontal gene acquisition has played a significant role in the evolution of the pathogen's genome [30, 31]. The bacterium's genome is one of the largest, genetically diverse genomes sequenced to date [11, 30, 32]. The 7.25-megabase *B. pseudomallei* genome is comprised of a 4.07-megabase large chromosome, chromosome 1, and a smaller 3.17-megabase chromosome, chromosome 2, [11] with approximately 6,332 protein-coding sequences [32]. Sequences in chromosome 1 encode

for proteins considered core to the *B. pseudomallei* genome, these are required for growth and metabolism functions such as macromolecule metabolism, nucleotide and protein biosynthesis, amino acid metabolism, chemotaxis and motility, among other components with shared genetic order in other prokaryotes [31, 32]. Chromosome 2 primarily encodes for proteins with accessory functions for adaptation and survival in different environments such as secondary metabolism, osmotic protection, iron acquisition, horizontally acquired DNA, hypothetical proteins and other components associated with plasmid replication, but with little to no conserved genetic order is shared with other prokaryotes [2, 32]. The smaller replicon also contains coding sequences critical for growth and metabolic functions, such as tRNA genes, an rRNA gene cluster and components of the replication and transcription machineries, thus chromosome 2 is classified as a chromosome rather than a megaplasmid [11]. Approximately 80 to 86% of the *B. pseudomallei* core genome distributed between both chromosomes is homologous among more than 111 *B. pseudomallei* clinical, environmental and animal isolates [11, 12, 31, 32], and of the core genome, ~8% of genes are considered essential [33]. Clinical isolates of the bacillus cluster together in phylogenetic trees based on genomic variability, which is suggestive of differential virulence potential among different isolates [12]. Although the *B. pseudomallei* large chromosome shares discrete regions of conserved genetic order with the large chromosome of other pathogens such as *R. solanacearum*, the smaller chromosome does not share conserved gene order, strongly suggesting differential ancestry for the smaller chromosome [11].

Genomic or pathogenicity islands, which are regions of DNA likely acquired through horizontal gene transfer, are variably found in clinical *B. pseudomallei* strains

and other pathogenic bacteria and are often associated with virulence in many bacterial pathogens [34]. The *B. pseudomallei* genome contains 16 genomic islands, 12 in chromosome 1 and 4 in chromosome 2, which make up ~6.1% (~4.4 Kb) of the bacterium's genome, consistent with the principle that genomic or pathogenicity islands occupy large genomic regions in pathogenic bacteria [11, 34]. *B. pseudomallei*'s fitness in diverse niches is reasoned to be directly mediated by the bacterium's genetic plasticity and diversity supplemented in part by genomic islands [12, 32] and the presence of these genomic islands in *B. pseudomallei* clinical isolates suggest that these regions may play key roles in the bacterium's virulence by predisposing these strains to cause disease in humans [12].

1.5 *Burkholderia pseudomallei* intracellular life cycle

Following internalization into target cells *B. pseudomallei* is contained within membrane-bound vacuoles, followed by bacterial escape into the cytoplasm [35]. Following escape of the bacterium from endocytic vesicles, *B. pseudomallei* is free to replicate in the cytoplasm of host cells, polymerizing actin at one pole resulting in intracellular motility and intercellular spread, eventually lysing the host cell (Figure 2). Vacuoles containing *B. pseudomallei* T3SS3 mutants incapable of vacuolar escape colocalize with the lysosome marker LAMP-1 and with the autophagy marker LC3 [36]. However, T3SS3 mutant-containing vacuoles do not possess the double membrane characteristic of autophagosomes, suggesting that *B. pseudomallei* infection does not trigger autophagy in host cells [36]. Alternatively, it has been proposed that LC3 may be recruited to T3SS3 mutant-containing vacuoles through LC3-associated phagocytosis,

resulting in decreased bacterial survival [37]. Accordingly, vacuolar escape is critical for the bacterium's intracellular lifestyle, thus this process must occur rapidly following internalization. The precise time *B. pseudomallei* escapes from vacuoles remains unknown, yet the kinetics of vacuolar escape of other cytosolic pathogens such as *Francisella tularensis*, *Shigella flexneri*, *Listeria monocytogenes* and *Rickettsia* spp. range from 15 to 60 minutes post internalization, suggesting that *B. pseudomallei* escapes phagosomal vesicles in a comparable time frame [35]. Vacuolar escape of cytosolic pathogens is a bacterial-driven process and for *B. pseudomallei* the T3SS3 mediates this event (discussed in section 1.6.3) [38].

1.6 *Burkholderia pseudomallei* virulence determinants

Characteristics of melioidosis such as difficulty in treating infection and instances of prolonged quiescent periods after initial infection followed by relapse years later, suggest that *B. pseudomallei* is a facultative intracellular pathogen [39-41]. Further, the bacterium is capable of surviving and replicating within human polymorphonuclear leukocytes, monocytes and phagocytic and non-phagocytic cultured cells [39-41]. *B. pseudomallei* and other pathogenic bacteria possess the ability to cause disease in humans through the use of virulence factors that allow the bacteria to successfully overcome host immune mechanisms. Key *B. pseudomallei* virulence factors include the capsular polysaccharide (CPS), type 6 secretion system (T6SS), type 3 secretion system (T3SS), quorum sensing, lipopolysaccharide, flagellin, type 2 secretion system, type 4 pili and phospholipase C among other undescribed factors [7]. These virulence systems are required for different aspects of *B. pseudomallei* host intracellular, extracellular and

environmental survival, herein we concentrate on T3SS3, CPS and T6SS5, which are the focus of our studies.

1.6.1 Type 3 Secretion Systems

The type 3 secretion system is a needle-like apparatus that translocates effector proteins across both Gram-negative bacterial membranes into the cytoplasm of eukaryotic cells [42, 43]. The Gram-negative type 3 machinery is made up of ~15-20 scaffolding or structural proteins that make up the basal body that spans both bacterial membranes, and the secretion apparatus or needle that delivers effectors to its host target [7, 42, 44]. In its genome, *B. pseudomallei* encodes 3 type 3 secretion loci [38, 45, 46]. Clusters 1 and 2 share homology with the plant pathogens *Ralstonia solanacearum* and *Xanthomonas* spp. [45] T3SS and cluster 3 (T3SS3) shares homology with the *Salmonella typhimurium* Inv/Spa/Prg and the *Shigella flexneri* Ipa/Mxi/Spa type 3 secretion systems, required for intracellular survival of both pathogens [46].

The T3SS is critical for the intracellular life cycle and survival of pathogenic bacteria such as *Shigella* spp., *Salmonella* spp., *E. coli*, *Yersinia* spp. and *Pseudomonas aeruginosa* [43]. The intracellular life cycle of *B. pseudomallei* and other pathogenic cytosolic bacteria such as *Shigella flexneri* consists of escape from host cell vacuoles following internalization, replication in the cytoplasm of the host cell (Figure 2) and manipulation of host cell signaling pathways that promote the bacterium's intracellular fitness [35]. *B. pseudomallei* has evolved to rapidly escape from endocytic vacuoles through the use of the type 3 secretion system cluster 3 [35]. Upon contact with the vacuolar membrane, the *B. pseudomallei* type 3 secretion apparatus forms a channel

between bacteria and host, secreted translocon proteins and the needle tip form a pore in the vacuolar membrane translocating very small amounts of effector proteins into the cytoplasm of the target cell [42, 44, 47]. *B. pseudomallei* injects type 3 secretion effectors across vacuolar membranes following internalization to rapidly escape to the cytoplasm, where the bacteria can continue its life cycle, bypassing killing by the host cell and eventually lysing the cell [39]. Translocated effectors may interact with host cell proteins facilitating the rapid escape of *B. pseudomallei* from endocytic vesicles by manipulating signal transduction pathways in the cell, promoting bacterial survival and spread [43]. Major hallmarks of type 3 secretion effector functions in other bacterial pathogens include inhibition of phagocytosis, cytoskeletal rearrangement, mediation of escape of the bacterium from host vacuoles, manipulation of cellular signaling pathways that promote bacterial survival, down-regulation of host cell inflammatory response or inhibition of apoptosis [43].

The *B. pseudomallei* T3SS3 is the only type 3 secretion system of critical importance for *B. pseudomallei* virulence in mammals, as it is the only cluster required for virulence in a Syrian golden hamster model of systemic melioidosis [7, 19]. Conserved type 3 secretion apparatus components were named Sct by Attree and Attree, but were later designated *bsa* (*Burkholderia* secretion apparatus) by Stevens et al., leading to multiple nomenclatures for T3SS3 [38, 46]. A mutant in a component of the T3SS3 export apparatus, *sctU*, exhibits no effector secretion and almost no intracellular replication in cultured macrophages when compared to wild type strains, strongly suggesting that T3SS3 is critical for intracellular fitness of *B. pseudomallei* [38, 48]. This mutant remains trapped in endocytic vesicles of cultured macrophages up to 12

hours post infection, although early in infection ~95.1% of bacteria were associated with the lysosomal marker lysosome-associated membrane glycoprotein-1 (LAMP-1) [38]. Actin tail formation, a hallmark of *Shigella* spp., *Rickettsia* spp. and *L. monocytogenes* in the cytoplasm of host cells, is also impaired in this mutant, again supporting the previously observed escape deficient phenotype of the *sctU* mutant [38]. These data demonstrate that the *B. pseudomallei* T3SS3 is critical for intracellular survival of the bacterium by mediating the bacterium's rapid escape to the cytoplasm of host cell.

Translocation of T3SS3 effectors is mediated by a set of translocon proteins and the T3SS3 apparatus needle tip termed *Burkholderia* invasion proteins (Bips), which form a pore in the vacuolar membrane of the host cell and include BipB, BipC and BipD [19, 38]. The Bip proteins, BipB, BipC and BipD, make up the translocon proteins and needle tip, respectively, of the T3SS3 apparatus [44]. BipB and BipC form a pore in the eukaryotic host cell membrane, but are also secreted into the cytoplasm; therefore it is possible that these translocon proteins may have additional roles during *B. pseudomallei* infection [44]. Accordingly, *bipB* and *bipC* mutants exhibit impaired invasion of non-phagocytic cultured cells and reduced intracellular fitness, strongly suggesting that efficient interaction of *B. pseudomallei* with host cells and efficient delivery of T3SS3 effectors to the cytoplasm of the cell is required for full virulence of the bacterium [49, 50]. Notably, inactivation of *bipC* also leads to delayed escape of *B. pseudomallei* from endocytic vacuoles, leading to a 2-fold reduction in intracellular burden in cultured cells [50]. It is possible that inactivation of *bipB* leads to a similar phenotype, given that defective formation of a translocon pore likely leads to inefficient effector delivery, compromising the fitness of the bacterium in host cells. In addition, BipB may also have

a role in *B. pseudomallei* late infection, as it has been shown to be required for efficient cell-to-cell spread of the bacterium by promoting fusion of the plasma membrane of cells infected with *B. pseudomallei* and that of neighboring cells [49]. These data suggests that other effectors may also be required for optimal cell-to-cell spread by host membrane fusion events and that effectors function during early and late events in the infection process, yet cell-to-cell spread by membrane fusion has only been observed during *B. pseudomallei in vitro* infection of cultured cells, so whether cell-to-cell spread by fusion events take place *in vivo* remains unknown [49]. Lastly, both *bipB* and *bipC* mutants are significantly attenuated in an intranasal BALB/c model of respiratory melioidosis, validating the requirement for formation of a translocon pore for full *B. pseudomallei* virulence in mammals [49, 50]. Thus taken together, these data suggest that efficient formation of a translocon pore by *B. pseudomallei* T3SS3 translocon proteins is required for adherence, invasion, translocation of effectors and overall fitness of *B. pseudomallei* in mammalian infection.

BipD the tip of the T3SS3 needle is also required for the efficient and timely delivery of effector proteins, stalling secretion in the absence of host cell contact [44]. Consequently, inactivation of *bipD* renders the bacterium incapable of efficient escape from endocytic vesicles, impaired intracellular replication and decreased intracellular survival in cultured macrophages, consistent with the phenotypes observed for *bipB* and *bipC* mutants, which make up the translocon pore [50, 51]. Crystal structures of BipD and its *Shigella* homologue IpaD, suggest that BipD may play a role as an extracellular chaperone, by guiding and mediating the insertion of BipB and BipC into the host cell membrane and by potentially tethering the translocon pore to the T3SS needle [51].

Notably, the crystal structure of BipD shows that the protein contains a highly conserved region at its C-terminal end that may be involved in protein-protein interactions with the translocon pore [51, 52]. Importantly, purified BipD, as well as BipB and BipC, strongly react with serum from convalescent melioidosis patients and other T3SS3 components have been successfully used in experimental vaccines in animal models, strongly suggesting that these proteins may constitute potential therapeutic and vaccine candidates [38]. Yet, vaccination of BALB/c mice with purified BipB, BipC or BipD did not confer immune protection against intraperitoneal challenge with wild type *B. pseudomallei* protein, suggesting that these proteins may be secreted in very low amounts or that host antibodies may not have access to these proteins as *B. pseudomallei* is a facultative intracellular pathogen [53].

B. pseudomallei effector proteins were named *Burkholderia* outer proteins or Bops and constitute BopA, BopC and BopE, named in a similar manner to *Salmonella*'s outer proteins [19, 38]. The *Burkholderia* secretion apparatus (Bsa) associated proteins or Baps (BapA, BapB and BapC), have no known function as of yet in type 3 secretion [19, 38], although recent studies confirmed that BapA [54, 55] and BapC [55] are secreted *in vitro* in a T3SS3-dependent manner, suggesting that the Bap proteins may contribute to the intracellular survival of the bacterium in host cells. Bop and Bap T3SS3 effector proteins are translocated into the cytoplasm of host cells by the T3SS3 apparatus during infection [19, 38].

The *Burkholderia* outer proteins, BopA, BopC, BopE, BapA and BapB are the *B. pseudomallei* T3SS3 putative translocated effectors, which most likely contribute to replication, survival, spread and ultimately persistence of the bacterium within its host.

BopA is critical for the rapid escape of *B. pseudomallei* from endocytic vacuoles of cultured macrophages, as *bopA* mutants exhibit delayed escape from RAW264.7 phagosomes, demonstrating that BopA directly mediates vacuolar rupture in cultured phagocytic cells [36]. In addition, the vacuole containing this mutant co-localizes with the autophagy marker microtubule-associated protein light chain-3 (LC3) and the lysosome marker LAMP-1 for longer periods of time than the wild type vacuole, leading to increased killing by LC3-associated phagocytosis and subsequent decreased intracellular replication in cultured macrophages [36]. Yet the *bopA* mutant does not trigger cellular autophagy, rather reduced intracellular bacterial numbers during infection are a result of delayed escape of the mutant into the cytoplasm, confirmed by electron transmission microscopy [36]. In addition, the *bopA* mutant is capable of inducing actin tail formation at later times during infection, supporting the previously observed delayed escape phenotype [36]. Further studies are needed to demonstrate the mechanism by which BopA mediates vacuolar escape and other potential contributions of this effector to the intracellular life cycle of the bacterium.

BopE is also secreted in a T3SS3-dependent manner *in vitro* [48]. Consistent with phenotypes observed with inactivation of its *Salmonella*-homologues SopE and SopE2, which promote bacterial invasion of non-phagocytic cells, inactivation of *bopE* is associated with significant reduction in invasion of HeLa cells [48]. Yet, *B. pseudomallei* is only weakly invasive when compared to *Salmonella* and is phagocytosed into cells rather than promoting its own uptake [39]. BopE is an effective guanine nucleotide exchange factor (GEF) for the SopE and SopE2 mammalian target proteins Cdc42 and Rac1, but with a lower exchange rate, suggesting that BopE may target other host

GTPases and may be required for effector functions other than invasion of host cells [48]. Notably, the invasion rate of *B. pseudomallei* in numerous epithelial and fibroblast cell lines is low compared to invasive *Salmonella*, again suggesting that Cdc42 and Rac1, which are involved in cytoskeleton rearrangement, are not targeted by *B. pseudomallei* for invasion. In a similar manner, BopC *in vitro* secretion is dependent on a functional T3SS3 apparatus and inactivation of this effector is also associated with reduced invasion of the human A549 epithelial cell line [56]. But, very little data is available on the functions of BopE and BopC during infection, thus further studies to discern the contributions of these effectors to the *B. pseudomallei* intracellular life cycle are of pressing concern, as no role has been attributed to either effector during infection of host cells. Overall, these data strongly suggest that a functional *B. pseudomallei* T3SS3 and efficient delivery of T3SS3 protein effectors is critical for the pathogenesis of the bacterium in host cells. Specifically, T3SS3 is critically required for efficient adherence, invasion, rapid vacuolar escape and intracellular fitness, promoting and mediating the survival of *B. pseudomallei* in mammalian hosts. Importantly, translocation of effectors and interaction of these effectors with host proteins, as evidenced by *S. flexneri* and *S. enterica* T3SS3 effectors, promotes intracellular fitness of *B. pseudomallei*. Accordingly, extensive studies are needed to elucidate the individual contributions of type 3 effectors to the intracellular life cycle of *B. pseudomallei* in efforts to find potential vaccine targets or therapeutics against *B. pseudomallei* infection.

1.6.2 Capsular Polysaccharide

The capsular polysaccharide makes up the outermost layer of Gram-negative bacterial cells. It is composed of highly hydrated homo- or heteropolymers of repeating monosaccharides joined together by glycosidic bonds in distinct numbers of configurations, resulting in highly diverse capsular structures synthesized by different bacterial species [57]. Capsule production has been associated with virulence in bacteria that cause serious human diseases, given that capsule mediates interactions between bacterial cells and their environment [58]. As a result, the capsular polysaccharide is characterized as a key virulence determinant for many pathogenic bacteria [57]. Importantly, the bacterial capsule has been implicated in protecting the bacterial cell against desiccation, promoting transmission and survival, adherence to target cells, resistance to opsonophagocytosis and protection against complement-mediated lysis and host specific immunity [59, 60].

The *B. pseudomallei* genome contains 4 operons (CPS I-IV) with genes predicted to be required for biosynthesis and export of 4 different capsular polysaccharides [58]. CPS I encodes a capsular polysaccharide similar to that produced by the human pathogens *Escherichia coli*, *Haemophilus influenzae* and *Neisseria meningitidis* [59, 61]. Genes with predicted biosynthetic functions in this operon share homology to genes required for synthesis of structures primarily composed of mannose, and genes with predicted functions in polysaccharide export share homology to those found in various bacterial species that serve the same function [58]. G+C content of this operon is ~58%, substantially lower than the 68% G+C content in the rest of the genome, suggesting potential acquisition of this operon through horizontal gene transfer [58]. The CPS I

operon is also found in *B. mallei*, a host adapted clone of *B. pseudomallei* that is pathogenic to mammals [58]. In contrast, CPS II, CPS III and CPS IV are also found in the *B. pseudomallei* avirulent relative *Burkholderia thailandensis* but not in *B. mallei* [58]. Accordingly, the CPS II, III and IV loci do not contribute to the virulence of *B. pseudomallei* in mammals, strongly suggesting that these loci may be required for environmental fitness of the bacterium [58].

To date, the *B. pseudomallei* the CPS I operon is one of the most important virulence determinants required for the bacterium to cause systemic melioidosis [59], given that capsule protects *B. pseudomallei* against specific and non-specific host immunity [58]. Capsular polysaccharide glycosyltransferase and mannosyltransferase genes are both required for production of major surface polysaccharides [61] and mutants in both genes exhibit up to 10,000-fold attenuation in an intraperitoneal hamster model of systemic melioidosis and a mouse model of acute melioidosis, respectively, corroborating the importance of capsule for *B. pseudomallei* virulence [59, 62]. Further, capsule is required for *B. pseudomallei* persistence in the blood by reducing complement factor C3b deposition on the bacterial surface and by protecting the bacterium from phagocytosis by polymorphonuclear leukocytes, which is consistent with the role of the capsular polysaccharide in *E. coli* [59, 63]. Glycosyltransferase mutants are incapable of colonizing the lung, liver and spleen of hamsters in a systemic model of melioidosis, highlighting the importance of the capsule for establishing systemic disease [59]. In a similar manner, the mutant strain JW270, which is missing the entire capsular polysaccharide operon, is attenuated ~2 log in an intranasal mouse model of acute melioidosis and is incapable of colonizing the blood at similar levels than the isogenic

parental strain, consistent with the requirement of capsule for *B. pseudomallei* persistence in the blood previously observed [60]. Yet, this mutant is capable of colonizing the lung and liver at similar levels to that of the parental strain, and the spleen at lower levels during lethal challenge, yet tissue damage to the liver and spleen is less severe than that of the isogenic parental strain, suggestive of an altered host immune response against acapsular bacteria [60]. These results also suggest that the *B. pseudomallei* capsular polysaccharide may not play the same critical role for the bacterium for pneumonic disease relative to its critical role for systemic disease.

In vitro, acapsular JW270 is internalized and capable of intracellular replication and survival within cultured macrophages up to 9 hours post infection at levels similar to those of the isogenic parental strain [60]. These results strongly suggest that the *B. pseudomallei* capsule is not antiphagocytic for macrophages in the absence of opsonization [60]. Bioluminescent detection of an isogenic acapsular light producing strain in infected macrophages showed a reduction in bacterial burdens of this mutant when compared to the parental strain at late stages of macrophage infection (>9 hours post infection), strongly suggesting that capsule is dispensable for early stages of macrophage infection [64]. Overall, these results highlight the importance of capsule as a virulence determinant for systemic fitness of *B. pseudomallei* in mammalian hosts and that genes required for capsular polysaccharide biosynthesis may be considered potential therapeutic and vaccine targets for systemic disease.

1.6.3 Type 6 Secretion Systems

Type 6 secretion systems (T6SS) are bacterial virulence-associated injectisomes

that translocate effector proteins into target eukaryotic or prokaryotic cells [65]. T6SS are found in the genomes of ~25% of all sequenced Gram-negative bacteria and have been implicated in cell-to-cell contact killing during host cell invasion and during inter-bacterial community competition [65-67]. The T6SS is comprised of ~15-20 open reading frames encoding various apparatus components that are structurally homologous to the components of the bacteriophage tail [68]. The apparatus is comprised of a base plate complex that spans the inner and outer bacterial membranes and a bacteriophage tail-like injectisome, it is highly dynamic and is hypothesized that it may be driven by a phage tail-like contraction mechanism [65, 68]. Assembly of the base complex initiates the polymerization of the injectisome inner tube protein Hcp and the outer phage tail-like sheath made up of the ClpV-interacting proteins A and B (VipA and VipB) in an extended conformation [65]. An unknown stimulus causes the contraction of the VipA/VipB sheath leading to translocation of effector proteins to neighboring cell targets and secretion of the tail spike protein VgrG and Hcp tubule [65]. Activity of the AAA+ ATPase ClpV is critical for disassembly of the contracted sheath in the cytoplasm of the bacterial cell and apparatus components are recycled for use in *de novo* machinery assembly [67].

The *B. pseudomallei* genome encodes for six evolutionary distinct T6SS comprising ~2.3% of the bacterium's genome, strongly suggesting that these systems play key roles in the fitness of *B. pseudomallei* in diverse environments [66, 69]. Type 6 secretion phylogenetic trees show that the only *B. pseudomallei* type 6 locus that clusters with eukaryotic cell targeting systems, such as those found in *Vibrio cholerae* and *Aeromonas hydrophila*, is cluster 5 (T6SS5) and that the remaining loci cluster with

bacterial cell targeting systems such as those found in *Pseudomonas aeruginosa* [66]. Importantly, T6SS5 is the only locus demonstrated to have a critical role during mammalian virulence [66].

Secretion of the T6SS inner tube needle protein Hcp is a hallmark of a functional type 6 secretion system [70]. Importantly, recombinant Hcp5 but not Hcp1, -2, -3, -4 or -6, strongly react with sera from melioidosis patients, suggesting that only T6SS5 is expressed during *B. pseudomallei* human infection and that this protein is highly immunogenic [70]. Expression of the *B. pseudomallei* VirAG two-component regulon *in trans* results in transcriptional activation of T6SS5 and secretion of Hcp5 in RAW264.7 macrophages [70]. The T6SS5 genes *tssM*, *tssI* and *tssH* are expressed in *B. pseudomallei* during growth in macrophages, demonstrating that cluster 5 encodes a functional type 6 secretion apparatus expressed *in vivo* [69]. In addition, an *hcp5* mutant is ~1000-fold attenuated in a Syrian hamster model of systemic melioidosis, but not *hcp1*, -2, -3, -4 or -6 mutants, again demonstrating that T6SS5 is a major virulence determinant for *B. pseudomallei* for systemic melioidosis and that the other T6SS clusters may be required for bacterial survival in environmental niches. Vaccination of BALB/c mice with recombinant Hcp1, -2, -3, -4, -5 or -6 showed that the recombinant proteins elicit specific antibody responses in mice, but the immune responses elicited were not protective, suggesting that individual proteins alone may not constitute strong vaccine candidates, but may be targeted for diagnostic testing of *B. pseudomallei* infection [70]. In RAW264.7 cultured macrophages, an *hcp5* mutant exhibits a significant intracellular fitness defect and reduced cytotoxicity [70]. This result contrasts with previous observations, which showed that a mutant in the *tssH-5* gene, a homolog of the AAA+

ATPase ClpV is as fit as a wild type strain in the same cell line, yet it is possible that if intracellular bacterial burdens would have been quantified at more than two time points, then the intracellular fitness defect of the mutant would have been noticeable [69].

A mutant in the *tag-AB* gene, encoding a hypothetical protein located in the T6SS5 locus, is highly attenuated in an intranasal BALB/c model of respiratory melioidosis [71]. And *in vitro* a *tag-AB* mutant exhibits an intracellular fitness defect in both RAW264.7 cells and the human lung epithelial cell line A549 [71]. Importantly, inactivation of *tag-AB* leads to a pronounced defect in Hcp5 export, strongly suggesting that *tag-AB* is critical for expression of functional T6SS5 machinery. Thus, taken together, these results highlight the importance of T6SS5 to the intracellular lifestyle of *B. pseudomallei*, yet very little is known about the functions of this virulence system inside host cells. Significantly, these data demonstrate that T6SS5 is a key virulence determinant for systemic melioidosis and that genes in these loci may serve as potential vaccine and therapeutic targets for melioidosis in humans.

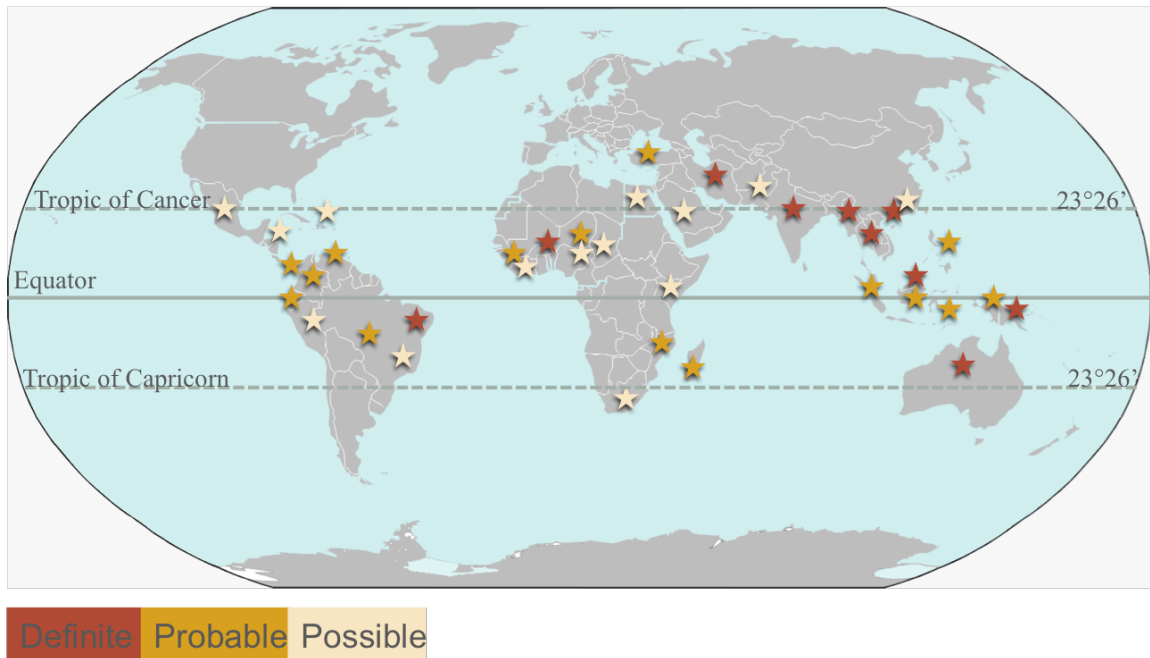


Figure 1. Worldwide distribution of *Burkholderia pseudomallei* endemicity. *B. pseudomallei* is highly endemic to regions of Southeast Asia and Northern Australia. Endemic pockets of melioidosis are also found in Africa and South America. Regions where endemicity of the bacterium is definite, probable and possible are highlighted. Current reports indicate that the bacterium may inhabit tropical and subtropical regions worldwide located between 20° N and 20° S of the Equator.

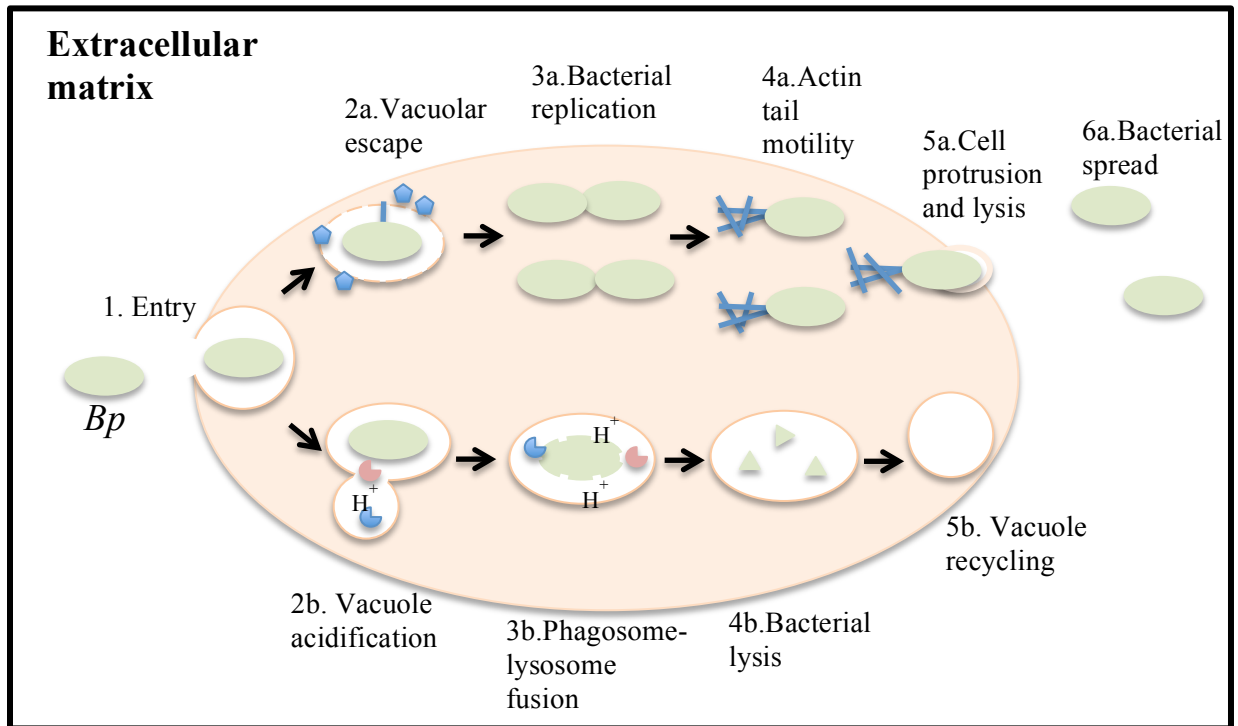


Figure 2. The *Burkholderia pseudomallei* intracellular life cycle. *B. pseudomallei* (*Bp*) is internalized into a membrane-bound vacuole during host cell entry (1). Inside the vacuole, the bacterium translocates effector proteins via the T3SS3 to disrupt the vacuolar membrane and rapidly escape into the cytoplasm (2a) or risk getting killed by the host cell through vacuole acidification (3b and 4b). Once free in the cytosol, bacteria can replicate (3a) and polymerize actin for intracellular mobility and intercellular spread (4a). These events lead to lysis of the host cell by *B. pseudomallei* (5a) and dissemination of the bacterium to other sites of infection (6a).

1.7 Specific Aims

The goal of this dissertation is to define the role(s) of the *Burkholderia pseudomallei* type 3 secretion system cluster 3 (T3SS3) in mediating respiratory disease. Type 3 secretion systems are significant contributors to the pathogenesis of numerous Gram-negative bacterial species, which utilize this injectisome to subvert host cellular defense mechanisms by translocating effector proteins into the cytoplasm of host cells. The *B. pseudomallei* T3SS3 is an important virulence determinant in both respiratory and systemic models of disease. The T3SS3 system potentially mediates bacterial escape from endocytic vesicles of phagocytes by employing its translocated effector proteins. However, the overall mechanisms by which *B. pseudomallei* T3SS3 effectors mediate vacuolar escape have not been elucidated. The results of this research project will further our understanding of the pathogenesis of Gram-negative bacteria, particularly on how T3SS and its effectors act either alone or in concert to modulate host cellular processes to the pathogen's benefit and importantly may provide vaccine and/or therapeutic targets against *B. pseudomallei* infection. Accordingly, we hypothesize that the *B. pseudomallei* T3SS3 is one of the most critical virulence determinants in a lung-specific mouse model of respiratory melioidosis and that is also critically required for the bacterium's intracellular life cycle. Herein, we propose 3 Specific Aims to test this hypothesis.

Aim 1. Develop a lung-specific mouse model of respiratory melioidosis. Hypothesis: Lung-specific delivery of *B. pseudomallei* would provide a more human-like model of respiratory melioidosis.

- A. Compare *in vivo* disease kinetics of mice inoculated via the intranasal route or via intubation-mediated intratracheal (IMIT) instillation.
- B. Determine the course of disease of capsule and T3SS3 mutants in an IMIT mouse model of melioidosis.

Aim 2. Identify *Burkholderia pseudomallei* virulence determinants required for respiratory melioidosis and spread to secondary sites of infection. Hypothesis: A human-like model of respiratory melioidosis would identify novel and characterized virulence determinants required by *B. pseudomallei* to cause respiratory melioidosis and subsequent dissemination to the liver and spleen.

- A. Create a transposon insertion library in the genome of *B. pseudomallei*.
- B. Validate the role of virulence determinants identified by the Tn-Seq screen in the pathogenesis of *B. pseudomallei*.

Aim 3. Define the contributions of T3SS3 effectors to the intracellular life cycle of *Burkholderia pseudomallei*. Hypothesis: T3SS3 effectors mediate *B. pseudomallei*'s rapid escape from host cell phagosomes by potentially modulating host signal transduction pathways.

- A. Assess the kinetics of growth of wild type *B. pseudomallei*, a T3SS3 structural mutant and effector mutants.
- B. Assess the individual contribution of a specific effector in mediating rapid escape of *B. pseudomallei* from host cell phagosomes.

CHAPTER II

MATERIAL AND METHODS

2.1 Bacterial strains and culture

Burkholderia pseudomallei and *Escherichia coli* strains were routinely cultured in Lennox Broth (LB) at 37°C. In preparation for infection studies, *B. pseudomallei* strains were subcultured 1:25 from overnight LB cultures into dialyzed and chelated Trypticase Soy Broth (TSBDC) [72] supplemented with 50 µM monosodium glutamate and grown for 3 hr at 37°C with shaking. When appropriate, antibiotics were used at the following concentrations: kanamycin (Km), 25 µg/ml; polymyxin B (Pm), 50 µg/ml; streptomycin (Sm), 100 µg/ml; and gentamicin (Gm), 20 µg/ml.

2.2 Luminescent *Burkholderia pseudomallei*

Luminescent *B. pseudomallei* strains JW280 and JW280 Δwcb were generated and described elsewhere [73]. JW280 $\Delta sctU_{Bp3}$ was generated by allelic exchange by using the S17-1/pKAS46-araP_{tolC}lux construct [73] to add the *luxCDABE* operon to DD503 $\Delta sctU_{Bp3}$ [19], as previously described.

2.3 Ethics Statement

All animal studies were conducted under Biosafety Level 3 conditions using eight to ten week old female albino C57BL/6J mice (B6 (Cg)-Tyr^{c-2J}/J, Jackson Laboratories) bred at the University of Louisville (Protocol Number 11113). These studies were approved by the University of Louisville's Institutional Animal Care and Use Committee (Protocol numbers 10073 and 13053), in agreement with National Institutes of Health guidelines and the "Guide for the Care and Use of Laboratory Animals" (NRC).

2.4 Mouse respiratory infections

Animal studies were conducted under Biosafety Level 3 conditions using eight to ten-week-old female or male albino C57BL/6J mice (B6(Cg)-Tyr^{c-2J}/J, Jackson Laboratories and in-house breeding). Freshly grown bacteria were washed into phosphate buffered saline (PBS) to appropriate concentrations for infection using OD₆₀₀-based calculations. Intranasal infections were carried out as previously described using 30 µl *B. pseudomallei* suspensions [60]. Intubation-mediated intratracheal (IMIT) instillation was performed, as previously described, to facilitate non-surgical lung-specific disease [74, 75]. Briefly, mice were isoflurane-anesthetized and 2% lidocaine was applied to the back of the mouth as a local anesthetic. Mice were intubated using a 20-gauge catheter, and catheter placement was confirmed by flow meter. Bacterial suspensions were directly instilled into the lung using a 22-gauge blunt needle inserted through the catheter. Optical diagnostic imaging was conducted with an IVIS Spectrum (Caliper Life Sciences) as described previously [73, 76], with once to twice-daily imaging through day 5, and once

daily thereafter until the study completion at day 14. Animals were euthanized at the onset of moribund disease, which was defined by loss of righting reflex.

2.5 Bacterial enumeration at key sites of infection

Infected animals were euthanized and necropsied to enumerate bacteria from infected tissues. Blood samples were collected by cardiac puncture, while bronchoalveolar lavage (BAL) was collected in 1 ml of PBS. Necropsied tissues were subjected to bioluminescence imaging (IVIS Spectrum) in a 24-well black plate before serial dilution enumeration of bacterial burden from tissue homogenate, as described elsewhere [76]. We have defined correlations between tissue counts per second (cps) and colony forming units (CFU) specifically for each tissue as follows: Lung, $\log(\text{cps}) = 1.219\log(\text{CFU}) - 2.999$ ($R^2 = 0.68$); Liver, $\log(\text{cps}) = 1.238\log(\text{CFU}) - 3.502$ ($R^2 = 0.99$); Spleen, $\log(\text{cps}) = 1.088\log(\text{CFU}) - 1.741$ ($R^2 = 0.98$).

2.6 Tn-Seq Library Preparation

Plasmids used in this study are identified in Table 1. To construct the transposon delivery vector pSAM-DKm, the *mariner*-family transposon, *Himar1* C9 transposase and its upstream regulatory region were PCR amplified from pBTK30 and cloned as a *Bam*HI restriction fragment into pSAM-Bt to yield pSAM-DYH. The kanamycin resistance cassette from pEXKm5 was PCR amplified and inserted into the *Mfe*I and *Xba*I restriction sites in place of the erythromycin resistance cassette and the resulting plasmid, pSAM-DKm was verified by PCR. To generate the *B. pseudomallei* Tn-Seq library, the

E. coli S17-1 strain transformed with pSAM-DKm was conjugated with the luminescent *B. pseudomallei* parent strain JW280 for 2 hrs at 37°C. Transposon mutants were selected for on PmKm LB agar plates and grown at 37°C for 24 hrs. A library of 2×10^4 unique mutants were pooled, grown in PmKm LB broth with shaking at 37°C and cryopreserved.

2.7 Tn-Seq Screen

A *B. pseudomallei* Tn-Seq library TSBDC culture was washed into phosphate buffered saline (PBS) and OD₆₀₀ readings were used to estimate bacterial concentrations in order to prepare an inoculum of $10^{4.74}$ CFU/50 µl. A group of three mice were inoculated with 50 µl of bacterial suspension of the Tn-seq library by intubation mediated intratracheal (IMIT) instillation, as described [77]. Disease progression was monitored twice daily by optical diagnostic imaging of bioluminescent *B. pseudomallei* until study completion, as described [78]. Animals were euthanized at moribund endpoints (66 hrs post infection) and necropsied to collect lungs, liver and spleen. Tissues were homogenized and bacteria from these tissues were cultured in LB broth overnight at 37°C with shaking.

Bioluminescence imaging data was processed as described [77].

Chromosomal DNA was purified from triplicate biological samples [79] and pooled for each tissue. Genomic DNA was digested with the *MmeI* restriction enzyme overnight at 37°C, treated for 20 minutes at 80°C to inactivate the enzyme, purified using the QIAquick, PCR purification kit (Qiagen) according to the manufacturer's instructions, and concentrated with a speed vacuum to a final volume of 30 µl. Restricted fragments were separated by electrophoresis in a 1% agarose gel and fragments corresponding to

1.2 to 1.5 Kb were isolated using the QIAquick Gel Extraction Kit (Qiagen). Fragments were ligated to barcoded double stranded adaptors using T4 DNA ligase in 50 μ l reactions overnight at 16°C, treated at 65°C for 10 minutes to inactivate the ligase, and purified using the QIAquick PCR purification kit. Transposon-genome junctions were amplified by PCR using the LIB_PCR_5 (5'-CAAGCAGAAGACGGCATAACGAAGACCGGGGACTTATCATCCAACC TGT-3') and LIB_PCR_3 (5'-AATGATACGGCGACCACCGAACACTCTTTCCCTACAC GACGCTCTTCCGATCT-3') primers [80] using HiFi DNA Polymerase (KAPA Biosystems). Confirmation of a 125-bp product was conducted using 1% agarose gel electrophoresis, and libraries were sequenced using Illumina 50-bp single end sequencing at the Harvard Medical School Biopolymer Facility. Data was analyzed by sorting based on barcodes using a custom script in Java Eclipse, then using CLC Genomics Workbench v. 7.2 for subsequent bioinformatics. Reads were trimmed to remove adapter and transposon sequences and aligned to the *B. pseudomallei* 1026b genome using the default settings in the RNA-seq function in CLC. Reads that mapped to multiple locations were discarded. The resultant reads were counted and normalized to the reads per kilobase of transcript per million reads mapped (RPKM) and compared across sample sites. Significance was assessed using the On Proportions function of CLC using the Kals's test option and the Bonferroni multiple testing correction was applied to the comparisons. Initially, fold change measurements of less than -3 (reduced in the mouse samples compared to the input pool) with a Bonferroni-adjusted *p*-value of less than 0.05 were considered significant.

2.8 Early Dissemination Studies

Early dissemination studies were conducted using the *B. pseudomallei* Tn-Seq library strain to infect groups of three animals by IMIT as described above, euthanizing groups at 6, 12 and 24 hrs post infection. Lung, liver and spleen from individual animals were collected at necropsy, homogenized and serial diluted for bacterial enumeration as described [77].

2.9 Type 6 Secretion System Mutagenesis

To generate a Type 6 Secretion System cluster 5 (T6SS5) mutant in *B. pseudomallei*, an internal in-frame 1,437 bp region of the *tssC-5* gene was deleted. Briefly, flanking fragments in the 5' and 3' region of the *tssC-5* gene were amplified with the following primer sets: 5-tssC-F, GAAGAATTCGCGTAGAACAGCAGCAGCAGCAGCCCCGC; 5-tssC-R, GTCAAGCTTCGGGGATTGCAGGTGTTTCGCCTTCCATGGTC; 3-tssC-F, GTCAAGCTTTCGCTCGTCGGCAAGCTCGAAAAGCGCTAGG; 3-tssC-R, GGCGGTACCTTGCGCGAAGCCGCCGCGAG. The amplified 5' *tssC-5* fragment was cloned into pSK as an *EcoRI/HindIII* fragment to yield pSK-5'tssC. The amplified 3' *tssC-5* fragment was cloned into pSK-5'tssC as a *HindIII/KpnI* fragment to yield pSK-*ΔtssC-5*. The assembled fragment was cloned into pKAS46 as an *EcoRI/KpnI* fragment to yield pKAS46-*ΔtssC-5* and conjugated with the parent *B. pseudomallei* strain DD503. Finally, the bioluminescent strain JW280 *ΔtssC-5* was constructed by conjugation of DD503 *ΔtssC-5* with S17-1/pKAS46-*araP_{tolC}lux*, as described previously [64].

2.10 Virulence Assessment of a T6SS5 Mutant in Respiratory Melioidosis

Animal studies were conducted to compare the virulence of JW280 and the JW280 *AtssC-5* mutant by IMIT infection, as described above. Groups of five animals were euthanized at moribund end point defined as loss of righting reflex. Mice were necropsied and lung, liver and spleen were isolated and imaged for bioluminescence in 24-well black plates. Correlations between bioluminescent signal and colony forming units (CFU) have been previously defined [78].

2.11 Competition Studies

A gentamicin resistance cassette was amplified with flanking *NotI* restriction sites from the pGSV4 vector [78] with the primers Gm cass NotI(+) (GCGGCCGCAGATTTAAATTAATTAAGAGCTAGAATTGACATAAGCCTG) and Gm cass NotI(-) (GAAGCGGCCGCGGCGTTGTGACAATTTACCGAACAACCTC). The Gm cassette was cloned into the pCR®-Blunt II-TOPO cloning vector (Invitrogen) and was then cloned into the pUC19-*araP_{tolC}lux* vector as a *NotI/NotI* fragment to yield pUC19-*araP_{tolC}lux*-Gm. The *araP_{tolC}lux*-Gm fragment was cloned into pKAS46 to generate the pKAS46-*araP_{tolC}lux*-Gm and was transformed into S17-1 cells to generate the S17-1/pKAS46-*araP_{tolC}lux*-Gm strain. This strain was conjugated with the *B. pseudomallei* parent strain DD503, capsule polysaccharide mutant (JW270), Type 3 Secretion System translocation-deficient mutant (DD503 *ΔsctU_{Bp3}*) and Type 6 Secretion System mutant (DD503 *ΔtssC-5*) to generate MGBP001, MGBP001 *Δwcb*, MGBP001 *ΔsctU_{Bp3}*, and MGBP001 *ΔtssC-5*, respectively, by allelic exchange as previously

described [19]. Competition studies were conducted by challenging animals by IMIT with $\sim 10^{4.0}$ CFU of a 1:1 mixture of non-luminescent *B. pseudomallei* DD503 plus one of the four luminescent, gentamicin-resistant MGBP001 strains. The study was completed at 67 hrs post infection at which point lung, liver and spleen were isolated and homogenized. Homogenates were plated in replicate on both LB and LB-Gm plates for bacterial enumeration and competitive index calculations.

2.12 Infection of cultured cells

J774A.1 and RAW264.7 cultured macrophages were maintained in DMEM supplemented with 10% fetal bovine serum and grown at 37° C with 5% CO₂. For growth kinetics studies, J774A.1 macrophages were seeded at 7.5×10^4 cells per well (100 μ l) in black, solid bottom 96-well plates 1 day prior to infection. Bioluminescent *B. pseudomallei* strains were grown as previously indicated. Bacterial concentrations were estimated from OD₆₀₀ readings and bacterial suspensions were diluted in PBS to desired concentrations. Cells were infected with 5 μ l of the diluted bacterial suspension. Infections with individual strains were done in triplicate at multiplicities of infection (MOI) ranging from 2.4 to 3.6 for the parental strain and 6.0 to 2.2 for mutant strains. Sample wells were treated with gentamicin (20 μ g/ml final concentration) 1 hr post infection for the duration of the experiment. For siRNA knockdown studies, RAW264.7 macrophages were infected at an MOI of 10. Bioluminescence measurements were taken every 10 minutes for a total of 14 h post infection using the IVIS Spectrum Imaging System (Caliper Sciences).

2.13 Cell transfection

HEK293 cells were maintained in DMEM supplemented with 10% fetal bovine serum and grown at 37°C with 5% CO₂. Cells were seeded at 6 x 10⁴ cells per well (1 ml) on glass coverslips in clear 24-well plates 1 day prior to infection. 600 ng of p3XFLAG-bopA was transfected into the cells for 24 hrs using PEI as per manufacturer's instructions. For siRNA transfection, 20 µl of 0.165 µM Silencer siRNA targeting TRAPPC8 diluted in Opti-MEM was mixed with 10 µl of Lipofectamine RNAi Max/Opti-MEM as per manufacturer's instruction. 30 µl of siRNA-Lipofectamine complex was added to each well of a black, solid bottom 96-well plate, incubated for 10 min and 1 x 10⁴ RAW264.7 macrophages suspended in 80 µL of DMEM + 10% fetal bovine serum were added to the wells. Cells were incubated for 48 hrs at 37°C with 5% CO₂ before infection. Cells were infected as previously mentioned.

2.15 Immunofluorescent staining and confocal microscopy

For confocal microscopy, cells were fixed to coverslips with 2.5% paraformaldehyde for 15 min and washed 3 times following incubation. An anti-3XFLAG antibody diluted 1:200 in PBS was used for BopA-3XFLAG detection and cells were incubated in 17 µl of the diluted antibody. Unbound antibody was washed 3 times with PBS and 17 µl of Alexa Fluor 488 antibody diluted 1:4000 was used to detect the primary antibody. Unbound antibody was washed 3 times with PBS and 17 µl of Phalloidin-Tetramethylrhodamine diluted 1:4000 was used for F-actin staining. Unbound antibody was washed 3 times with PBS and glass cover slips were mounted on glass slides using

Prolong Gold mounting media with DAPI. For vacuolar membrane staining, RAW264.7 macrophages were incubated with the lipophilic styryl dye FM4-64FX for 1 hr prior to infection as per manufacturer's instructions. Unbound FM4-64FX dye was washed 3 times with PBS and cell infections and vacuole isolation were conducted as previously described. For BopA localization studies, sample plates were placed on ice to stop the progression of infection at 2 hrs post infection. Extracellular bacteria were labeled with mouse anti-BpMAB2 primary antibody and detection of the primary antibody was done with an AMCA donkey anti-mouse secondary antibody. Cells were then fixed with 2.5% paraformaldehyde for 15 minutes. Loading of anti-BpMAB2 primary antibody into the cytoplasm of RAW264.7 cells for detection of cytoplasmic bacteria was accomplished by selective permeabilization of the cells' plasma membrane with the mild detergent digitonin, at a concentration of 10 ng/mL. And detection of the primary antibody was done with donkey anti-mouse Alexa® 547-Tetramethylrhodamine. Samples were analyzed with the Zeiss LSM Duo-LSM5 Confocal Microscope.

2.16 Statistical analyses

Student T-test, one-way ANOVA followed by Tukey's Multiple Comparison test, two-way ANOVA followed by the Bonferroni post-test, student T-test, Log-rank survival analyses (Mantel-Cox test and Gehan-Breslow-Wilcoxon test) were conducted in GraphPad Prism. Probit analysis (Finney Method, StatPlus 2009 Professional) was used to calculate LD₅₀ +/- standard error, which was subsequently subjected to Student T-test analysis to investigate significant differences of LD₅₀ values of different *B. pseudomallei* strains.

Table 1. Strains used in this study.

Strain	Description	Reference
S17-1	<i>E. coli</i> conjugation strain, λ pir	[81]
S17-1/pKAS46- <i>araP</i> _{tolC} <i>lux</i>	Bioluminescence allelic exchange construct	[73]
S17-1/pKAS46- Δ <i>tssC-5</i>	T6SS5 mutant allelic exchange construct	This study
DD503	<i>B. pseudomallei</i> 1026b derivative, Pm ^R Sm ^R Km ^S Gm ^S , lacking AmrAB-OprA efflux pump	[82]
DD503 Δ <i>tssC-5</i>	T6SS5 mutant	This study
DD503 Δ <i>sctU</i> _{Bp3}	T3SS3 mutant	[19]
JW270	DD503 Δ <i>wcb</i> capsule mutant	[60]
JW280	DD503::P _{tolC} - <i>luxCDABE</i>	[73]
JW280 Δ <i>bopA</i>	Bioluminescent <i>bopA</i> mutant	This study
JW280 Δ <i>bopC</i>	Bioluminescent <i>bopC</i> mutant	This study
JW280 Δ <i>bopE</i>	Bioluminescent <i>bopE</i> mutant	This study
JW280 Δ <i>bapA</i>	Bioluminescent <i>bapA</i> mutant	This study
JW280 Δ <i>bapC</i>	Bioluminescent <i>bapC</i> mutant	This study
JW280 Δ <i>tssC-5</i>	Bioluminescent T6SS5 mutant	This study
MGBP001	DD503::P _{tolC} - <i>luxCDABE</i> -Gm	This study
MGBP001 Δ <i>tssC-5</i>	Bioluminescent, Gm ^R T6SS5 mutant	This study
MGBP001 Δ <i>sctU</i> _{Bp3}	Bioluminescent, Gm ^R T3SS3 mutant	This study
MGBP001 Δ <i>wcb</i>	Bioluminescent, Gm ^R capsule mutant	This study
MGBP002	Green Fluorescent Protein expression, JW270	This study
MGBP002 Δ <i>sctU</i> _{Bp3}	Green Fluorescent Protein expression, JW270	This study
MGBP002 Δ <i>bopA</i>	Green Fluorescent Protein expression, JW270	This study

Table 2. Plasmids used in this study.

Plasmid		
pBTK30	Vector containing <i>HimarI</i> C9 transposase	[83]
pSAM-Bt	Tn-seq vector for use in <i>Bacteroides thetaiotaomicron</i>	[84]
pSAM-DYH	pSAM_Bt with the transposase from pBTK30 inserted as a <i>BamHI</i> fragment to replace the native transposase and promoter	[85]
pEXKm5	Gene replacement vector for <i>Burkholderia</i> species	[86]
pSAM-DKm	Tn-seq vector	This study
pKAS46	Allelic exchange vector providing Km ^R and Sm ^S in DD503 genetic background	[87]
pGSV4	Promoterless bioreporter vector harboring <i>luxCDABE</i> operon	[78]
pCR®-Blunt II-TOPO	Topoisomerase-conjugated cloning vector	Invitrogen
pUC19	Cloning vector	New England Biolabs

CHAPTER III

TYPE 3 SECRETION SYSTEM CLUSTER 3 IS A CRITICAL VIRULENCE DETERMINANT FOR LUNG-SPECIFIC MELIOIDOSIS

3.1 Introduction

Naturally acquired melioidosis typically involves percutaneous inoculation or inhalation of pathogen by susceptible hosts, with many risk factors such as diabetes and alcoholism leading to the presentation of clinical melioidosis [88]. Under exceptional conditions, such as natural disasters, otherwise healthy individuals are also susceptible to melioidosis [89-92], suggesting that dose and route of inoculation are key elements to determining whether or not a healthy individual acquires disease. The ability of *B. pseudomallei* to establish a lethal respiratory disease combined with its inherent resistance to numerous classes of antibiotics and the lack of licensed vaccines against the bacterium, highlights the importance of characterizing respiratory melioidosis for the purposes of biodefense.

Respiratory melioidosis has been well studied in surrogate animal models for both basic science investigations as well as therapeutic studies. *B. pseudomallei* has a significant lung tropism, irrespective of the route of acquisition [88], and is able to spread

to other tissues to cause a lethal systemic disease. Bioluminescent *B. pseudomallei* strains have been generated which allow for the temporal assessment of disease progression in individual animals using optical diagnostic imaging. In the first of such studies, a non-lethal intranasal challenge revealed that *B. pseudomallei* prominently colonizes the upper respiratory tract (URT) of mice, leading to a rapid development of meningitis within 24 hours, likely resulting from spread to the olfactory bulbs via olfactory nerve endings [93]. Interestingly, the symptoms of a prominent URT colonization (rhinitis, sinusitis, tonsillitis, laryngitis, and otitis media) have not been described as common presentations of melioidosis [94, 95], suggesting that URT infections do not play a prominent role in humans as that observed in murine models. Indeed, a large clinical sampling study of throat swabs revealed no carriage of *B. pseudomallei* in healthy volunteers, while melioidosis patients had culturable *B. pseudomallei* from the throat in 36.1% of cases [96], less than the presentation rate of pneumonia at 50% [97]. Additionally, paired analyses of throat and sputum carriage from the same patient demonstrated that *B. pseudomallei* culture from the throat is underrepresented relative to sputum culture, suggesting that presence of *B. pseudomallei* in the lung is not a direct result of a descending infection from a colonized throat [96]. These clinical trends, combined with the relatively rare presentation of meningitis at an incident rate of 4-5% [97, 98], suggest that murine models in which *B. pseudomallei* is delivered intranasally over-represent the incidence of URT disease and central nervous system (CNS) involvement in studies of respiratory melioidosis. Significant URT colonization was also observed by diagnostic optical imaging in a lethal intranasal murine

model of respiratory melioidosis [73], suggesting that the URT colonization phenotype is not specific to sub-acute disease.

The role of murine URT colonization on studies of respiratory melioidosis is poorly understood though may have a significant impact on both basic and translational studies. A recent study investigating an intratracheal instillation of *B. pseudomallei* directly into the lungs successfully demonstrated that avoidance of initial URT colonization could limit both CNS involvement and late stage URT colonization [99]. This finding is consistent with other studies demonstrating the mechanism by which melioidosis-associated meningitis arises from spread to the brain from the nasal cavity within 24 hours using both olfactory and trigeminal nerves [100]. Because intratracheal delivery is capable of avoiding such URT and CNS involvement, an unanswered question is what impact these cephalic disease presentations have on disease outcome of pneumonic and systemic disease. We have developed a non-surgical approach to deliver bacteria directly into the lung as a novel instillation strategy termed intubation-mediated intratracheal (IMIT) inoculation, which we have validated to provide >98% efficiency in pulmonary delivery [75], and we therefore used this highly accurate lung inoculation approach to study the impact of lung-specific melioidosis on dissemination and disease outcome. Additionally, we investigated whether lung-specific administration of capsular polysaccharide and type 3 secretion mutants exhibit modified courses of disease relative to previous characterization in other respiratory murine models. Using a combination of optical diagnostic imaging, targeted lung-specific delivery of *B. pseudomallei*, and previously characterized virulence system mutants, we demonstrate that the presence or

absence of URT infection in murine models exhibits significant disease outcome differences, with potential impacts on both basic and translational studies.

3.2 Results

3.2.1 Lung-specific delivery of *Burkholderia pseudomallei* impacts disease progression

Opportunistic URT colonization by *B. pseudomallei* is associated with high rates of meningitis in murine respiratory models [93, 101], and avoidance of bacterial deposition on the nasal mucosa by intratracheal instillation is associated with reduced CNS involvement [99]. We decided to investigate whether the URT colonization typical of current respiratory melioidosis models impacts the moribund disease presentation. To investigate this, we employed a non-surgical approach that would facilitate direct instillation of bacteria directly into the lungs of mice with >98% efficacy [75], termed intubation-mediated intratracheal (IMIT) delivery [74]. Albino C57BL/6J mice were used as a model system in these studies given the myriad of transgenic tools available in the C57BL/6J background, and the importance of coat color in optimizing detection of bioluminescent bacterial pathogens [76]. Thus, albino C57BL/6J mice were infected with 10^4 CFU of luminescent *B. pseudomallei* strain, JW280, using either intranasal or IMIT delivery and monitored twice daily by optical diagnostic imaging. While challenge with 10^4 CFU by both routes of inoculation resulted in moribund disease over a similar time frame, the foci of disease in moribund animals was dramatically different (Figure 3). As observed in our previous work with a BALB/c model [73], C57BL/6J mice infected

intranasally developed a significant URT infection with a reduced bioluminescent signal associated with the thoracic cavity/lung (Figure 3). Interestingly, mice infected in a lung-specific manner by IMIT developed a pulmonary infection earlier than by intranasal delivery of the same inoculum, consistent with estimates that 10% of an intranasal inoculum is delivered to the lung for other respiratory pathogens [102]. Importantly, the early involvement of the lung in the IMIT model led to more severe pneumonic disease than that observed in the intranasal model, with subsequent systemic spread not previously observed in the intranasal model. This suggests that mice are capable of sustaining an advanced systemic disease than previously thought possible in the intranasal model, and therefore that URT colonization by *B. pseudomallei* directly contributes to the host morbidity of the intranasal model. These data indicate that avoiding initial deposition of bacteria in the upper respiratory mucosa represents an important modification for studying the development of pneumonia and subsequent systemic spread.

3.2.2 Respiratory melioidosis models exhibit similar disease kinetics

We decided to examine whether the kinetics of respiratory disease vary as a function of the method of delivery in order to investigate whether the involvement of different foci of infection impacts the median time to death (MTTD). Mice were infected by either intranasal or IMIT instillation and both respiratory disease models were able to establish an acute course of disease in C57BL/6J mice with a typical MTTD of ~4 days (Figure 4). We observed typical dose response disease susceptibility in the intranasal

model with a transition from 100% survivors to 100% fatality over a 32-fold dose range (Figure 4A). Interestingly, we observed a much sharper dose transition in host susceptibility to disease in the IMIT-infected groups, which occurred over a single ten-fold dose range (Figure 4B). We calculated the LD₅₀ of the intranasal C57BL/6J model to be $12.1 \pm 2.4 \times 10^3$ CFU, while the IMIT model significantly lowered the LD₅₀ to $5.4 \pm 2.0 \times 10^3$ CFU (P = 0.04). Thus, targeting of *B. pseudomallei* directly into the lungs of mice resulted in a lowering of the LD₅₀ and resolved host susceptibility into a more discrete dose range transition from susceptibility to clearance of pathogen. Importantly, the small 2.2 fold change in the LD₅₀ and similar MTTD at equivalent doses suggest that the ultimate course of disease takes place over a similar time frame, regardless of the method of inoculation, but that the disease presentation is dramatically altered dependent on whether *B. pseudomallei* spreads specifically from the lung, or whether initial inoculation prominently colonizes the URT. We conclude that intranasal and IMIT respiratory infections therefore cause very different morbidity in the host as a result of either primarily URT or systemic endpoints, respectively.

To further investigate the role of URT colonization on disease endpoints, we subsequently investigated the bacterial burdens of tissues isolated from moribund mice to further characterize differences in bacterial dissemination. Tissues were necropsied from moribund mice infected with ~LD₁₀₀ doses of JW280 by either the intranasal or IMIT routes of infection, and we compared the tissue burdens of moribund animals for the lung, liver, spleen, BAL and blood of mice infected with (i.n.) or without (IMIT) involvement of the URT. Consistent with the findings of Figure 3, we found that IMIT delivery of *B. pseudomallei* facilitates significant disease in all monitored tissues, both at

the primary site of infection in the lung, as well as in the disseminated infection of the liver and spleen (Figure 5). Further, we observe a >3 log CFU difference of bacterial dissemination through the blood, indicating that moribund mice exhibit a greater degree of septicemia in the IMIT model relative to the i.n. model. Consistent with *in vivo* diagnostic imaging, bacterial tissue burden analysis reveals that *B. pseudomallei* infections involving prominent URT colonization result in host morbidity associated with reduced disease maturation in core body sites, suggesting that the host morbidity of the i.n. model is directly influenced by the bacterial colonization of the nasal cavity.

3.2.3 Sex difference influence host susceptibility to lung-specific melioidosis

Given a recent focus in the scientific community on understanding disease progression in both male and female model systems [103], we additionally performed survival analyses in male albino C57BL/6J mice to investigate whether sex differences impact susceptibility to lung-specific respiratory melioidosis. Male disease progression closely mirrored that observed in the female models (Figure 4 and 6), where in both cases, the 100% minimally lethal dose was observed at $10^{4.2}$ CFU by IMIT, with a 91 hr MTTD. We calculated the LD₅₀ for lung-specific melioidosis in male mice as $1.9 \pm 1.2 \times 10^3$ CFU, which was 2.9 fold reduced relative to the female LD₅₀ ($P = 0.25$). Thus, male mice are not significantly different in their susceptibility to respiratory melioidosis relative to female mice in the C57BL/6J IMIT model system.

3.2.4 Type 3 Secretion is more critical for respiratory melioidosis than capsule

We observed that URT colonization impacts disease outcome in the murine respiratory melioidosis model, and we therefore hypothesized that URT colonization could impact our basic understanding of the role of virulence determinants in mediating *B. pseudomallei* pathogenesis. Previous murine studies demonstrated that a capsule mutant LD₅₀ is attenuated 10^{1.8} fold in a respiratory melioidosis model [60], and that T3SS3 is also required for the full virulence in an equivalent dose challenge [104]. We therefore examined the response of albino C57BL/6J mice infected with increasing doses of either a luminescent capsular polysaccharide mutant (JW280 Δwcb) or a T3SS3 mutant (JW280 $\Delta sctU_{Bp3}$). We found that a capsule mutant inoculated by IMIT was not significantly attenuated relative to the wild type strain, with a capsule mutant LD₅₀ calculated to be 10^{4.57} CFU (6.8 fold attenuation, P = 0.60). We observed a MTTD of 72 hrs at an \sim LD₁₀₀ challenge (Figure 7A), which represents a faster course of disease than the \sim LD₁₀₀ dose of wild type at 91 hrs, albeit with a larger challenge dose. Thus, the JW270 capsular polysaccharide mutant is not significantly attenuated in the lung-specific IMIT model, contrasting with our prior findings in the i.n. model. In the IMIT model, the T3SS3 mutant had a calculated LD₅₀ of 10^{6.19} CFU, which represents a significant attenuation of 10^{2.5} fold (P= 0.004). The course of disease of the T3SS3 was observed to have a MTTD of 79 hr at the minimally lethal dose (Figure 7B), which like the capsule mutant strain was faster than the wild type MTTD, albeit with a larger challenge dose. Thus, in a lung-specific respiratory melioidosis model, T3SS3 is a critical virulence

determinant for *B. pseudomallei* in the lung, whereas the capsular polysaccharide appears to play a more minor role.

3.2.5 Capsule and T3SS3 mutants are defective in spread from the lung

We decided to further investigate whether abrogation of URT colonization in our lung-specific disease studies impacts the dissemination potential of the capsule and T3SS3 mutants. We performed optical diagnostic imaging of \sim LD₁₀₀ infections of the wild type strain as well as both the capsule and T3SS3 mutants to characterize bacterial burdens at moribund disease. We found that the wild type strain is capable of dissemination beyond the lung to colonize all sites of the body at high titer (Figure 8). The capsule and T3SS3 mutants developed significant bacterial pneumonia yet exhibited a spread deficiency with minimal bacterial burden outside of the lung (Figure 8). We further characterized the dissemination defects of these mutants by enumerating bacteria from the lung, liver and spleen, from mice infected with minimally lethal doses of each strain. We found that while all tested strains established bacterial pneumonia of 10^8 - 10^9 CFU per tissue, the capsule and T3SS3 mutants exhibited significant dissemination defects to the liver and spleen in both tissues (Figure 9). These data demonstrate that a capsule mutant exhibits reduced fitness to disseminate from the lung, consistent with the previously characterized role of capsular polysaccharide in mediating complement protection [59]. Thus, a capsule mutant is capable of producing a lethal pneumonia with a similar LD₅₀ as wild type, yet without the wild type-ability to spread beyond this organ. In contrast, the T3SS3 virulence determinant exhibits significantly reduced fitness in the

lung by LD₅₀ analysis, and this reduced fitness is also associated with a reduced dissemination potential to the liver and spleen. Thus, both the capsule and T3SS3 mutants are spread deficient when delivered specifically to the lung, highlighting a major difference between the current lung-specific respiratory melioidosis model versus our previous work with i.n. models. This finding suggests that the differences in respiratory melioidosis models, with respect to URT involvement in dissemination and endpoint, dramatically influences our interpretation of basic science investigations of the role of *B. pseudomallei* virulence determinants.

3.2.6 T3SS3 mutant exhibits reduced fitness in lung over the course of disease

We hypothesized that the reduced fitness characterized at moribund disease would similarly be associated with a reduced fitness throughout the course of disease. We therefore performed optical imaging of mice infected at a ~LD₁₀₀ dose of JW280, JW280 Δwcb , or JW280 $\Delta sctU_{Bp3}$ and quantified the *in vivo* bioluminescence until moribund endpoints were reached. We identified an *in vivo* logarithmic increase in bioluminescence of all strains in the lung, but observed that the T3SS3 mutant exhibited reduced fitness relative to both wild type and capsule mutant strains (Figure 10). The bioluminescence-doubling rate was calculated for all strains and we found non-significant differences of the doubling rates of the wild type and capsule mutant strains of 9.88 and 9.24 hrs, respectively (One-way ANOVA/Tukey not significant). However, the T3SS3 mutant bioluminescence doubled at a significantly reduced rate of 13.64 hrs (P<0.001), suggesting that the T3SS3 mutant is less fit to grow in host niches and/or is subject to enhanced clearance by the host. This finding is consistent with our study data,

highlighting T3SS3 as a critical virulence determinant for *B. pseudomallei* lung colonization, whereas the capsular polysaccharide plays a lesser role in disease of the lung.

3.3 Discussion

We have previously developed an optical diagnostic imaging model of intranasal respiratory melioidosis and observed that the URT of mice infected in this manner are subject to prominent infection [73]. URT colonization is associated with infection of the nasal-associated lymphoid tissue (NALT) as well as infection of the olfactory bulbs/CNS [93, 100]. As discussed above, descriptions of disease states associated with URT infections have not been described in human melioidosis, and paired analysis of culture sputum and throat swabs suggests that pneumonia gives rise to the presence of *B. pseudomallei* at the top of the respiratory tract rather than URT carriage seeding a primary infection which descends to the lung [96]. The over-representation of these symptoms in mice have led us, and others, to investigate alternatives to the standard approaches of inoculating mice with *B. pseudomallei* through the nares. A recently developed intratracheal model of respiratory melioidosis succeeded in abrogating CNS infections, suggesting that URT colonization is directly responsible for the high levels of meningitis reported in the murine model [99, 105]. Our current studies focused on advancing these findings by identifying whether URT infection in the mouse impacts the overall course of disease and ask whether these impacts might influence both basic and translational studies of respiratory melioidosis.

Importantly, we found that inoculation of *B. pseudomallei* directly into the lung dramatically altered disease outcome, where we observed significant increases in both lung burden and septicemic spread not previously observed in intranasal inoculation studies. Our survival analysis of intranasal and IMIT-infected mice revealed that both routes of infection supported a disease process with very similar timing of inoculation to moribund endpoint; however, the major difference between the models was the difference in which host tissues supported the dominant site(s) of infection. IMIT also lowered the LD₅₀ relative to the i.n. model and provided an earlier development of pneumonia which progressed to advanced systemic disease. Intranasal infection exhibits a clear bias to nasal cavity colonization, and conversely the IMIT model achieves systemic disease at moribund endpoints. This difference in infection site at moribund disease strongly suggests that the causation of moribund presentation is very different in these models, with IMIT providing systemic, general organ failure disease, while the moribund disease of the intranasal model is very directly related to the bacterial burden in the nasal cavity. Pathological analysis of the URT of mice infected by the i.n. route revealed significant blockage by inflammatory cell debris in the nasal turbinates [105], thus the severe pathology/rhinitis of the intranasal model likely promotes moribund disease. Both IMIT and i.n. models have moribund disease symptoms which include labored breathing of mice, and given that mice are obligate nasal breathers, we hypothesize that nasal cavity occlusion in the intranasal model drives moribund endpoints while the labored breathing of the IMIT model may reflect greater lung pathology, as the IMIT model supported >1 log more bacteria per lung than the i.n. model. Future studies will be required to investigate whether the aerosol model, which would also involve the nasal mucosa as a

primary site of infection, is similarly subjected to preferential colonization of the URT over systemic spread.

The IMIT inoculation method we developed is distinct from other non-invasive intratracheal instillation methods, including those used previously for *B. pseudomallei* instillation [99]. IMIT inoculation is a two-step process in which mouse intubation is followed by instillation of bacteria via a long blunt needle, and the approach facilitates an intermediate confirmation of correct catheter placement into the trachea (rather than the esophagus), and is therefore not prone to user error associated with unintentional misinoculation of the GI tract [106]. IMIT inoculation also benefits from being a non-invasive approach, which avoids overt deposition of bacteria into the blood stream, which could occur as a result of surgical intratracheal inoculation.

This study incorporated use of albino C57BL/6J mice as a novel host model system in which to study respiratory melioidosis. A vast array of murine transgenic lines are available to the research community, the majority of which are available in the C57BL/6J background, which have been, and will continue to be important tools in melioidosis studies. C57BL/6 mice are commonly referred to as representing a chronic model of melioidosis, however both in the intranasal and IMIT infection studies we found that C57BL/6J mice develop an acute disease with a MTTD of 3-4 days. While C57BL/6J mice do appear to have a higher resistance to respiratory melioidosis with intranasal LD₅₀ values 1-3 logs higher than their BALB/c counterparts [107], we conclude that C57BL/6J mice successfully model an acute respiratory disease presentation. We further made use of tyrosinase-negative mice, which have albino coats

and therefore offer greater sensitivity over black-coated mice to detect bioluminescent bacteria, which is necessary to monitor the early stages of disease progression *in vivo*.

We hypothesized that the improved ability to study disease maturation of respiratory melioidosis in the absence of URT colonization might influence the role of virulence determinants in mediating *B. pseudomallei* pathogenesis. Given our prior interest in studying the role of capsular polysaccharide in mediating *B. pseudomallei* dissemination from the lung, we investigated the role of a capsule mutant using IMIT inoculation. Unlike our previous work which identified an attenuation of the Δwcb capsule mutant of $10^{1.8}$ - $10^{2.3}$ fold in intranasal models [60, 73], we found a non-significant attenuation of just 6.8 fold ($10^{0.8}$) in the IMIT model, suggesting that the capsular polysaccharide is not absolutely critical for the initial stages of lung colonization. From our growing understanding of the difference between i.n. and IMIT models, we conclude that the capsule mutant is attenuated in its ability to colonize the nasal mucosa as the contributor to its greater attenuation in the i.n. model, and conversely that capsular polysaccharide is not as critical for disease in the lung. More importantly, we further characterized whether the capsule mutant is required for dissemination beyond the lung. In our previous studies, we had found that there was no significant defect in dissemination of the capsular polysaccharide mutant when studied at the minimally lethal dose in the murine intranasal model [60]. This previous observation had not been anticipated given the previous demonstration that capsular polysaccharide is required to resist opsonization by host complement likely during dissemination through the blood stream [59], and further that capsule is a critical virulence determinant in systemic disease models of both the hamster and mouse with an attenuation of $\sim 10^5$ fold [61, 62].

Importantly, our current studies provide a modified understanding of the role of capsular polysaccharide in mediating dissemination beyond the lung, as we now observe that a capsule mutant is defective in lung-specific dissemination both optical diagnostic imaging as well as tissue burden analysis. We retrospectively interpret our previous studies to suggest that capsular polysaccharide mutants are attenuated for colonization of the URT mucosa, and that a capsule mutant is competent to disseminate from the URT to the liver and spleen at wild type levels, possibly involving the NALT and lymphatic system, as has been proposed for *B. pseudomallei* spread by others [93]. Only through studying the capsule mutant in a lung-specific model system have we identified a dissemination defect for this mutant, consistent with a dominant role for capsular polysaccharide as a defense to innate immunity, thereby facilitating disseminated disease. Thus, the study of the role of virulence determinants in respiratory melioidosis may give different phenotypes dependent on whether disease is mediated by URT infection (i.n.) or systemic disease progression (IMIT).

Type 3 Secretion has been characterized as an important *B. pseudomallei* virulence determinant in hamster and murine systemic disease models as well as a murine intranasal model system [19, 104]. *B. pseudomallei* possesses three T3SS clusters in its genome [45, 46, 108], of which only cluster 3 was found to be important for mammalian virulence, with a calculated attenuation of $10^{2.8}$ fold in a systemic hamster intraperitoneal model [19]. Given that our IMIT model revealed a reduced importance for the role of capsule in *B. pseudomallei* pulmonary pathogenesis, we investigated whether T3SS3 is an important *B. pseudomallei* virulence determinant in the lung, or whether it too is required preferentially for systemic infection rather than initial lung colonization.

Interestingly, we found that a T3SS3 translocation defective mutant was attenuated $10^{2.5}$ fold, similar to the $10^{2.8}$ fold attenuation reported in a systemic model. Thus, unlike the capsule mutant, which is critical for systemic, but not respiratory, disease, T3SS3 is required ubiquitously for both systemic and respiratory disease. It is understood that a critical phenotype associated with the T3SS3 locus is mediating the ability of *B. pseudomallei* to rapidly escape from the phagosome of professional phagocytes [38, 109]. Thus, T3SS3 mutants exhibit growth defects in intracellular niches associated with delayed vacuolar escape, suggesting that the decreased fitness, which we have observed for the T3SS3 mutant in the lung, is associated with reduced fitness in the intracellular environment. Our data suggests that *B. pseudomallei* inhabits intracellular niches, not only in the lung, but also in other tissues, which might explain why a similar degree of attenuation is observed for the T3SS3 mutant in both systemic and respiratory disease models. We are therefore interested in identifying how specific effector proteins delivered by the T3SS3 apparatus participate in mediating vacuolar escape and increase the fitness of *B. pseudomallei* in the lung.

In summary, we have demonstrated that respiratory melioidosis in the murine model may be associated with severe upper respiratory inflammation, which directly drives host morbidity. We have further demonstrated that simple approaches facilitating a lung-specific disease progression allow for abrogation of URT infection, and therefore allow mice to act as much better surrogates for human melioidosis, minimizing the role of URT-based morbidity and CNS involvement. This approach has profound impact both in translational studies as well as basic science investigations. In the case of the former, full disease progression in the mouse will allow an investigation of the efficacy of pre-

and post-exposure prophylaxis to protect against an advanced septicemic disease state. With regards to basic science investigations, we have successfully used the IMIT model to meet prediction of the role of capsular polysaccharide in facilitating dissemination of *B. pseudomallei* from the lung, whereas our former intranasal model system did not allow us to draw these predicted conclusions. The IMIT model has also revealed a critical role for the T3SS3 in facilitating respiratory melioidosis.

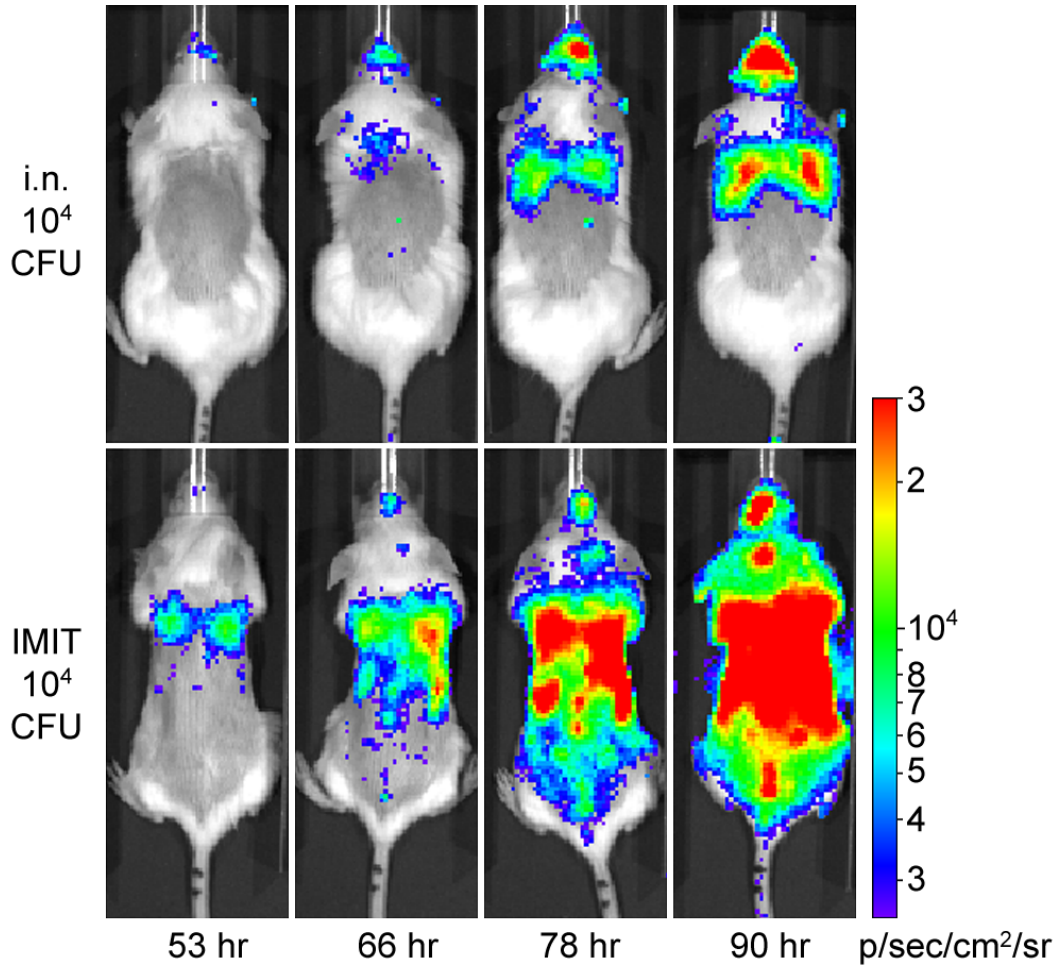


Figure 3. *In vivo* optical diagnostic imaging of respiratory melioidosis.

Female albino C57BL/6J mice were challenged with 10^4 CFU of luminescent *B. pseudomallei* strain JW280 by either the intranasal (Top panel) or IMIT (Bottom panel) routes of infection. Mice were imaged twice-daily beginning at 18 h post infection. Images were uniformly adjusted to a range of 2.5×10^3 to 3×10^4 p/s/cm²/sr on a logarithmic scale. A representative panel of images beginning 53 hr post infection is presented for both infection routes, where the last image of each panel represents the moribund disease endpoint.

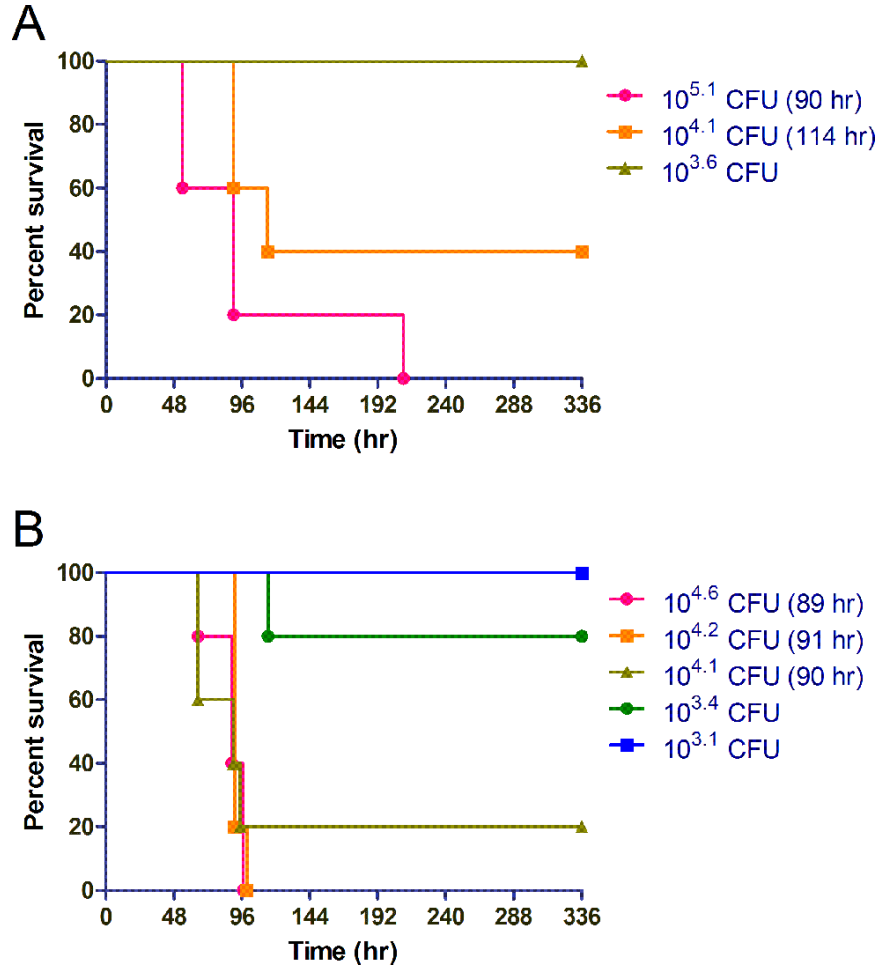


Figure 4. Host response to lung-specific delivery of *Burkholderia pseudomallei*.

Groups of 5 female albino C57BL/6J mice were challenged with increasing doses of luminescent *B. pseudomallei* strain JW280 by either the intranasal (A) or IMIT (B) routes of infection. Mice were monitored for 14 days (336 hr) for disease progression and euthanized at the onset of moribund disease presentation. Survival curves are used to present the dose-dependent response of the host to increasing bacterial challenges. The MTTD was calculated for groups with $\geq 50\%$ mortality, as indicated.

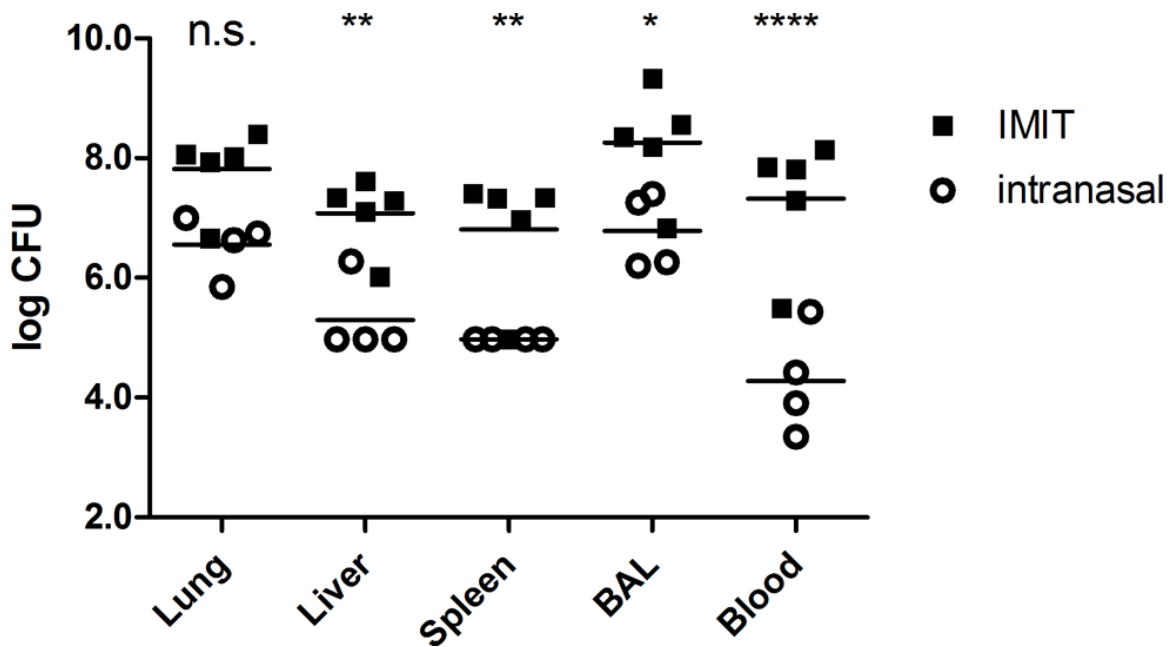


Figure 5. Bacterial enumeration at moribund disease for respiratory melioidosis

models. Groups of 5 female albino C57BL/6J mice were infected by either the i.n. ($10^{5.1}$ CFU) or IMIT ($10^{4.6}$ CFU) routes of infection and euthanized at moribund disease endpoints. Bacteria were enumerated from tissues homogenized in 1 ml PBS, from a 1 ml PBS BAL collection, or from cardiac-drawn blood. Bacterial burden was calculated as CFU/tissue (lung, liver, and spleen) or bacteria per ml of body fluid (BAL and blood). Significant differences between log transformed data were evaluated by 2-way ANOVA with Bonferroni multiple comparisons (n.s., not significant; *, $p < 0.05$; **, $p < 0.01$; ****, $p < 0.0001$).

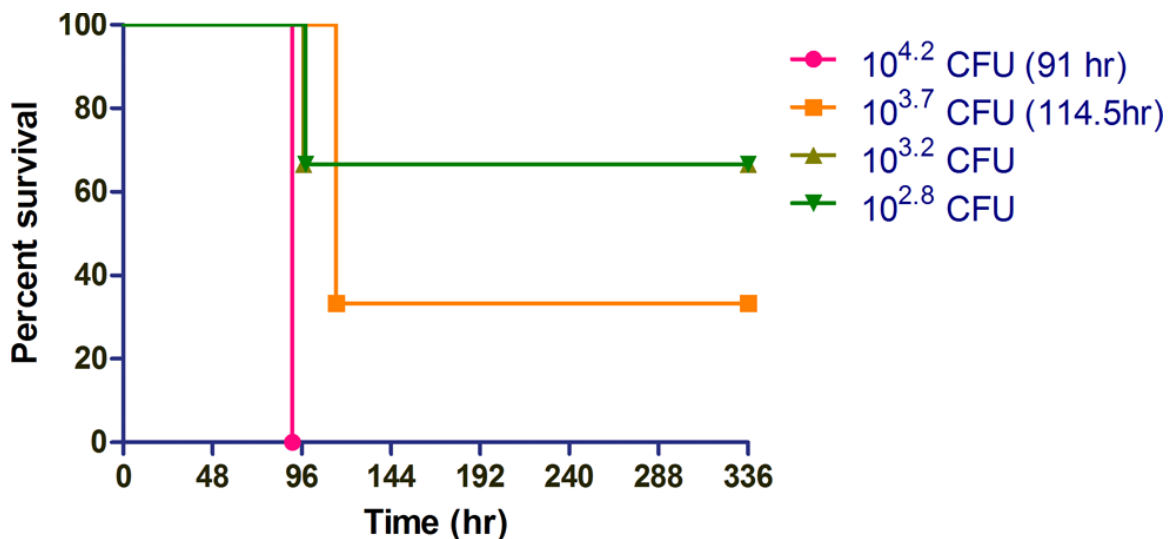


Figure 6. Male host response to lung-specific delivery of *Burkholderia pseudomallei*.

Groups of 3 male albino C57BL/6J mice were challenged with increasing doses of luminescent *B. pseudomallei* strain JW280 by IMIT infection. Mice were monitored for 14 days (336 hr) for disease progression and euthanized at the onset of moribund disease presentation. Survival curves are used to present the dose-dependent response of the host to increasing bacterial challenges. The MTTD was calculated for groups with $\geq 50\%$ mortality, as indicated.

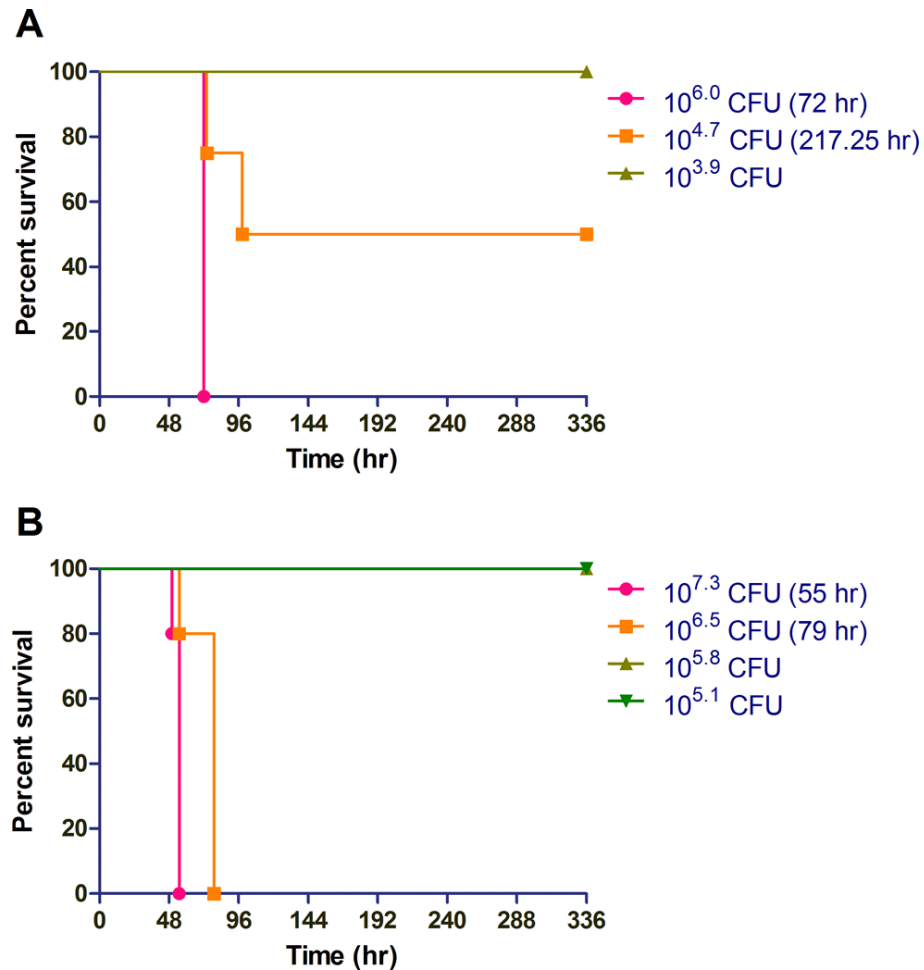


Figure 7. Host response to capsule and T3SS3 mutants of *Burkholderia*

pseudomallei. Groups of 5 female albino C57BL/6J mice were challenged by the IMIT route of infection with increasing doses of either Δwcb capsule mutant (A) or $\Delta sctU_{Bp3}$ T3SS3 mutant (B) in the luminescent *B. pseudomallei* strain JW280 background. Mice were monitored for 14 days (336 hr) for disease progression and euthanized at the onset of moribund disease presentation. Survival curves are used to present the dose-dependent response of the host to increasing bacterial challenges of *B. pseudomallei* mutants. The MTTD was calculated for groups with $\geq 50\%$ mortality, as indicated.

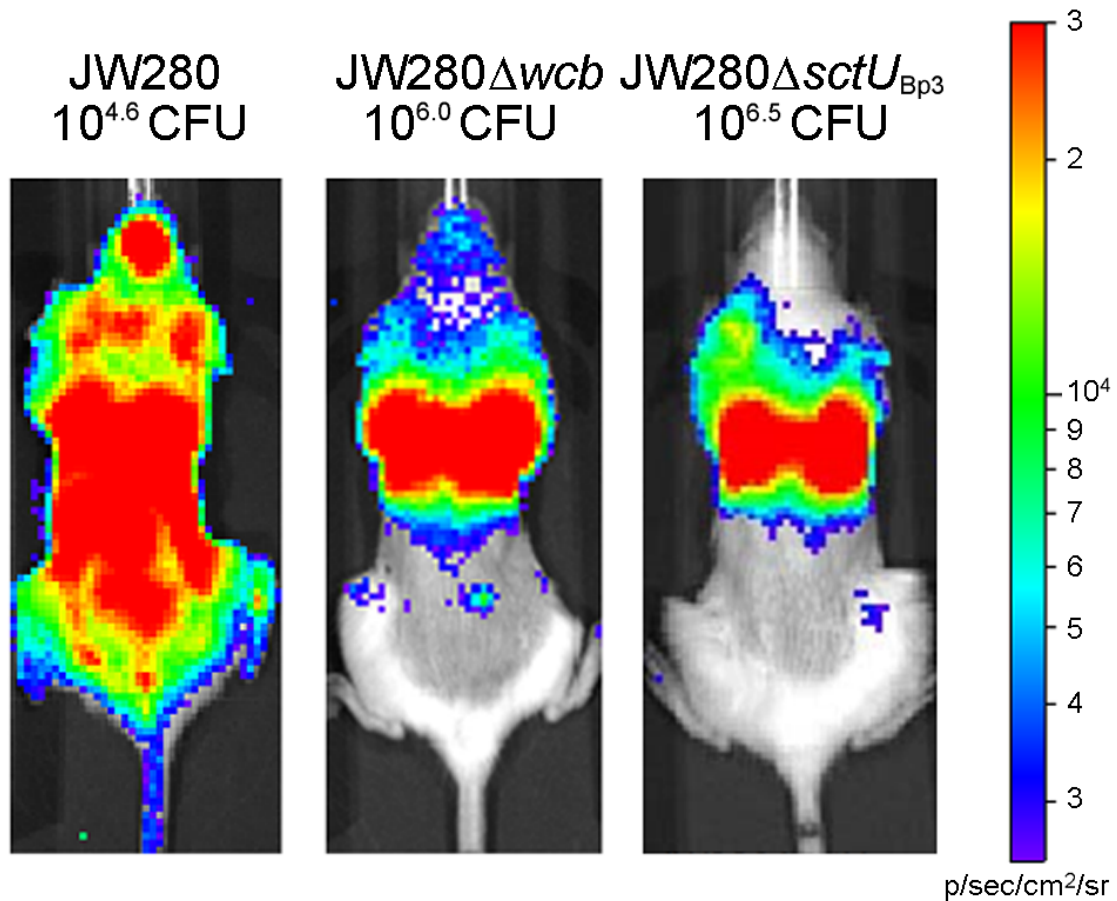


Figure 8. Detection of dissemination of *Burkholderia pseudomallei* mutants by optical imaging. Groups of 5 female albino C57BL/6J mice were challenged by the IMIT route of infection with either wild type luminescent *B. pseudomallei* strain JW280, the Δwcb capsule mutant, or the $\Delta sctU_{Bp3}$ T3SS3 mutant. Representative images of disease endpoints are presented, with uniform image settings adjusted to a range of 2.5×10^3 to 3×10^4 p/s/cm²/sr on a logarithmic scale.

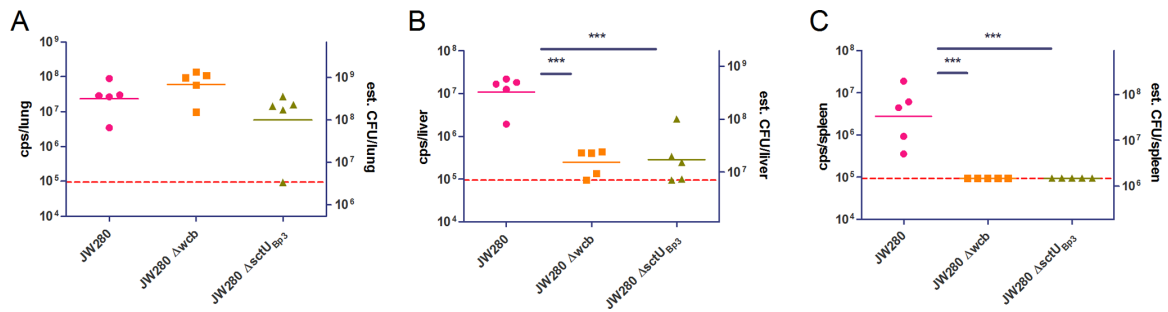


Figure 9. Bacterial enumeration of *Burkholderia pseudomallei* mutants in moribund

respiratory disease. Groups of 5 female albino C57BL/6J mice were infected with wild type JW280 ($10^{4.2}$ CFU), Δwcb capsule mutant ($10^{6.0}$ CFU), or $\Delta sctU_{Bp3}$ T3SS3 mutant ($10^{6.5}$ CFU), and euthanized at moribund disease endpoints. Bacteria were enumerated from tissues *ex vivo* by optical imaging (left Y-axis: cps/tissue) with presentation of the estimated tissue CFU burdens based on calculated tissue-specific cps:CFU correlation (right Y-axis: CFU/tissue est.) for lung (A), liver (B) and spleen (C). The 95% LOD was calculated as a technical background luminescence and indicated as a dotted horizontal line. Data points below the 95% LOD were set to the 95% LOD value. Significant differences (1-way ANOVA with Tukey posttest) between log-transformed data sets are indicated with an adjoining line (*, $p < 0.05$; **, $p < 0.01$; ***, $p < 0.001$).

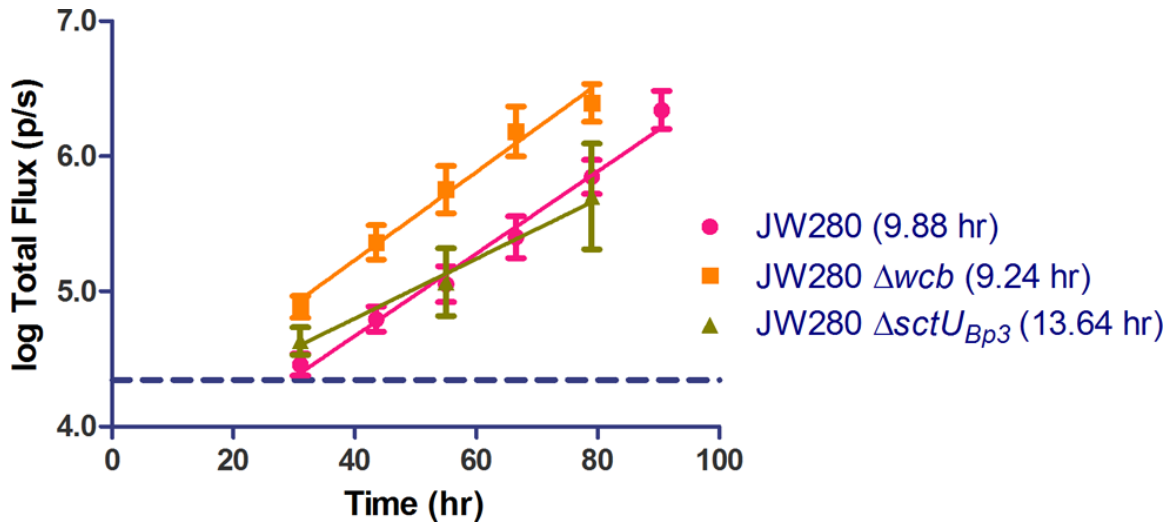


Figure 10. Detection of pulmonary growth rates of *Burkholderia pseudomallei* mutants *in vivo*. Groups of 5 female albino C57BL/6J mice were infected with wild type JW280 ($10^{4.2}$ CFU), Δwcb capsule mutant ($10^{6.0}$ CFU), or $\Delta sctU_{Bp3}$ T3SS3 mutant ($10^{6.5}$ CFU), and monitored by optical diagnostic imaging once to twice daily. ROIs from the dorsally-imaged thoracic cavity were plotted as a function of infection time for each mutant. The 95% LOD was calculated for the background luminescence of uninfected mice and indicated as a dotted horizontal line. The calculated doubling rate of bioluminescent signal of each strain is indicated.

CHAPTER IV

COMPREHENSIVE IDENTIFICATION OF VIRULENCE FACTORS REQUIRED FOR RESPIRATORY MELIOIDOSIS USING TN-SEQ MUTAGENESIS

4.1 Introduction

Respiratory melioidosis is a disease presentation of high relevance to both naturally occurring and biodefense-related studies. Both our laboratory and others have previously shown that the nasal cavity represents the predominant site of *B. pseudomallei* colonization in intranasally inoculated mice [73, 93], whereas direct lung instillation of bacteria can abrogate nasal cavity colonization and the associated central nervous system involvement [78, 99]. We have further characterized that lung-specific instillation of *B. pseudomallei* results in a shift of moribund endpoint from a predominant nasal cavity infection in the intranasal model to greater bacterial proliferation in the lung and disseminated spread [78], more closely resembling descriptions of human melioidosis. Furthermore, the intubation-mediated intratracheal (IMIT) inoculation method facilitated the discovery of a spread-deficiency phenotype for a capsular polysaccharide mutant from the lung [78], which had not been discovered in mice succumbing to nasal cavity colonization [73], and yet meets the predicted role for capsule in mediating

protection from complement during dissemination [59]. Thus, the IMIT lung-specific melioidosis model has begun to provide unique insights into the roles of *B. pseudomallei* virulence determinants that have not been identified in other respiratory melioidosis models.

We sought to identify additional *B. pseudomallei* virulence determinants by combining our IMIT mouse model of lung-specific instillation with transposon mutagenesis. Tn-seq is a powerful tool used to identify genes required for an organism's fitness in a selective environment by combining saturation mutagenesis and Next Generation Sequencing [110]. Recent Tn-seq studies identified essential genes required to support *in vitro* growth for the *Burkholderia pseudomallei* K96243 strain [33] and the closely related *Burkholderia thailandensis* E264 strain [111, 112]. These studies identified potential antimicrobial drug targets in key constituents of metabolic pathways, cell structure and genes required for nucleotide and amino acid synthesis, and further estimated that ~8% of the *Burkholderia* genome represent essential genes [33, 111]. Importantly, Tn-seq has not been previously used to identify *B. pseudomallei* genes required to support growth in the selective pressure of mammalian host tissues. In the present study, we investigated the potential of Tn-seq to identify virulence determinants required by *B. pseudomallei* to colonize mammalian lungs in a mouse model of respiratory melioidosis as well as to disseminate to the liver and spleen. These studies take advantage of our IMIT respiratory melioidosis model to non-invasively target delivery of a Tn-seq library directly into the lungs of mice to specifically identify genes supporting pulmonary disease in the absence of potential interplay between upper and lower respiratory tract infections.

4.2 Results

4.2.1 Lung-specific mouse infection with the Tn-Seq insertion library

We sought to identify virulence determinants required by *B. pseudomallei* to cause disease specifically in the lung, as well as subsequent disseminated spread to the liver and spleen. Accordingly, we generated a transposon insertion library composed of 20,000 insertion mutants in the genome of the *B. pseudomallei* luminescent strain JW280, a derivative of the 1026b clinical strain. To select against transposon-inactivated genes required for lung colonization and systemic spread *in vivo*, we challenged groups of three C57BL/6J albino female mice with $10^{4.74}$ CFU of a transposon insertion library. This inoculum was within 10 median lethal doses (LD_{50}) of the JW280 strain [78], and achieved approximately 4x coverage of the genome and 4x mutant strain representation in the challenge inoculum. We monitored the growth rate of the mutant library by bioluminescence starting at 19 hours post infection and observed that in the lungs, the library pool exhibited logarithmic growth at a rate consistent with our previously observed JW280 parent strain growth rate [78] (Figure 11A). By 66 hours post infection, all animals had reached moribund stage, characterized by acute respiratory infection and systemic spread (Figure 11B) and at this point all animals were euthanized and lungs, liver and spleen were isolated. These data indicate that *in vivo* disease progression in C57BL/6J mice infected with the transposon insertion library followed an acute course of infection comparable to that of the parent *B. pseudomallei* strain [78].

4.2.2 Transposon insertion sequencing and mapping

Our collaborator Dr. Deborah Yoder-Himes performed sequencing of the input transposon insertion library to determine transposon insertion density and homogeneous coverage of the *B. pseudomallei* JW280 genome. Sequencing of the input mutant library mapped 1.1268 million reads to the *B. pseudomallei* 1026b genome and the mapped reads showed that 88% percent of genes contained a transposon insertion. Approximately 8% of the *B. pseudomallei* genome is estimated to represent essential genes based on *in vitro* growth [33]; thus our input library coverage approached the maximum potential coverage of 92%. As might be expected, larger genes received better coverage efficiency and genes larger than 400 base pairs in length had over 94% coverage (Figure 12A).

We hypothesized that lung-specific delivery of the *B. pseudomallei* mutant library would sustain selective pressure in the lung, which would lead to an initial loss of library diversity and subsequent additional diversity loss following spread to the liver and spleen. Tn-seq analyses typically investigate changes in library diversity between two conditions using a 2-fold cutoff criteria [85, 113, 114], however, given the smaller size of our mutant library tailored for animal infection studies, we increased the stringency of our initial data analysis to a 3-fold cutoff. Sequencing of the output libraries showed that at a 3-fold loss relative to the input library, transposon mutants in the lungs sustained selective pressure leading to clearance of 1455 transposon-inactivated genes required for lung colonization (Figure 12B). As expected, the transposon library was further reduced in the spleen (2862 genes), suggestive of loss of library diversity both in the lung and due to loss of genes required for disseminated spread. Surprisingly, we observed a greater retention of diversity of the transposon library in the liver relative to the lung (765

mutants lost in the liver compared to 1455 in the lung), suggesting that a representative library pool reached this site prior to effects of the selective pressure exhibited in the lung (Figure 12B). Further, the retention of library diversity in the liver relative to the lung suggests that the liver does not exhibit as strong a selective environment as the lung, and that the early spread to the liver is at high titer so as to avoid potential bottlenecking effects of spread from one tissue to another. Taken together, these data suggest that *B. pseudomallei* spread from the lung to the liver is a prominent dissemination path, which occurs as an early event resulting in reduced selective pressure in the liver.

4.2.3 *Burkholderia pseudomallei* early hepatic dissemination

To characterize the kinetics of disseminated spread from the lung, a time course analysis was conducted. Groups of three C57BL/6J female albino mice with $10^{4.62}$ CFU, isolated lungs, liver and spleen at 6, 12 and 24 hours post infection and enumerated bacterial numbers from each organ. Transposon mutants were cultured from the lungs with higher numbers than the original instilled amount by 6 hours, and grew exponentially throughout the course of infection (Figure 13), consistent with growth patterns observed by optical diagnostic imaging (Figure 11A). At 6 hours post infection, transposon mutants were also present in the liver at similar numbers to those found in the lungs (Figure 13), confirming the findings of the Tn-seq data that hepatic spread is early and at high titer. Colonization of the spleen was detected by 12 hours post infection at or below the limit of detection (100 CFU), where pronounced splenic colonization occurred 24 hours post infection (Figure 13). This suggests that the enhanced loss of Tn-seq library diversity in the spleen relative to the lung is associated with later spread from the

lung, subsequent to the effects of selective pressure in the lung. Thus, *B. pseudomallei* colonize host lungs very early during infection and persist at this site through the onset of acute respiratory disease. Similarly, bacteria can spread from the lungs at high titers to colonize the host liver very early following infection but bacterial numbers at this site remain constant until late in infection. This finding corroborates a unique observation made from the Tn-seq data set, shedding new light on *B. pseudomallei* dissemination.

4.2.4 Identification of virulence determinants required for *Burkholderia pseudomallei* colonization of host lungs

We initially focused our analysis of the Tn-seq data set on identifying virulence determinants required by *B. pseudomallei* to colonize the lungs of mammalian hosts, of which 1455 genes were required to colonize the murine lung at a 3-fold relative abundance cutoff ratio relative to the input pool (Figure 12B). As a refined stringency to focus our identification of key virulence determinants, we made use of a targeted analysis of the capsular polysaccharide (CPS or CPS I [115]) biosynthetic cluster. We have previously demonstrated that a capsule mutant was attenuated 6.8-fold relative to the isogenic parent strain in the IMIT model, but that this level of attenuation was not statistically significant [78]. We therefore performed a detailed analysis of the Tn-seq lung results for the CPS I biosynthetic cluster as a benchmark genetic system, which exhibits a marginal level of attenuation by LD₅₀ analysis. We found that while the majority of CPS I genes were reduced in the lung relative to the input pool, pronounced variation in degree of response was observed across the genetic cluster (Figure 14). This variation was suggestive of bottlenecking effects, which are possible under the

parameters of the current study, which was designed for a biologically relevant infection while achieving saturating library coverage. While variation was observed across the CPS I locus, the locus itself exhibited an average 14.92-fold reduction in mutant prevalence for the lung versus input pool. Thus to further analyze the Tn-seq lung data set, we applied a more stringent fold-change cut off of 15-fold, reflecting the magnitude of the average fold gene reduction of the CPS I locus. Further, we decided to identify clusters of genes, which meet this 15-fold cutoff to mitigate the impact which bottlenecking might have on dataset variation at the individual gene level.

A total of 548 genes underwent selective pressure in the lung at a 15-fold cutoff relative to the input pool. These genes were heat mapped for nearest neighbor relationship (Figure 15) to identify genetic clusters with consecutive hits of no more than a 4-gene distance from the previous hit. The three genetic loci which provided the largest assemblage of genes meeting these criteria included: i) CPS I (8 genes), ii) Type 6 Secretion System cluster 5 (T6SS5; 8 genes), and iii) Type 3 Secretion System cluster 3 (T3SS3; 7+5 genes) (Table 2). The T6SS5 is identified as cluster 5 by the NCBI database [69], and this same cluster is identified as cluster 1 in *Burkholderia mallei* [116]. Numerous additional small genetic clusters may provide important contributions to the fitness of *B. pseudomallei* in the lung. However, these data indicate that the three prominent genetic systems contributing to *B. pseudomallei* lung pathogenesis are CPS I, T3SS3 and T6SS5. Given that we have previously characterized the contribution of CPS I and T3SS3 to respiratory melioidosis using the IMIT model [78], we decided to address the impact of the T6SS5 system on *B. pseudomallei* virulence.

Only a single gene met the 15-fold cutoff criterion in the liver (thioredoxin: -16.2-fold reduced), suggesting that the liver does not offer a strong selective pressure against *B. pseudomallei* relative to that of the lung. Conversely, 2255 genes met this more stringent 15-fold cutoff criterion in the spleen, thus this criterion did not effectively reduce the number of hits in the spleen from the 2862 hits at a 3-fold cutoff criterion. Due to the late spread to the spleen and the large number of gene hits, we interpret that the colonization of the spleen in this current model system is a bottle-necked event that does not facilitate a biologically relevant data interpretation. This study therefore focused on validating the results from the lung dataset, specifically the identification of capsule, T3SS3 and T6SS5 as the largest genetic loci contributing to respiratory melioidosis.

4.2.5 T6SS5 mutant is not attenuated in the IMIT model

We previously calculated the LD₅₀ of a *B. pseudomallei* luminescent strain JW280 to be 10^{3.87} CFU, a T3SS3 translocation-deficient mutant, JW280 Δ *sctU_{Bp3}* to be 10^{6.19} CFU and a CPS I operon mutant to be 10^{4.57} [78]. While CPS I, T3SS3, and T6SS5 all contributed to *B. pseudomallei* pulmonary fitness by the Tn-seq screen, single strain challenge with a CPS mutant did not reveal an attenuation by LD₅₀, whereas a T3SS3 mutant was significantly attenuated >200-fold [78]. We therefore challenged C57BL/6J albino female mice with 10^{3.95} CFU of the JW280 luminescent strain and 10^{4.25} CFU of the JW280 Δ *tssC-5* luminescent T6SS5 mutant strain to investigate the role of T6SS5 in respiratory melioidosis. Infection with the parent JW280 strain close to its LD₅₀ resulted in 67% mortality (Figure 16A), whereas infection with the luminescent T6SS5 mutant

was 100% lethal with the $10^{4.25}$ CFU dose, which is 0.52-log above the parent LD_{50} . Thus, the LD_{50} of the *tssC-5* mutant is $<10^{4.25}$ CFU, which was not significantly attenuated by Log-rank survival analysis relative to the parent control (Figure 16A). Therefore, like the CPS mutant, the T6SS5 mutant is not attenuated in a single strain respiratory model challenge. Optical diagnostic imaging was used to monitor bacterial proliferation in the lung of lethally infected mice and by 19 hours post infection both the parent and the T6SS5 mutant were detectable by bioluminescent imaging. However the bioluminescent signal intensity increased at similar rates in the thoracic cavity (Figure 16B). While the T6SS5 mutant appeared to be slightly less fit than parent strain in proliferation rate, this difference was not significant. We characterized the bacterial tissue burden in moribund mice and found no significant difference between the T6SS5 and parent bacterial numbers in the lungs, liver and spleen (Figure 16C-D). Thus, although our Tn-Seq analysis revealed that the T6SS5 cluster is required for the full fitness of *B. pseudomallei* in the lung, single strain pulmonary challenge studies did not support this role for T6SS5.

4.2.6 A *Burkholderia pseudomallei* T6SS5 mutant is attenuated in competition studies

Given that Tn-Seq is a genome-wide competition study, and initial validation of our Tn-Seq results using traditional LD_{50} estimations did not identify attenuation for the *tssC-5* mutant, we decided to investigate whether this T6SS5 mutant is attenuated by direct competition studies. We generated a novel gentamicin-marked $P_{tolC}luxCDABE$ bioluminescence reporter strain, MGBP001, which we also generated for the CPS I,

T3SS3 and T6SS5 mutants and used these in competition studies against gentamicin-sensitive, non-luminescent, DD503. Accordingly, four groups of three C57BL/6J albino female mice were inoculated with $\sim 10^{4.0}$ *B. pseudomallei* at a 1:1 ratio of DD503 combined with either: i) MGBP001, ii) MGBP001 Δwcb (CPS I-), iii) MGBP001 $\Delta sctU_{Bp3}$ (T3SS3-), or iv) MGBP001 $\Delta tssC-5$ (T6SS5-). Infections persisted for 67 hr (late stage disease) before lungs, liver and spleen were collected and homogenates differentially plated on agar to identify proportions of gentamicin resistant and sensitive strains. The MGBP001 parent strain exhibited a competition index which was not significantly different from a ratio of 1.0 (Figure 17A), indicating that DD503 and MGBP001 shared the same virulence potential in all tissues, suggesting that neither the luminescence operon nor gentamicin resistance impact the virulence of *B. pseudomallei*. Interestingly, all three mutant strains exhibited significantly reduced competition indices in the lungs, liver and spleen of mice relative to the non-luminescent DD503 competition partner (Figure 17A). Furthermore, optical diagnostic imaging of the thoracic cavity demonstrated that the parent MGBP001 strain proliferated within the lung (Figure 17B), consistent with the pulmonary colonization observed by the JW280 strain [78]. Imaging was able to successfully monitor the decreased fitness of the three mutants in the lung during the course of infection (Figure 17B), with significant differences in bioluminescence for all but the capsule mutant by 39 hr, and for all strains by 50 hr, indicating that optical diagnostic imaging can be used to monitor fitness defects *in vivo* during competition studies. Therefore, CPS I, T3SS3, and T6SS5 are all critical virulence determinants to support the fitness of *B. pseudomallei* in the lung, but importantly, attenuation of these virulence systems by single strain challenge studies has

only been able to identify a role for T3SS3. We propose that competition analyses, including Tn-seq, provide a higher resolution assay by which to assess the role of *B. pseudomallei* virulence determinants in the lung, and that our current Tn-seq screen successfully identified CPS I, T3SS3 and T6SS5 as the largest genetic loci required to facilitate respiratory melioidosis.

4.3 Discussion

In this study, we performed Tn-seq analysis to identify virulence determinants required to cause respiratory disease in a mouse model of lung-specific melioidosis. The primary design criteria of our screen were achieving the balance of saturating transposon mutagenesis while also limiting the challenge dose to allow for a biologically relevant disease progression. Previous transposon-directed insertion site sequencing and Tn-seq libraries have been generated in the *Burkholderia pseudomallei* strain K96243 [33] and its close relative *Burkholderia thailandensis* [111, 112] to identify essential genes required for survival of these pathogens *in vitro*. Importantly, these *in vitro* screens allowed for much larger library sizes to accurately identify essential genes which were not amenable to transposon mutagenesis, which for *B. pseudomallei* was estimated to be 8.0% of the genome [33]. In spite of limiting library size in our study to allow for infection studies, we achieved coverage of 88% of the genome, where the theoretical maximum coverage is 92% based on estimates of number for essential genes. Thus, we achieved near saturating coverage of the genome while still challenging mice with <10 LD₅₀s of bacteria.

An unexpected result of our Tn-seq dataset was the revelation that *B. pseudomallei* is capable of reaching the liver very early in the course of infection, which was subsequently validated by a time course infection study. These findings were facilitated by using IMIT instillation which has been reported to efficiently deliver ~98% of an instilled dose directly into the lung [77]. Within 6 hrs of delivery directly into the lung by IMIT instillation, *B. pseudomallei* not only replicates in the lung, but also spreads to the liver at numbers similar to that cultured from the lung. Interestingly, few genes were critical for *B. pseudomallei* to maintain a presence in the liver, relative to the lung, suggesting that the lung does not persistently seed the liver over the course of infection, nor is the liver a source of a strong selective pressure to *B. pseudomallei*. Furthermore, *B. pseudomallei* does not appear to replicate in the liver until late in the infection, suggesting that the systemic fitness of the host may impact the replication potential of *B. pseudomallei* in the liver, again given that Tn-seq results do not support the possibility that the late infection increase in hepatic burden results from spread from the lung. It is noteworthy that in other respiratory models, the liver becomes colonized at later time points; for instance, aerosol delivery of *B. pseudomallei* did not result in detection of bacteria in the liver until 3 days post infection [117]. Thus, the observation of rapid dissemination from the lung to the liver may be a unique feature of the IMIT model, as is the prominent moribund septicemia, which is not observed in other respiratory melioidosis models. Future work will be required to understand the role of the liver as a replicative niche for *B. pseudomallei* during respiratory melioidosis.

We developed a high specificity filter to prioritize follow-up analysis of the Tn-seq results of the lung. The selection criteria was benchmarked to the capsule

polysaccharide genetic locus which we previously demonstrated was not a critical virulence determinant in the IMIT model of respiratory melioidosis, yet was attenuated 6.8-fold relative to parent [78]. Thus, our criteria were chosen to capture all virulence systems, including those that may not be significantly required by LD₅₀ analysis. Our screen identified 548 genes, 8.7% of the genome's predicted open reading frames (ORFs), to be required by the bacterium for mammalian lung colonization, and of these, 32% (175 ORFs) accounted for hypothetical proteins, suggesting that additional novel virulence systems may participate in mediating fitness within the mammalian lung. Using cluster analysis to further prioritize the Tn-seq data set, we identified the three dominant genetic loci contributing to respiratory melioidosis as CPS I, T3SS3 and T6SS5. Interestingly, these systems have been previously identified as virulence systems in systemic animal models [19, 61, 70]; however, other virulence determinants described as important in systemic disease models did not meet our selection criteria, including the lipopolysaccharide (LPS) biosynthetic locus which had just two genes meeting our 15-fold selection criterion. Thus, virulence determinants required to support systemic infection might not be the same as those required in the lung. Our Tn-seq analysis was notably biased to the identification of large genetic systems, which contribute to respiratory melioidosis, and it is therefore likely that additional genetic loci have also been identified by this Tn-seq dataset, which will be the subject of future investigation.

Most *B. pseudomallei* virulence factors have been characterized primarily in systemic infection models, including intravenous, subcutaneous, and intraperitoneal inoculation. Indeed, the three major virulence systems targeted from our Tn-seq screen have been well studied as major contributors to disease in hamster and mouse systemic

intraperitoneal infection models. The capsular polysaccharide has been characterized by several groups as providing one of the most significant contributions to the systemic disease potential of *B. pseudomallei*, with capsule mutants being attenuated approximately 5-log in these infection models [59, 62]. The significant role for capsule in *B. pseudomallei* systemic disease is consistent with a demonstrated role of this virulence factor in resisting complement opsonization of the bacteria [59], and therefore likely a critical virulence factor for traffic between tissues, suggestive of *B. pseudomallei* spread as an extracellular pathogen. Interestingly, the capsule mutant does not appear to have a major role in the respiratory system of mice with attenuation levels of <2 log by intranasal delivery and <1 log by IMIT instillation [60, 78]. Importantly, the T3SS3 system is known to allow for escape of *B. pseudomallei* from phagosomes to facilitate rapid replication in the cytoplasm of phagocytes [38], and the ubiquitous requirement for T3SS3 in both systemic [19] and respiratory disease models [78] suggests that the intracellular lifestyle of *B. pseudomallei* is critical in all host tissues. Indeed, T3SS3 is the only virulence system examined thus far in the IMIT instillation method that exhibits significant attenuation by single strain challenge, suggesting that this virulence system is one of the most critical systems for both respiratory and systemic disease. The primary function of the T6SS5 system is not well described, though there is evidence that T6SS5 supports the intracellular lifestyle of *B. pseudomallei* and cell-to cell spread [118, 119]. T6SS5 system mutants are attenuated >3 log in a systemic hamster intraperitoneal model [118] and are attenuated ~2-3 log in intranasal murine models [119, 120]. In this current study, the role for T6SS5 in respiratory melioidosis using IMIT delivery does not appear to be a prominent role given that we were unable to demonstrate significant attenuation in

single strain challenge studies, which is in contrast to what has been previously reported for the intranasal models. We have previously demonstrated that intranasal inoculation of *B. pseudomallei* in mice results in a moribund disease state primarily associated with the nasal cavity rather than the systemic disease state observed following IMIT inoculation [78]. Thus, T6SS5 may be an important virulence factor for nasal cavity colonization, but does not play the same critical role in the lung as seen for the T3SS3 system.

A key finding of our studies was the ability of competition studies to provide a higher resolution identification of virulence factors in the fitness of *B. pseudomallei* in the lung than single strain challenges/LD₅₀ analyses. Similar findings have been made for other disease model systems, where competition indexes provide a higher resolution methodology for defining the contribution of virulence genes to a pathogen's fitness in animal model systems [121-123]. We had previously reported that a CPS I mutant was not significantly attenuated by LD₅₀ in the IMIT model [78], but presently that CPS I was significantly attenuated by competition study in the IMIT model. Similarly, we were unable to validate a significant attenuation for a T6SS5 mutant by single strain challenge, but identified a significant attenuation by competition index. The Tn-seq screen itself is a genome wide competition assay, thus our competition studies were able to successfully recapitulate the phenotypes we identified from the Tn-seq screen results. However, single strain challenges did not have the resolution to defined roles in respiratory melioidosis to either capsular polysaccharide or T6SS5. These observations indicate that competition studies have a higher resolution to ascribe roles in virulence to both CPS I and T6SS5 in respiratory melioidosis, and thus far, T3SS3 is the sole virulence

determinant which exhibits attenuation by LD₅₀ in the IMIT respiratory melioidosis model [78]. As an added feature of our competition assay, we have included a unique optical imaging approach which is further capable of detecting significant fitness defects in competition studies as early as 39 hrs post infection.

In summary, we provide the first phenotypic screen for *B. pseudomallei* virulence factor function in the mammalian lung, and have identified the largest critical genetic systems as CPS I, T3SS3 and T6SS5. While previously identified as virulence systems, this study represents the first comparative study to identify these as the primary genetic systems for respiratory melioidosis. These virulence systems therefore represent excellent targets for the future development of therapeutics against this Tier 1 Select Agent pathogen.

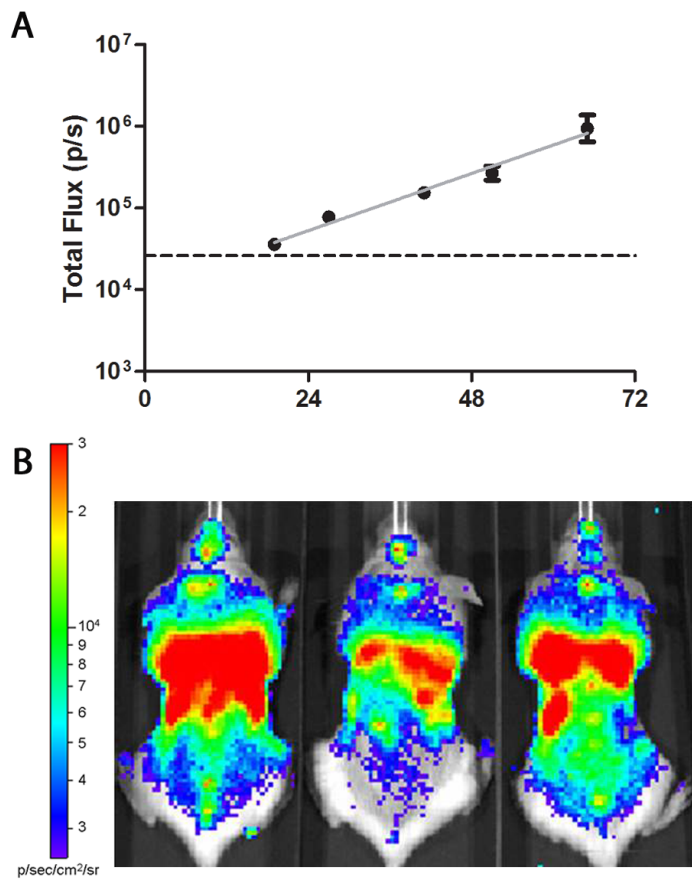


Figure 11. *In vivo* disease progression of *Burkholderia pseudomallei* Tn-seq

transposon library. (A) *In vivo* growth of the *B. pseudomallei* transposon library in the thoracic cavity of three C57BL/6J female albino mice infected by IMIT was monitored twice daily with an *in vivo* imaging system using luminescence as a read out for bacterial replication. Total luminescence was enumerated using a region of interest (ROI) centered on the thoracic cavity. The dashed line indicates technical 95% limit of detection. (B) Whole body imaging of moribund C57BL/6J mice infected with *B. pseudomallei* transposon library at 66 hours post infection. The logarithmic scale bar is provided for the standardized data presentation of 2.5×10^3 - 3×10^4 p/s/cm²/sr.

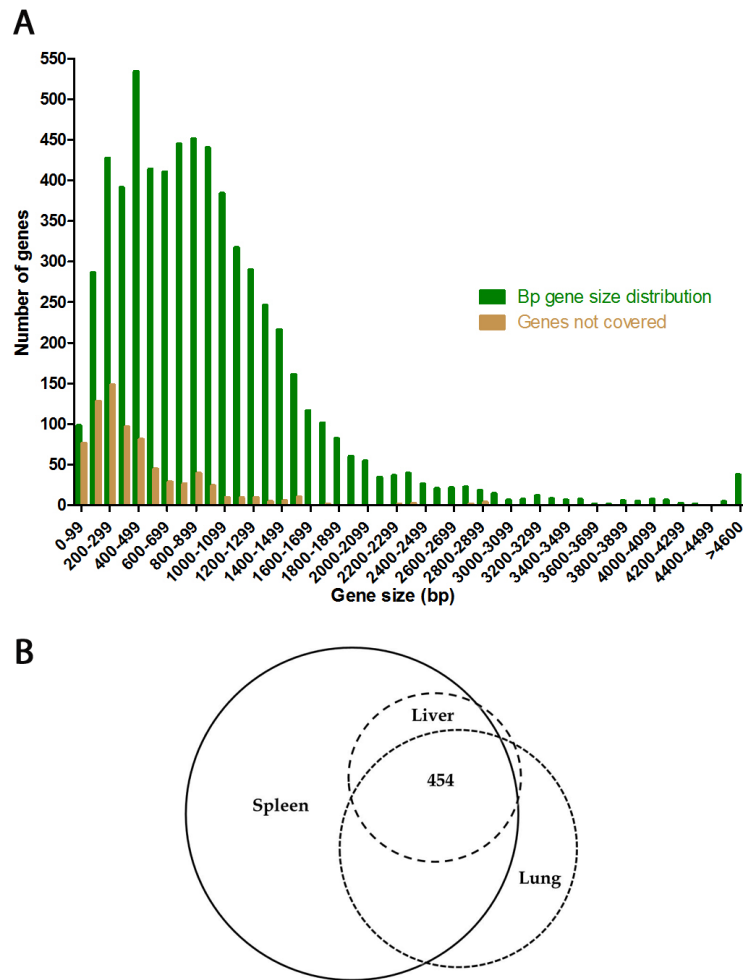


Figure 12. Gene size distribution of the *Burkholderia pseudomallei* genome and transposon insertion coverage. (A) Histogram of the *B. pseudomallei* genome (green bars) and percentage of genes lacking transposon insertions (brown bars), both binned at 100 bp gene size intervals. (B) Tn-seq data sets were analyzed for *B. pseudomallei* Tn-seq mutants lost by selective pressure in the lung (1455); liver (765); spleen (2862) at a 3-fold reduction in relative abundance relative to the input pool. Venn diagram illustrating mutants lost in the three tissues, with 454 genes being selected against in all three tissues.

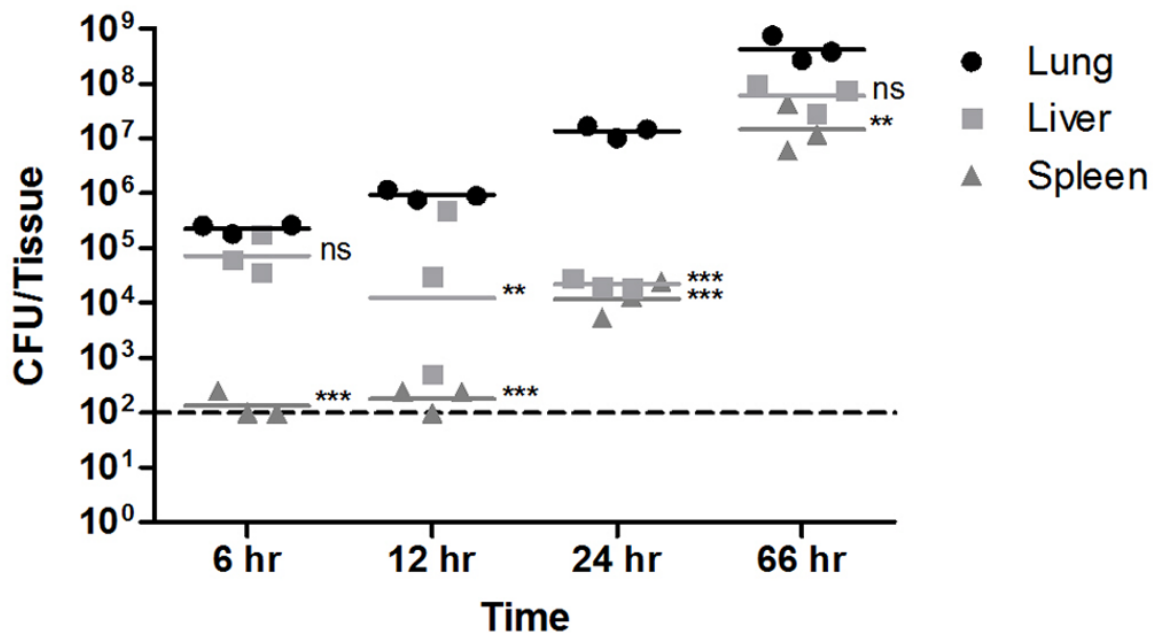


Figure 13. *Burkholderia pseudomallei* Tn-seq transposon library tissue burdens at key sites of infection. Groups of three C57BL/6 female albino mice infected with the *B. pseudomallei* Tn-seq transposon library were euthanized at 6, 12 and 24 hours post infection. Bacterial numbers in the lungs, liver and spleen were enumerated by plate counting and compared to bacterial numbers of moribund mice at 66 hours post infection from the initial Tn-seq transposon library challenge. A dashed line indicates the limit of detection of bacterial enumeration from host tissues. Tissue counts below the limit of detection were set to the limit of detection for statistical analysis. Statistical significance was calculated by Two-way ANOVA followed by Bonferroni post test (**, $P < 0.01$; ***, $P < 0.001$; ns, not significant).

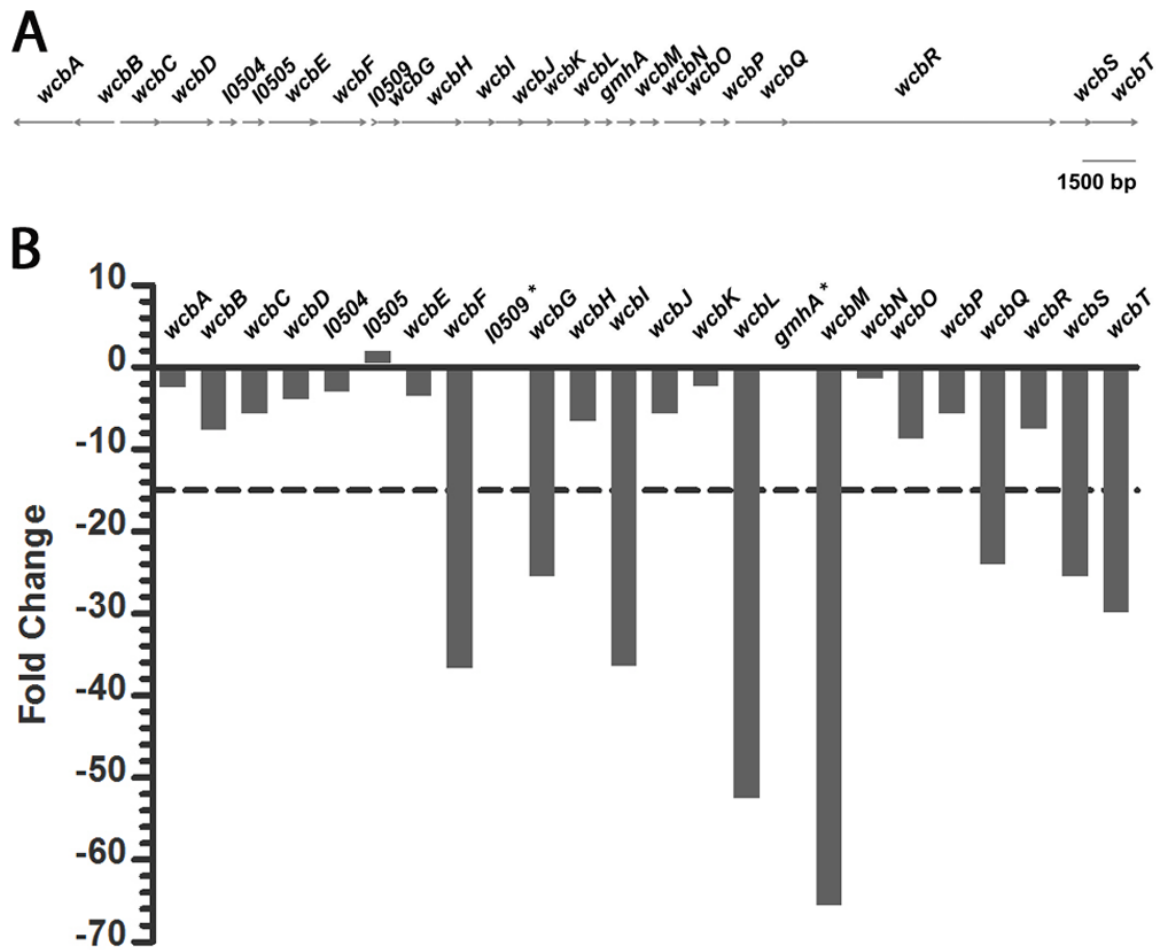


Figure 14. Analysis of variation within capsular polysaccharide I operon genes required for lung colonization by Tn-seq. (A) Scale representation of the capsular polysaccharide genetic locus. (B) Variation in fold-change of capsule genes by Tn-seq analysis of the lung data set relative to the input pool. The average fold reduction across all capsule genes was 14.92-fold (dashed horizontal line). * denotes genes not covered in the input library.

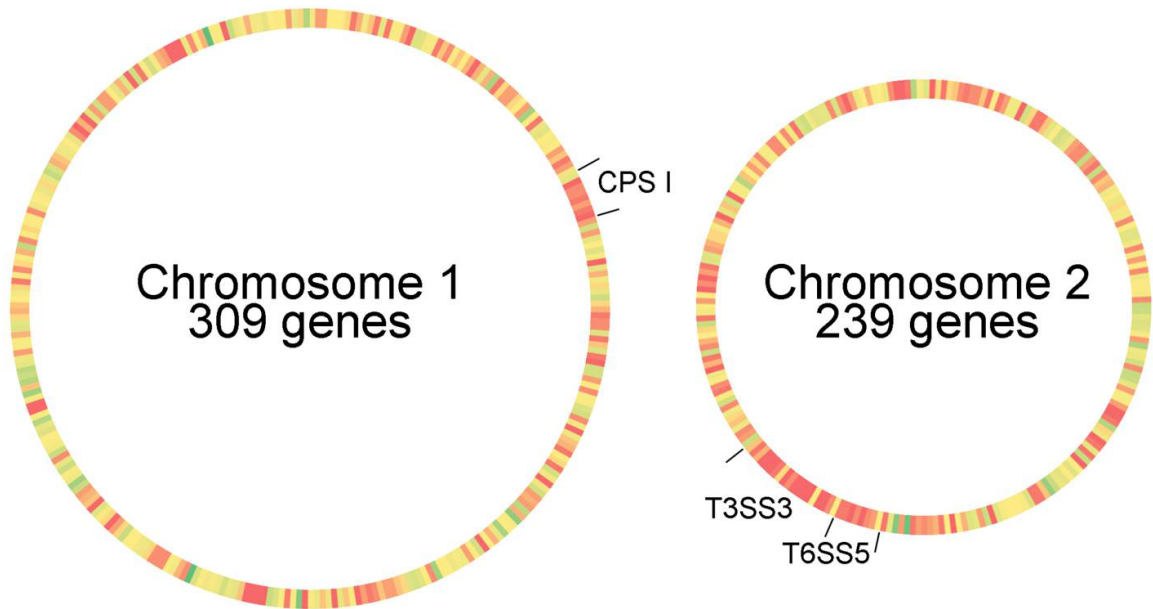


Figure 15. Proximity heat map of genes required for respiratory melioidosis. The Tn-seq lung data set was filtered for genes required by *B. pseudomallei* at a 15-fold reduction cut off relative to the input pool (548 genes). Genes were sorted for their arrangement on the two circular chromosomes of the *B. pseudomallei* genome, with similar distribution density found on the larger chromosome 1 (309 genes) and smaller chromosome 2 (239 genes). The heat map provides graphical cluster analysis of gene hits located in close proximity (red = 1 gene distance) or distal hits (green >70 gene neighbor distance). The three largest genetic clusters of hits separated by no more than 4 genes per hit are indicated: capsular polysaccharide (CPS I), Type 3 Secretion System cluster 3 (T3SS3), and Type 6 Secretion System cluster 5 (T6SS5).

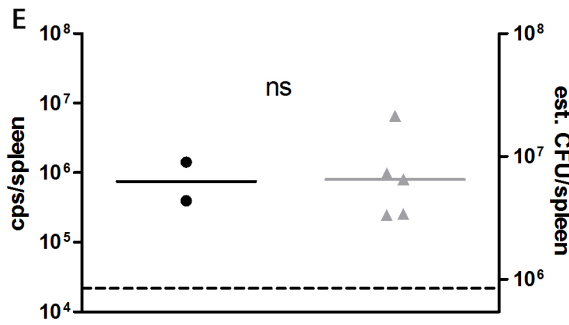
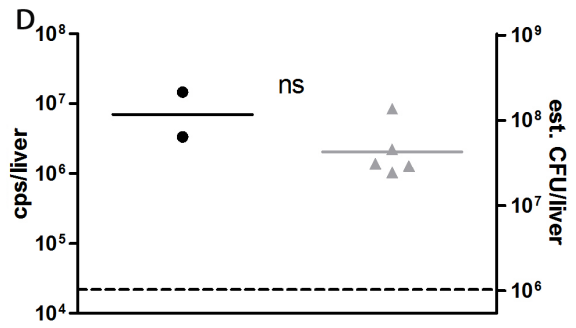
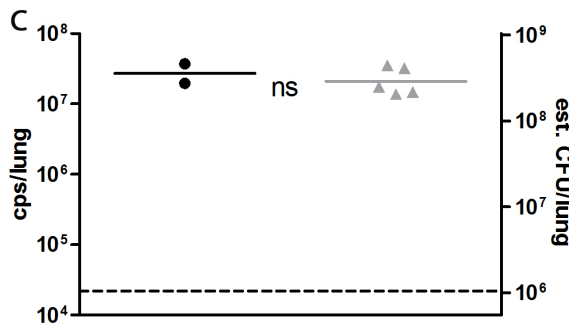
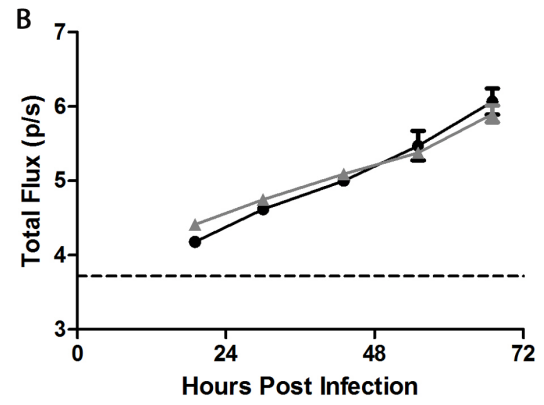
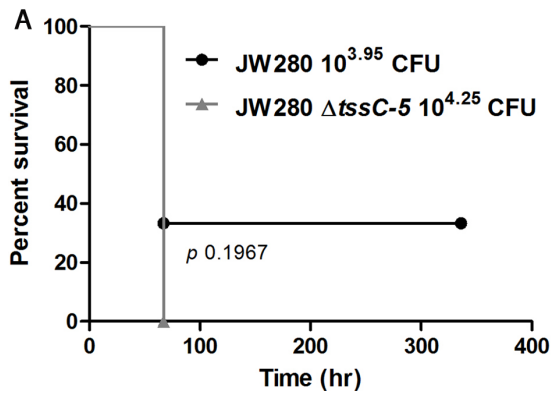


Figure 16. *In vivo* characterization of a T6SS mutant. (A) Survival curve of C57BL/6 female albino mice by IMIT infected with either JW280 or JW280 $\Delta tssC-5$. (B) *In vivo* growth of *B. pseudomallei* strains JW280 and JW280 $\Delta tssC-5$ infecting C57BL/6 mice, where bioluminescence was monitored twice per day and thoracic cavity total flux (p/s) was collected from region of interest measurements. A horizontal dashed line indicates the technical 95% limit of detection. Bacterial numbers in the lungs (C), liver (D) and spleen (E) of C57BL/6 mice infected with either JW280 or JW280 $\Delta tssC-5$ were enumerated by bioluminescence measurements of *ex vivo* tissues, as described [77]. Statistical significance was calculated using the Student's T test (ns: not significant).

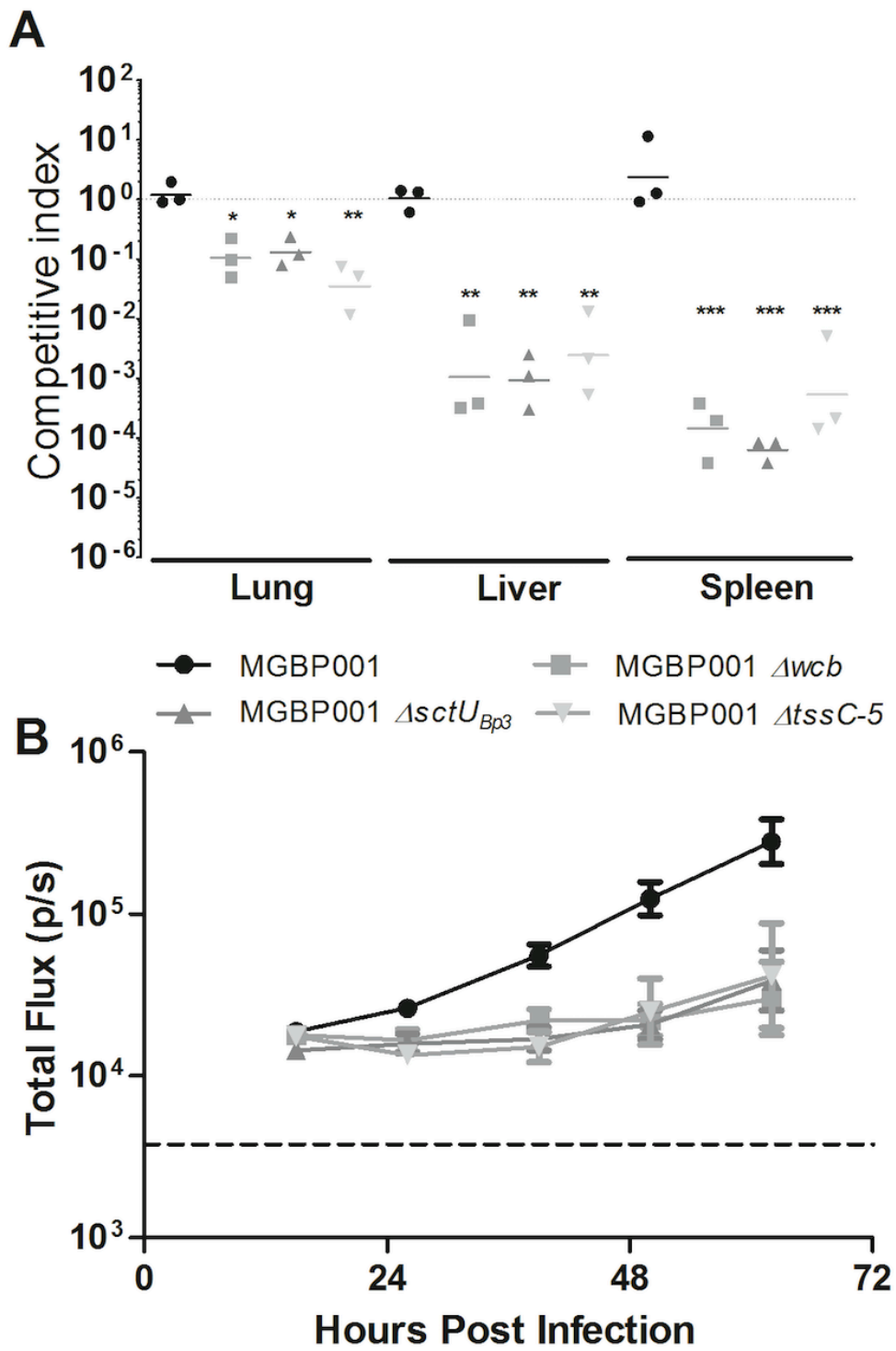


Figure 17. *Burkholderia pseudomallei* major virulence determinants are attenuated in competition assays. (A) Competitive index of luminescent, Gm-marked parent strain (MGBP001), capsular polysaccharide deletion mutant (MGBP001 Δwcb), T3SS3 (MGBP001 $\Delta sctU_{Bp3}$) and T6SS5 (MGBP001 $\Delta tssC-5$) mutants compared to Gm-sensitive, non-luminescent strain, DD503. Competitive index was calculated as the output ratio of mutant to parent divided by the input ratio of mutant to parent, having differentially plated lung, liver and spleen homogenates on agar plates with or without gentamicin selection. The horizontal dashed line indicates a competitive index of 1. Statistical significance was calculated using One-way ANOVA followed by Tukey's Multiple Comparison Test (*, $P < 0.01$; **, $P < 0.001$; ***, $P < 0.0001$). (B) *In vivo* growth of MGBP001, MGBP001 Δwcb , MGBP001 $\Delta sctU_{Bp3}$ and MGBP001 $\Delta tssC-5$ in the lungs was monitored twice daily using luminescence as a read out for bacterial replication, and total flux (p/s) measurements collected from regions of interest centered on the thoracic cavity. The horizontal dashed line indicates the 95% technical limit of detection.

Table 3. Identification of prominent genetic loci required for pulmonary disease.

Feature ID	Fold change	Distance to previous hit	Feature ID	Fold change	Distance to previous hit
T3SS3			T6SS5		
<i>bprA</i>	-70.3781		BP1026B_I11587	-83.2298	
<i>bipC</i>	-35.0191	1	hcp-5	-367.19	4
<i>bipB</i>	-15.6668	1	tssF-5	-22.3609	3
<i>bicA</i>	-15.2996	1	clpV-5	-23.6294	1
<i>bsaZ</i>	-56.991	1	tagB-5	-21.4194	3
<i>spaP</i>	-15.6396	3	tagC-5	-22.6434	1
<i>bsaV</i>	-26.665	1	tssK-5	-31.7466	2
<i>bsaO</i>	-82.8959	7	tssL-5	-111.177	2
BP1026B_I11643	-34.0416	2	Capsule		
BP1026B_I11644	-59.6684	1	wcbF	-36.6525	
BP1026B_I11645	-40.3909	1	wcbG	-25.4066	2
BP1026B_I11646	-33.6591	1	wcbI	-36.413	3
			wcbL	-52.5586	3
			wcbM	-65.6182	2
			wcbQ	-24.1121	4
			wcbS	-25.4738	2
			wcbT	-29.8059	1

CHAPTER V

TYPE 3 SECRETION SYSTEM CLUSTER 3 EFFECTORS MEDIATE *BURKHOLDERIA PSEUDOMALLEI*'S RAPID ESCAPE FROM HOST CELL PHAGOSOMES

5.1 Introduction

The type 3 secretion system (T3SS) is a needle-like apparatus that translocates effector proteins across both Gram-negative bacterial membranes into the cytoplasm of host cells [42, 43]. T3SS translocated effectors from several Gram-negative bacteria such as *S. flexneri* [124], *S. enterica* [125] and *P. aeruginosa* [126], interact with host cell proteins to subvert the cell's signaling pathways facilitating bacterial survival within this intracellular niche. In its genome, *B. pseudomallei* encodes for 3 T3SS loci [45, 46], yet cluster 3 (T3SS3) is the only cluster that plays an important role in the intracellular life cycle of the bacterium in mammalian cells, specifically by promoting vacuolar escape from endocytic vesicles [36] and overall intracellular fitness of the bacterium [38, 127].

B. pseudomallei like many other cytosolic pathogens, have evolved to rapidly escape from endocytic vesicles by using its T3SS, following internalization into host cells

[35]. Escape of the bacterium from the vacuolar compartment is a critical step for intracellular survival [38] and is estimated to take place within 3 hours of internalization [38]. However vacuole acidification occurs within 15 minutes of vacuole formation [128], suggesting that vacuolar escape occurs earlier, as is the case with *S. flexneri*, which escapes the vacuole in less than 10 minutes post internalization [129]. Once in the cytoplasm, *B. pseudomallei* establishes a replicative niche by manipulating host immune responses and signaling pathways to the bacterium's advantage through the concerted action of its T3SS3 translocated effectors [38]. Ultimately, *B. pseudomallei* lyses its host spreading to neighboring cells and continuing the cycle of infection (Figure 2) [35].

The contributions of *B. pseudomallei* T3SS3 effectors to vacuolar rupture of the bacterium are poorly understood, yet their concerted functions are critical for the bacterium's intracellular survival [36, 38, 48-50, 55, 56]. Putative *B. pseudomallei* T3SS3 translocated effectors (Table 4) include the *Burkholderia* outer proteins BopA, BopC and BopE and the *Burkholderia* secretion apparatus (Bsa) associated proteins BapA, BapB and BapC [38]. Of great significance is that the T3SS3 effector BopA is required for vacuolar rupture and rapid escape of *B. pseudomallei* from endocytic vacuoles, as *bopA* mutants exhibit delayed vacuolar escape from phagosomes, leading to decreased intracellular survival in RAW264.7 macrophages [36]. Other than BopA, no role in vacuolar escape has been attributed to any other T3SS3 protein effectors. BopC and BopE may play a role in invasion of non-phagocytic cells, as inactivation of both effectors has been associated with a significant reduction in invasion of non-phagocytes [48, 56]. A role of BopE in invasion of non-phagocytic cells as a guanine nucleotide exchange factor (GEF) is consistent with the roles of its *Salmonella* T3SS orthologues

SopE and SopE2, which act as GEFs for the Rho GTPases Cdc42 and Rac1, facilitating invasion of host cells through actin network rearrangements [130]. Yet, activity of BopE for these GTPases is much lower than that of SopE or SopE2 and notably *B.*

pseudomallei is only weakly invasive, suggesting that BopE may target other host GTPases involved in distinct signaling pathways. Both BapA and BapC are secreted *in vitro* in a T3SS3-dependent manner, but their effector functions during infection of host cells remain elusive [55]. While, BopA is the only T3SS3 effector protein that appears to directly contribute to *B. pseudomallei* vacuolar escape, escape of a *bopA* mutant is only delayed and not completely abrogated to levels of secretion-defective mutants, strongly suggesting that other T3SS3 effectors may also be involved in mediating the efficient escape of *B. pseudomallei* from phagosomes [36, 38].

We hypothesize that additional *B. pseudomallei* type 3 secretion effectors may possess distinct and complementary functions resulting in the bacterium's rapid escape from host cell endocytic vacuoles and full virulence in host cells. Yet, the contributions of *B. pseudomallei* T3SS3 effectors to vacuolar rupture remain elusive, yet their concerted functions are critical for the bacterium's intracellular fitness [36, 38, 48-50, 55, 56]. Accordingly, herein we assess the growth kinetics of the *B. pseudomallei* T3SS3 effector mutants *bopA*, *bopC*, *bopE*, *bapA* and *bapC* in cultured macrophages to investigate their impact on intracellular survival of the bacterium. We demonstrate that the five profiled effectors facilitate full virulence of *B. pseudomallei* in cultured macrophages. Finally, we investigate the role of a host cell protein with functions in vesicular trafficking, which is potentially targeted for BopA activity, and propose a

mechanism by which BopA interaction with this host factor results in the rapid escape of *B. pseudomallei* to the cytoplasm of host cells.

5.2 Results

5.2.1 Real-time growth kinetics of bioluminescent *Burkholderia pseudomallei* in cultured macrophages

We developed a high-sensitivity assay to assess the fitness of intracellular *B. pseudomallei* in cultured macrophages. We used the bioluminescent *B. pseudomallei* parental strain JW280, which contains a chromosomal insertion of the *Photorhabdus luminescens luxCDABE* operon and exhibits constitutive light production during *in vivo* and *in vitro* infections, allowing for the monitoring of bacterial numbers during intracellular replication [64]. To assess the fitness of intracellular *B. pseudomallei*, we infected J774A.1 cultured macrophages with JW280 and monitored the progression of infection for ~14 hours. Macrophages were infected at multiplicities of infection (MOI) of 5, 2, 0.5 and 0.2 in a 96-well plate format with gentamicin added to the culture media at 1-hour post infection and maintained throughout the assay. Using *in vivo* optical diagnostic imaging, we observed killing of the *B. pseudomallei* parental strain very early in infection following addition of gentamicin to the culture medium, suggestive of killing of extracellular bacteria. This early loss of bioluminescence was immediately followed by a logarithmic growth phase, which peaked between 8.5 hours to >13 hours depending on the MOI. Following the peak in bioluminescence, we observed a marked decrease in bacterial bioluminescence, suggestive of macrophage cell death resulting in exposure of bacteria to the gentamicin maintained in the culture media (Figure 18). These findings

are consistent with previous results that showed corresponding growth patterns of non-luminescent [38, 127] and luminescent [64] *B. pseudomallei* parental strains.

Accordingly, we demonstrate that by using *in vivo* optical diagnostic imaging we can accurately track the progression of bioluminescent *B. pseudomallei* infection in host cells in real-time at very high resolution, and that this approach is amenable for use to study the progression of infection of distinct *B. pseudomallei* bioluminescent strains.

5.2.2 A bioluminescent T3SS3 structural mutant exhibits a significant fitness defect during infection of host cells

The *B. pseudomallei* type 3 secretion system structural mutant *sctU* (*bsaZ*) is incapable of intracellular replication in cultured macrophages due to its impaired ability to escape from endocytic vesicles in these cells prior to 12 hours post infection [38, 60]. Accordingly, we assessed whether the bioluminescent T3SS3 structural mutant JW280 Δ *sctU*_{Bp3}, was similarly defective in intracellular replication as measured by bioluminescence. We infected J774A.1 cultured macrophages with the parental strain JW280 or JW280 Δ *sctU*_{Bp3} at an MOI of ~3 in a 96-well plate format for ~14 hours using a gentamicin protection assay. Gentamicin was added to the culture media in each well at 1 hr post infection and maintained throughout the duration of the experiment. As expected, the growth kinetics of the parental strain showed an initial period of bacterial loss succeeded by a logarithmic growth-phase that peaked and quickly decreased, suggestive of macrophage cell death resulting in exposure of bacteria to antibiotic in the culture media. Inactivation of the structural component *sctU* in the T3SS3 apparatus resulted in minimal intracellular replication of the mutant strain in J774A.1 macrophages

prior to 12 hours post infection (Figure 19), as previously reported [38, 127]. This reduction in intracellular replication of JW280 $\Delta sctU_{Bp3}$ is consistent with the mutant's inability to escape from macrophage phagosomes, as previously described [60]. However, the *sctU* mutant is capable of minimal intracellular replication after 12 hours post infection, suggestive of delayed vacuolar escape, consistent with previous observations, which demonstrated that a *sctU* mutant is capable of escaping endocytic vesicles and replicating in the cytoplasm of cultured macrophages after 12 hours post infection [127]. Accordingly, this study confirms prior findings that demonstrate that a functional T3SS3 apparatus is critically required for the intracellular fitness of *B. pseudomallei* in cultured macrophages. Most importantly, these results validate that *in vivo* optical diagnostic imaging is capable of distinguishing phenotypic differences in intracellular bacterial viability as a non-invasive approach to study intracellular fitness of *B. pseudomallei* and other intracellular pathogens.

5.2.3 T3SS3 effector proteins are required for full virulence of *Burkholderia pseudomallei* in host cells

Full virulence of *B. pseudomallei* during infection of host cells is dependent on the functions of the T3SS3 effector proteins [36, 48, 55, 56]. Notably, inactivation of the T3SS3 effector gene *bopA* results in delayed escape of *B. pseudomallei* from phagosomes of RAW264.7 macrophages, observed by transmission electron microscopy, demonstrating that BopA is critical for the bacterium's rapid vacuolar escape and intracellular fitness in cultured macrophages [36]. In order to assess the contributions of other Bop and Bap proteins to the intracellular fitness of *B. pseudomallei*, we infected

J774A.1 macrophages with the bioluminescent *B. pseudomallei* parental strain JW280 or the bioluminescent T3SS3 effector mutants *bopA*, *bopC*, *bopE*, *bapA* and *bapC* at matched multiplicities of infection in a 96-well format. Infections were allowed to proceed for ~14 hours, gentamicin was added to the culture media 1 hr post infection and maintained throughout the duration of the assay. The growth kinetics of the parental strain did not differ from the previously observed growth patterns (Figures 20 and 21). An initial period of bacterial loss followed by a logarithmic growth phase and a marked decrease in bacterial viability, as bacteria were exposed to gentamicin in the culture media as a result of cell death. We monitored the growth profiles of the T3SS3 effector-mutants *bapA* and *bapC* in cultured macrophages and noticed that both mutants displayed intracellular fitness defects when compared to the parental strain (Figure 20). Bacterial numbers for the *bapA* and *bapC* mutants only reached ~87% and ~78% of the parental strain intracellular numbers at the peak of their growth phase, respectively (Figure 20). In a similar manner, inactivation of *bopA*, *bopC* and *bopE* resulted in intracellular fitness defects when compared to the parental strain (Figure 21). Bacterial numbers for the *bopA*, *bopC* and *bopE* mutants only reached ~70%, ~89% and ~80% of the parental strain intracellular numbers at the peak of their growth phase, respectively (Figure 21). These results strongly suggest that all the T3SS3 effector proteins contribute to the intracellular fitness of *B. pseudomallei* in cultured macrophages. Notably, the growth profiles of the five T3SS3 effector mutants showed that inactivation of *bopA*, *bopE* or *bapC* resulted in the most pronounced fitness defects (Figures 20 and 21). BopA specifically has been shown to be involved in vacuolar escape [36], therefore this effector is important for

intracellular fitness of *B. pseudomallei* by potentially directly mediating vacuolar rupture during infection of host cells.

5.2.4 BopA exhibits delayed vacuolar escape in cultured macrophages

Previous observations through transmission electron microscopy demonstrated that inactivation of *bopA* results in delayed escape of *B. pseudomallei* from endocytic vesicles from cultured macrophages [36]. We showed that inactivation of *bopA* results in a significant defect in intracellular survival of *B. pseudomallei* in cultured macrophages. Accordingly, we aimed to validate the role of the *B. pseudomallei* T3SS3 effector BopA in vacuolar escape in host cells by determining the subcellular distribution of a *bopA* mutant strain early in infection. In this assay, we used the *B. pseudomallei* acapsular JW270 strain, which is internalized by macrophages at comparable levels to those of the parental strain, is capable of replicating at equivalent numbers to those of the parental strain by ~8 hours post infection [60, 64] and has been validated for intracellular survival assays at Biosafety Level 2 containment [131]. We infected RAW264.7 macrophages with JW270-GFP (MGBP002), or with isogenic *bopA* and *sctU_{Bp3}* mutants, MGBP002 Δ *bopA* and MGBP002 Δ *sctU_{Bp3}*, respectively. RAW264.7 cells were seeded on glass coverslips for later visualization by confocal microscopy. The infection was conducted in a 24-well format for 2 hours, gentamicin was added to the media culture at 1 hour-post infection and maintained through the duration of the experiment. Extracellular bacteria were labeled after infection, followed by selective permeabilization of the cells' plasma membrane with digitonin to label cytoplasmic bacteria and differential antibody staining was assessed by confocal microscopy to quantify subcellular *B. pseudomallei* strains. We

observed that ~40% of the parental strain MGBP002 was present in the cytoplasm of host macrophages at 2 hours post infection (Figure 22), consistent with previous estimations, showing that ~39% of wild type *B. pseudomallei* was found in the cytoplasm of RAW264.7 macrophages at 2 hours post infection [36]. As expected, MGBP002 Δ sctU_{Bp3} displayed a significant delay in escape when compared to the parental strain, ~20% less cytoplasmic numbers than that of the parental strain. This is consistent with previous reports demonstrating that a T3SS3 structural mutant exhibits significant delay in escape from RAW264.7 phagosomes [36]. Intracellular numbers of MGBP002 Δ bopA were comparable to those observed for the MGBP002 Δ sctU_{Bp3} structural mutant and remained trapped at significantly higher levels relative to the parental strain in endocytic vacuoles of RAW264.7 macrophages at 2 hours post infection (Figure 22). This is also consistent with reduced numbers of the *bopA* mutant when compared to the parental strain at later times in infected J774A.1 macrophages observed by optical diagnostic imaging, likely due to delayed escape from endocytic vesicles (Figure 18) as previously reported by Gong et al. [36]. Taken together these results demonstrate that the T3SS3 effector protein BopA directly contributes to the rapid escape of *B. pseudomallei* from host cell endocytic vesicles.

5.2.5 BopA is associated with punctate structures in the cytoplasm of host cells

We focused on elucidating the location of BopA in HEK293 cells as inactivation of *bopA* resulted in delayed vacuolar escape in host cells. A recent report of a yeast-two hybrid screen of *B. mallei* virulence proteins associated with specialized secretion systems, identified the host transport protein particle C8 (TRAPPC8) as a potential BopA

interaction partner [132]. TRAPPC8 is the mammalian orthologue of the recently identified Trs85 subunit of the yeast TRAPPIII complex, which has been implicated in mediating membrane expansion in macroautophagy and the cytoplasm to vesicle pathway [133]. Accordingly, TRAPPC8 may represent a target for BopA due to its role in intracellular vesicular trafficking. We therefore hypothesized that BopA may localize to distinct structures dispersed in the cytoplasm of host cells. To investigate the subcellular location of BopA in host cells, we generated a FLAG-tagged BopA fusion protein and transiently expressed this protein in HEK293 cells for 24 hours. Transient transfection of the BopA-FLAG fusion protein showed that BopA was associated with punctate structures localized to the cytoplasm of HEK293 cells (Figure 23). Accordingly, localization of BopA to puncta in the cytoplasm of host cells supports a potential interaction between this effector and vesicle-associated TRAPPC8, which localizes to both vacuolar and plasma membranes [134].

5.2.6 Contribution of host transport protein particle C8 to stabilizing the *Burkholderia*-containing vacuole during infection of host cells

TRAPPs are multi-subunit complexes with guanine nucleotide exchange factor activity involved in various vesicular trafficking processes [135]. Accordingly, we examined the role of TRAPPC8 during infection of RAW264.7 macrophages with the *B. pseudomallei* JW280 parental strain as BopA may directly interact with this host factor. We used siRNA to knockdown TRAPPC8 protein translation in RAW264.7 macrophages or we used non-specific scrambled siRNA as a negative control. Macrophages were treated with siRNA for 48 hours and were then infected with JW280 at an MOI of 10.

The assay was conducted in a 96-well format and *in vivo* optical diagnostic imaging was used to track the progression of infection for ~15 hours, using a gentamicin protection assay. Growth kinetics of *B. pseudomallei* in macrophages treated with scrambled siRNA exhibited the previously observed growth pattern (Figures 18 and 24), showing initial killing of bacteria by 4 hours post infection, followed by a phase of bacterial expansion and killing of the host cell by ~ 9 hours post infection (Figure 24).

Surprisingly, TRAPPC8 knockdown resulted in an early (~2 hours post infection) increase in bacterial numbers in infected macrophages, followed by a sharp decrease in numbers by 4 hours post infection, likely due to rapid loss of a viable niche for the bacteria resulting in exposure to gentamicin in the culture media (Figure 24). These results strongly suggest that absence of TRAPPC8 in host cells due to siRNA knockdown results in vacuolar destabilization, releasing *B. pseudomallei* to the cytoplasm of the cell to establish a replicative niche. These results also suggest that vacuolar destabilization through TRAPPC8 function inhibition may constitute a mechanism by which BopA promotes the rapid escape of *B. pseudomallei* from endocytic vesicles and ultimately intracellular survival of the bacterium in host cells.

5.3 Discussion

We used *in vivo* optical diagnostic imaging to study the growth kinetics and overall progression of *B. pseudomallei* infection in cultured macrophages. By using bioluminescent *B. pseudomallei* to infect these host cells, we are able to monitor the progression of disease noninvasively in a real-time, high-throughput manner and at very high resolution. This high-throughput screen confers great advantages when

investigating the impact of specific mutations or treatments on the fitness of diverse bacterial strains. Further, our approach facilitates the examination of the growth kinetics of distinct bacterial strains in different primary and cell culture models, at different multiplicities of infection and under diverse treatments such as siRNA knockdown or small compound libraries. Because the approach is noninvasive, observations on growth kinetics can be made at different time points during infection, minus sample vessel manipulation, which may reduce technical error across experimental samples. Notably, *B. pseudomallei* is classified as a Tier 1 Select Agent in the United States and this classification requires experimental use of the bacterium to be conducted under Biosafety Level 3 containment, so minimizing manipulation of infected samples maximizes user safety and reduces the utilization of laboratory resources such as personal protective equipment and other consumables.

In this study, we investigated the impact of T3SS3 effector proteins on the intracellular survival of *B. pseudomallei* in cultured macrophages and found that all effector mutants exhibited defects in intracellular fitness in these cells. These results strongly suggest that T3SS3 effectors act in concert to promote the bacterium's intracellular survival in host cells. Comparison of the intracellular fitness of the T3SS3 effector mutants *bopA*, *bopC*, *bopE*, *bapA* and *bapC* in cultured macrophages, demonstrated that BopA, BopE and BapC play prominent roles during *B. pseudomallei* infection that directly contribute to intracellular survival of the bacterium, and that other effectors may have supportive roles to also promote intracellular fitness. Yet, further studies are needed to validate the role of these effectors in primary cells. In addition, finding potential host cell protein targets for BopC, BopE, BapA and BapC would further

our understanding of *B. pseudomallei* pathogenesis and elucidate host proteins and pathways exploited by the bacterium to promote its own intracellular survival.

We focused on studying the role of BopA in facilitating *B. pseudomallei*'s escape from phagocytic vesicles, as *bopA* mutants exhibited the most profound defect in intracellular fitness of all the profiled effectors and this defect was previously demonstrated to be a result of delayed escape from host cell phagosomes [36]. The trafficking particle protein C8 (TRAPPC8) was identified as a potential host cell target for *B. mallei* BopA [132]. Importantly, TRAPPC8 function may facilitate vacuolar trafficking or fusion events important for *Burkholderia*-containing vacuoles in host cells, as siRNA knockdown of TRAPPC8 results in the rapid release of *B. pseudomallei* from vacuoles to the cytoplasm of infected host cells. TRAPPC8, an orthologue of the Trs85 subunit of the yeast TRAPP3 complex, is required for macroautophagy and for the cytoplasm to vacuole targeting pathway [136]. All three yeast TRAPP complexes regulate the Rab GTPase Ypt1, an orthologue of the mammalian GTPase RAB1, through their guanine nucleotide exchange factor domain [133] and are required for mediating initial tethering events between vesicles and their target membrane [137]. Limited data is available on the functions of mammalian TRAPP complexes and the attributed roles of these complexes in mammalian trafficking pathways are based on studies of orthologous yeast TRAPP complexes [133], although mammalian TRAPP complexes likely regulate vesicular trafficking through RAB proteins as well.

We explored the contribution of TRAPPC8 to *B. pseudomallei* fitness in cultured macrophages. Our results suggest that TRAPPC8 knockdown results in destabilization of vesicular membranes in RAW264.7 macrophages, as evidenced by the rapid increase in

B. pseudomallei intracellular numbers in these cells (Figure 24). Based on TRAPPIII functions in yeast, this also suggests that disruption of TRAPPC8 function in the vacuolar membrane of *Burkholderia*-containing vacuoles (BCVs) may inhibit tethering events of vesicles to BCVs, subsequent vesicle fusion and membrane expansions events leading to vacuolar destabilization. This is consistent with the role of the human papillomavirus L2 protein during infection of epithelial cells, which inhibits TRAPPC8 function in the Golgi, leading to fragmentation/destabilization of this compartment [134]. We propose that BopA binding to TRAPPC8 leads to inhibition of vesicular tethering by masking TRAPPC8 from incoming donor vesicles, hindering interaction of the TRAPPIII complex with the vesicle (Figure 25). Another possibility may be that BopA binding to TRAPPC8 inhibits interaction of TRAPPIII with host effector proteins required for SNARE assembly and membrane fusion and expansion at the donor/acceptor vesicle interface (Figure 25). Importantly, co-localization of TRAPPC8 to the *Burkholderia*-containing vacuole would validate this interaction and add to the overall knowledge of mammalian TRAPPIII function, the mechanisms involved in tethering and membrane fusion, and host factors and pathways exploited by *B. pseudomallei* to promote its intracellular survival in mammalian cells.

Overall, we demonstrated that we can monitor the progression of *B. pseudomallei* infection in cultured macrophages in a real time, high-throughput manner at very high resolution using *in vivo* optical diagnostic imaging and found that the T3SS3 effectors BopA, BopE and BapC greatly contribute to *B. pseudomallei*'s intracellular survival in cultured macrophages. Thus, we provide a novel approach to investigate the contribution of both host and pathogen proteins to the establishment of the *B. pseudomallei*

intracellular niche in host macrophages. Importantly, these studies will help to elucidate vesicular trafficking patterns of the mammalian TRAPPIII complex and provide potential host or bacterial targets for therapeutics and experimental vaccines for the prevention of *B. pseudomallei* infection in humans.

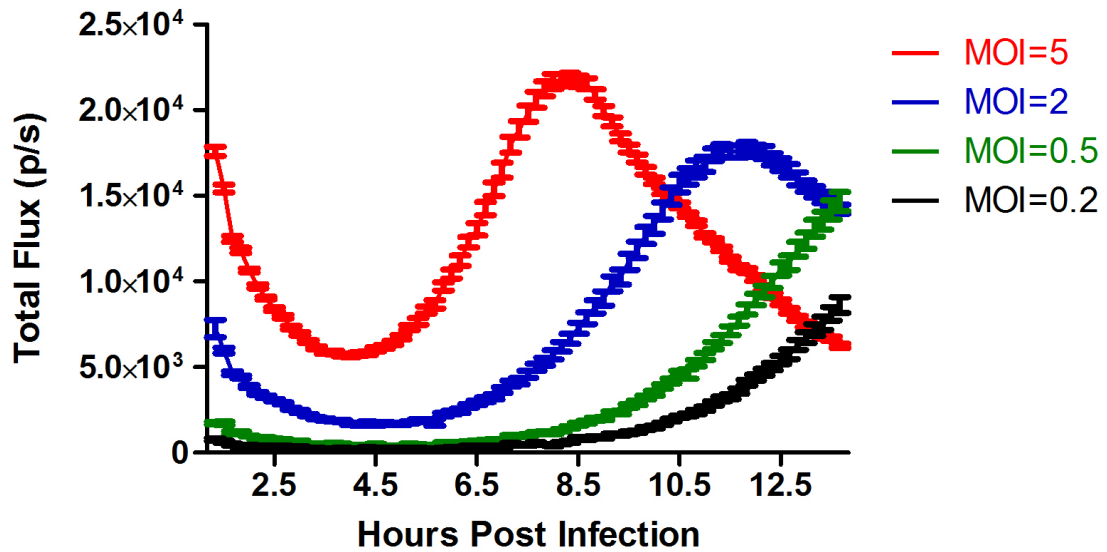


Figure 18. Growth kinetics of *Burkholderia pseudomallei* parental strain in J774A.1 macrophages. *In vivo* growth pattern of the bioluminescent *B. pseudomallei* parental strain JW280 in infected J774A.1 macrophages at multiplicities of infection (MOI) of 5, 2, 0.5 and 0.2 bacteria per macrophage using a gentamicin protection assay. Growth of *B. pseudomallei* was followed using *in vivo* imaging over a 14 hour time period using Total Flux (total luminescence) of bacteria in photons per second. Intracellular bacterial burden was plotted as the Total Flux of viable bacteria over time.

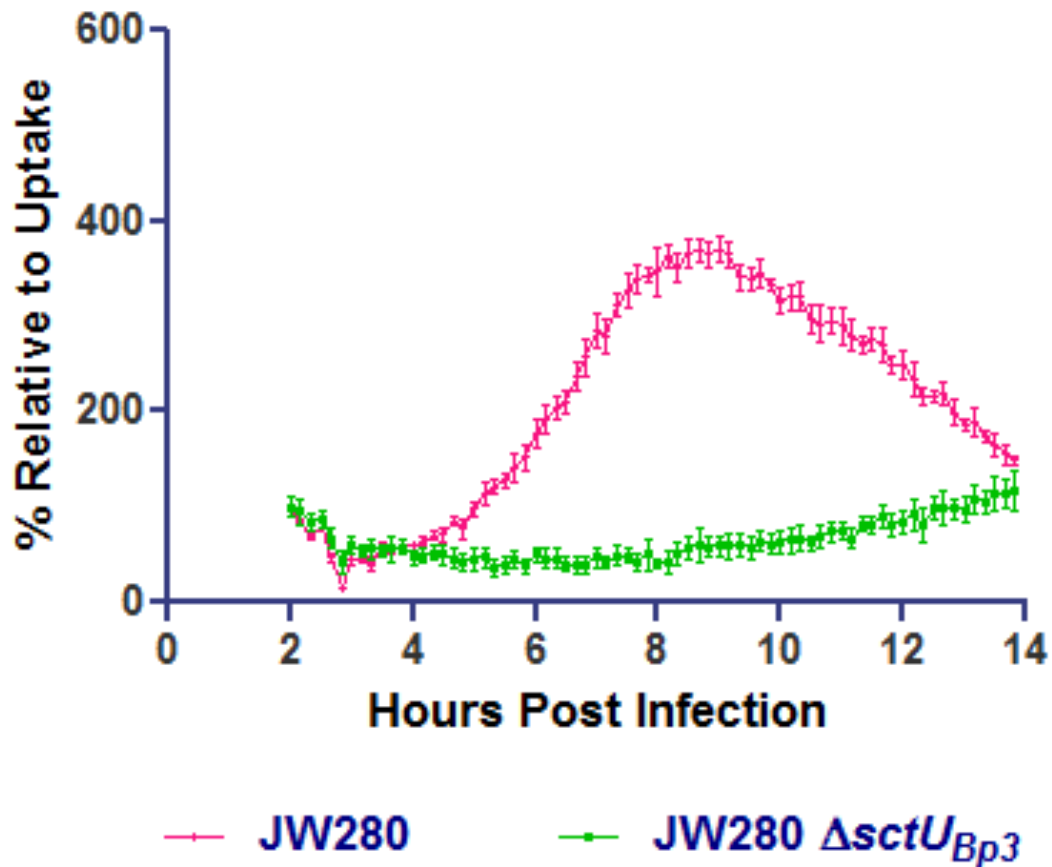


Figure 19. Growth kinetics of the *Burkholderia pseudomallei* type 3 secretion system cluster 3 structural mutant JW280 $\Delta sctU_{Bp3}$ in J774A.1 macrophages. Comparison of *in vivo* growth patterns of the *B. pseudomallei* parental strain JW280 and JW280 $\Delta sctU_{Bp3}$ mutant strain in infected J774A.1 macrophages. Growth of *B. pseudomallei* was followed using an *in vivo* imaging system over a 14 hour time period using Total Flux (total luminescence) of bacteria in photons per second. Intracellular bacterial burden was plotted as the relative percent of viable bacteria over time.

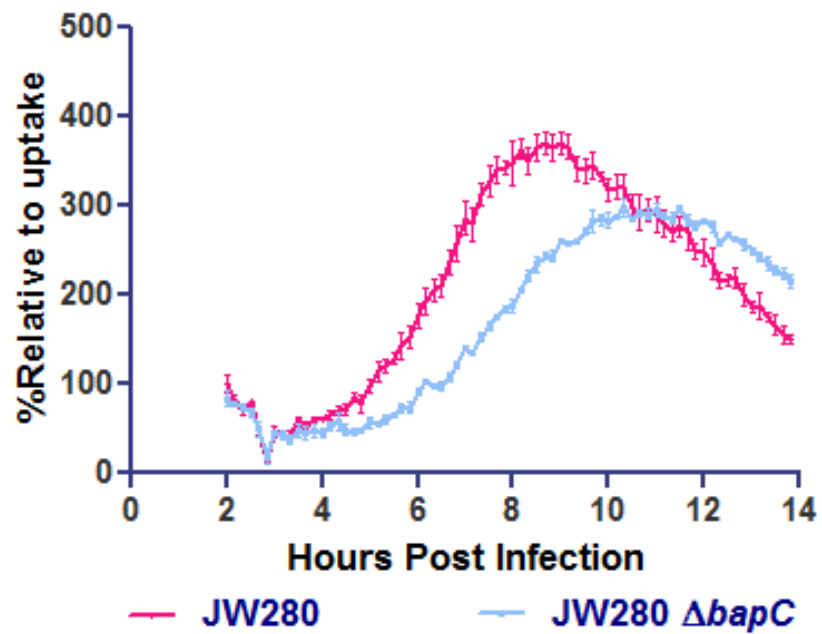
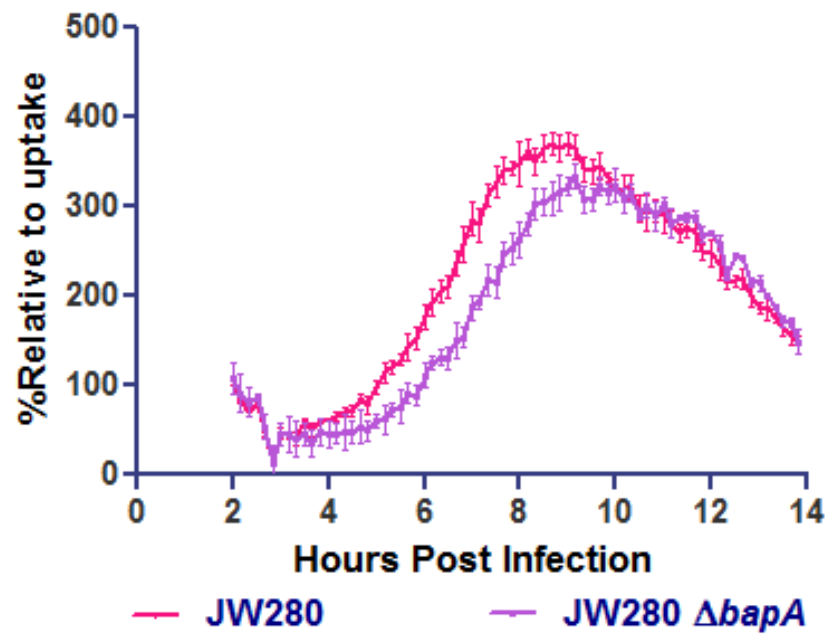


Figure 20. Growth kinetics of the *Burkholderia pseudomallei* type 3 secretion system cluster 3 effector protein mutants JW280 $\Delta bapA$ and JW280 $\Delta bapC$ in J774A.1 macrophages. Comparison of *in vivo* growth patterns of the *B. pseudomallei* parental strain JW280 and the effector mutant strains JW280 $\Delta bapA$ and JW280 $\Delta bapC$ in infected J774A.1 macrophages. Growth of *B. pseudomallei* was followed using an *in vivo* imaging system over a 14 hour time period using Total Flux (total luminescence) of bacteria in photons per second. Intracellular bacterial burden was plotted as the relative percent of viable bacteria over time.

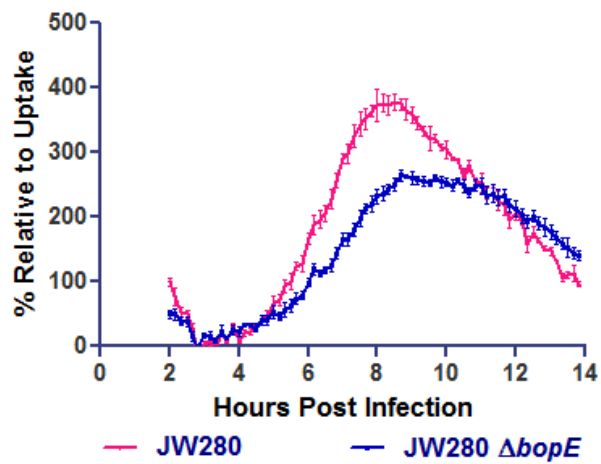
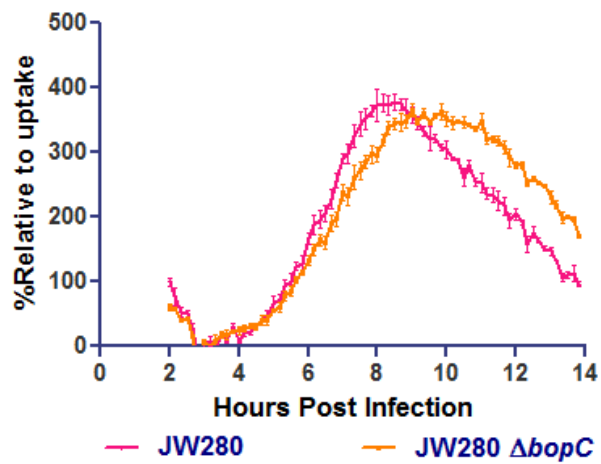
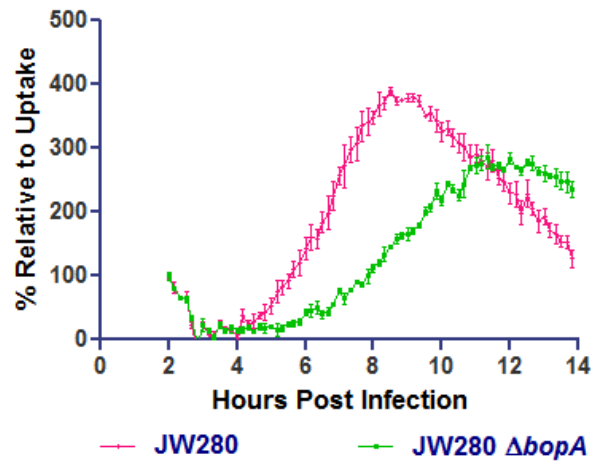


Figure 21. Growth kinetics of the *Burkholderia pseudomallei* type 3 secretion system cluster 3 effector protein mutants JW280 $\Delta bopA$, JW280 $\Delta bopC$ and JW280 $\Delta bopE$ in J774A.1 macrophages. Comparison of *in vivo* growth patterns of the *B. pseudomallei* parental strain JW280 with the JW280 $\Delta bopA$, JW280 $\Delta bopC$ and JW280 $\Delta bopE$ effector mutant strains in infected J774A.1 macrophages. Growth of *B. pseudomallei* was followed using an *in vivo* imaging system over a 14 hour time period using Total Flux (total luminescence) of bacteria in photons per second. Intracellular bacterial burden was plotted as the relative percent of viable bacteria over time.

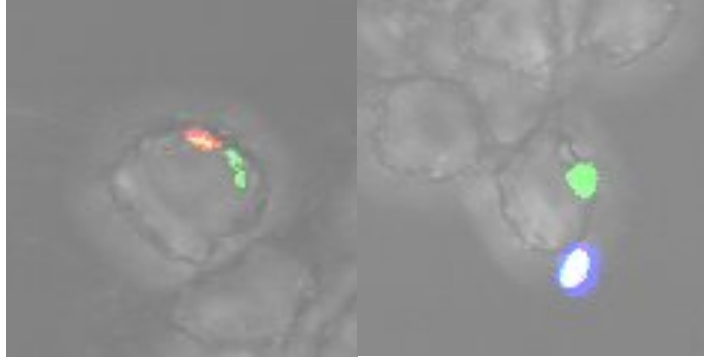
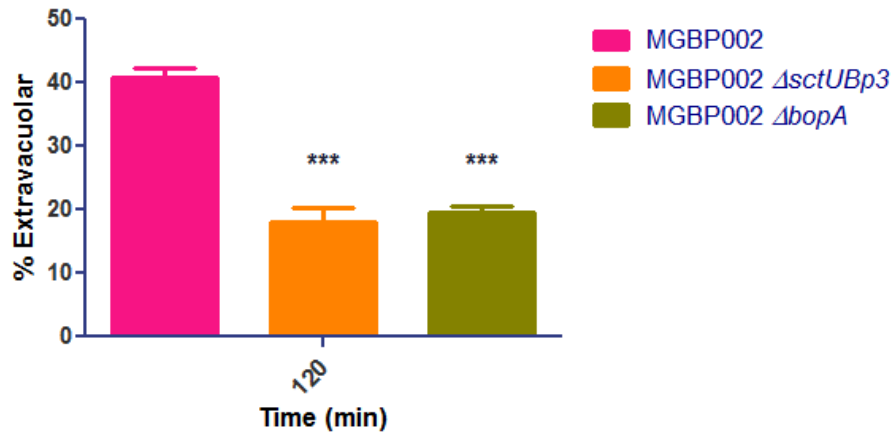
A**B**

Figure 22. A BopA effector mutant exhibits delayed vacuolar escape in RAW264.7 macrophages. (A) Representative confocal images of RAW264.7 macrophages infected with the *B. pseudomallei* strains MGBP002, MGBP002 $\Delta sctUBp3$ or MGBP002 $\Delta bopA$. Bacteria were pseudocolored, with extracellular bacteria shown in white (blue, red and green transposition) cytoplasmic bacteria shown in yellow (red and green transposition) and bacteria in vacuoles shown in green. (B) Percentage of *B. pseudomallei* MGBP002, MGBP002 $\Delta sctUBp3$ and MGBP002 $\Delta bopA$ located in vacuoles of infected RAW264.7 macrophages 2 hours post infection. Statistical significance determined by 1 way ANOVA; *** $p < 0.05$.

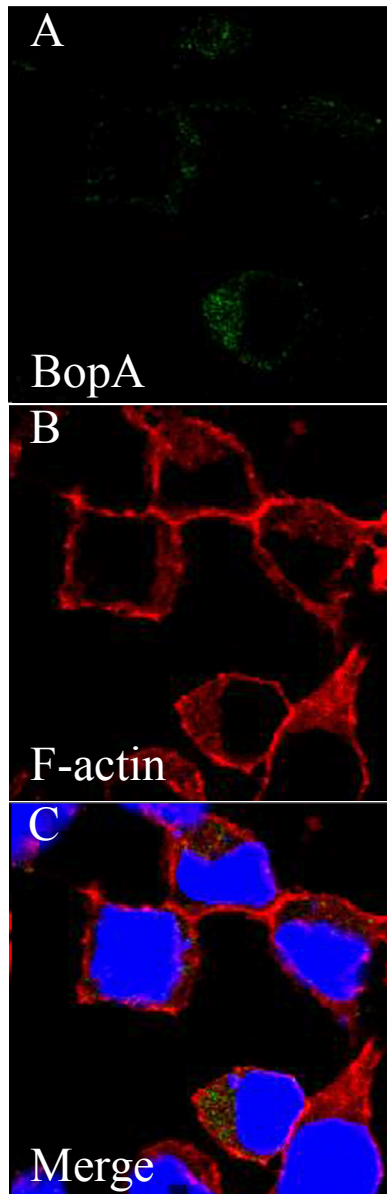


Figure 23. Ectopically expressed BopA is associated with punctate structures in the cytoplasm of HEK293 cells. Representative confocal microscopy image of HEK293 cells transiently transfected with p3XFLAG-BopA for 24 hrs. (A) BopA-FLAG fusion protein was detected in the cytoplasm of HEK293 cells with an anti-FLAG Alexa Fluor 488 antibody. (B) Phalloidin-TRITC binding of F-actin and (C) merged image plus DAPI nuclear staining.

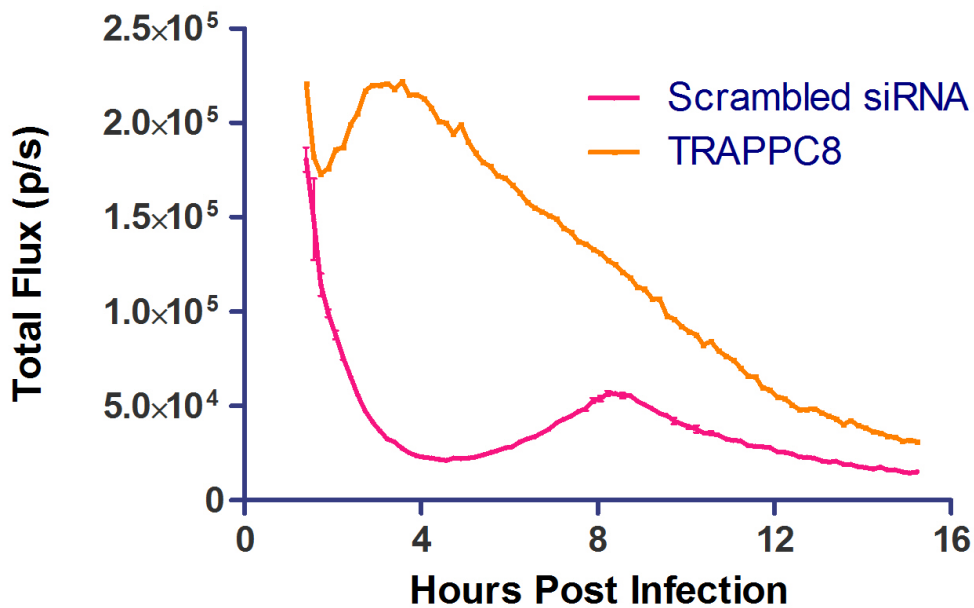


Figure 24. TRAPPC8 knockdown promotes intracellular survival of *Burkholderia pseudomallei*'s in RAW264.7 macrophages. Growth kinetics of the *B. pseudomallei* JW280 parental strain in infected RAW 264.7 macrophages treated with siRNA against TRAPPC8 (yellow line) and scrambled siRNA (pink line) for 48 hours prior to infection. Growth of *B. pseudomallei* was followed using an *in vivo* imaging system over a 15 hour time period using Total Flux (total luminescence) of bacteria in photons per second. Intracellular bacterial burden was plotted as the Total Flux of bacteria over time.

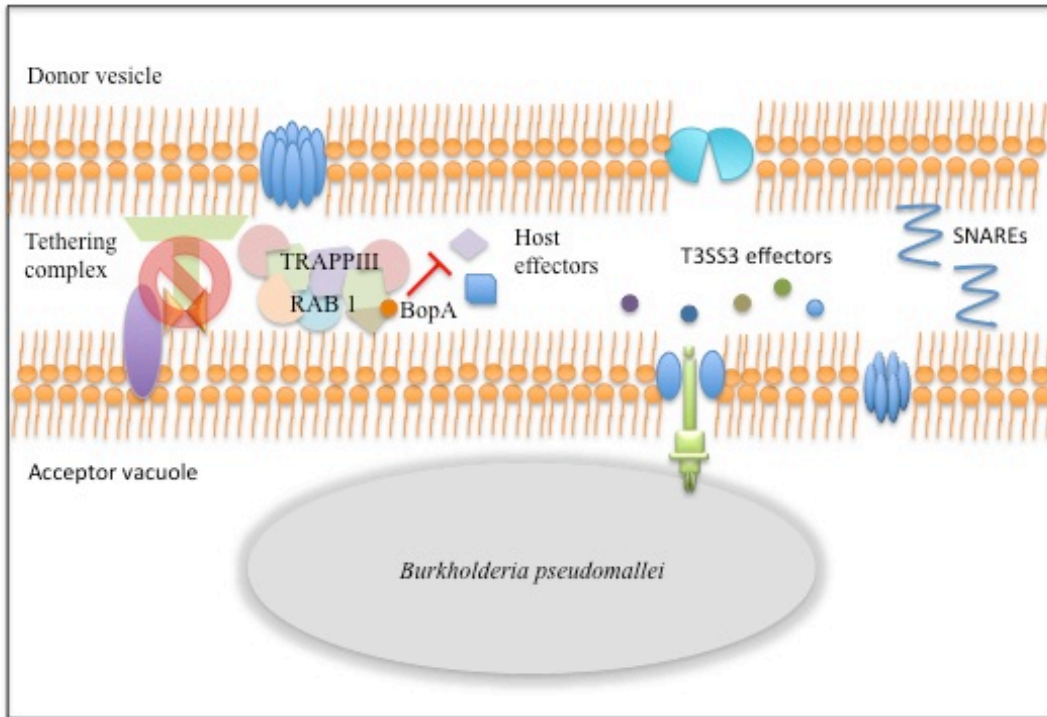


Figure 25. Model for BopA inhibition of TRAPPC8 function. Model for interaction of the T3SS3 effector BopA and TRAPPC8 at the donor vesicle and acceptor vacuole interface in the cytoplasm of host cells during *B. pseudomallei* infection. BopA binding of TRAPPC8 may interfere with early vesicle tethering events or formation of multi-subunit fusion complex formation, inhibiting vesicle expansion and leading to vacuolar destabilization.

Table 4. Type 3 secretion system cluster 3 putative secreted protein effectors.

Effector Protein	T3SS3-Dependent Secretion <i>In Vitro</i>	Putative Effector Function	Functional Domain/Superfamily	Domain/Superfamily Characteristics
BopA	Yes	Unknown	SicP-binding domain	Members of this family bind the chaperone SicP, which maintains effector stability and ensures effector secretion.
BopC	Yes	Unknown	Unknown	Unknown
BopE	Yes	Guanine nucleotide exchange factor	SopE-GEF superfamily	Members of this family contain a C-terminal guanine nucleotide exchange factor domain of the <i>Salmonella</i> type 3 secretion system effector SopE. This effector activates Rho family GTP-binding protein-dependent signaling cascades to induce cytoskeletal rearrangements.
BapA	Yes	Unknown	Unknown	Unknown
BapB	Yes	Acyl carrier protein	PP-binding superfamily	Carrier of growing fatty acid chain bound to a phosphopantetheine prosthetic group covalently bound to a serine residue during fatty acid biosynthesis.
BapC	Unknown	Unknown	Lytic transglycosylase domain	Members of this family include lytic transglycosylases in bacteria, bacteriophage lambda and eukaryotic lysozymes. Lytic transglycosylases catalyze cleavage of β -1,4-glycosidic bond between N-acetylmuramic acid and N-acetyl-D-glucosamine.

CHAPTER VI

DISCUSSION AND FUTURE DIRECTIONS

In these studies, we present results that greatly contribute to our overall knowledge of the pathogenesis of *B. pseudomallei* in mammalian hosts. Specifically, we demonstrate the importance of an effective lung-specific mouse model of respiratory melioidosis for the development of human-like melioidosis in mice. We identified the type 3 secretion system cluster 3 as critically required for respiratory melioidosis and other novel virulence determinants needed for *B. pseudomallei* lung colonization. Further, we found that the T3SS3 effector proteins BopA, BopC, BopE, BapA and BapC act in concert to mediate intracellular survival of *B. pseudomallei* in host cells. Yet, these studies also raise additional questions that can further our understanding of host-*B. pseudomallei* interactions. Accordingly, the following future directions could add to our understanding of T3SS3 effectors to the intracellular survival of *B. pseudomallei* in mammalian hosts.

6.1 Identification and efficacy evaluation of potential *Burkholderia pseudomallei* vaccine and therapeutic candidates using intubation-mediated intratracheal instillation

Herein we show that direct delivery of *B. pseudomallei* to mice lungs through tracheal intubation, leads to a course of disease with key hallmarks of human melioidosis in mice, specifically development of respiratory melioidosis and septicaemic disease [138]. This infection model provides a strong platform for studying the pathogenesis of *B. pseudomallei* in humans, has great implications for identifying potential vaccine and/or therapeutic candidates against *B. pseudomallei* infection and for evaluating the efficacy of these potential candidates. Commonly used intranasal and aerosol inoculation mouse models of *B. pseudomallei* generally result in colonization of the upper respiratory tract by deposition of bacteria in the nasal cavity [64, 139]. This leads to overrepresentation of neurological symptoms and incomplete disease progression with reduced spread of the bacterium to secondary sites of infection [140] and premature mortality in mice by suffocation [138]. Consequentially, it may be questionable to assess therapeutic protection against suffocation end points that likely do not elicit a complete immune response. Thus, inhalational and aerosol mouse models of melioidosis do not model human disease correctly [139], raising challenges for identifying protective antigens for acute and chronic melioidosis. Currently, there are no licensed vaccines available for the prevention of melioidosis; early diagnosis and subsequent antibiotic treatment are the only alternatives available for the management of *B. pseudomallei* infection [141], thus identifying vaccine candidates against the bacterium is of pressing concern.

We previously established that the type 3 secretion system cluster 3 is absolutely critical for respiratory melioidosis, strongly suggesting that the type 3 secretion apparatus and/or its associated proteins may constitute potential vaccine and/or therapeutic targets. However, a live attenuated mutant in the type 3 needle tip protein BipD and vaccination with purified BipB, BipC or BipD, did not confer protection against *B. pseudomallei* intraperitoneal challenge in BALB/c mice [53, 104]. We previously showed that different routes of infection lead to altered disease outcomes [138], accordingly, reevaluating protection and efficacy of these subunit vaccines in our lung-specific mouse model of infection, which is associated with respiratory and septicaemic melioidosis rather than suffocation end points, is appropriate.

Alternatively, T3SS3 structural components and associated effector proteins may constitute potential therapeutic targets. Given that the T3SS3 is critically required for the intracellular life cycle of the bacterium [38], it is possible that T3SS3 associated proteins may not be accessible to humoral immune responses. By developing therapeutics that may hinder the functions of T3SS3 key proteins or may compete for binding with target host cell interaction partners resulting in significant bacterial attenuation, we may be able to reduce the morbidity and mortality associated with acute melioidosis, prevent the onset of chronic melioidosis or patient relapse.

6.2 Tn-Seq screen: A source of novel virulence determinants

We used IMIT in combination with transposon mutagenesis to identify novel virulence factors required by *B. pseudomallei* to colonize the mouse lung and to spread to the liver and spleen; all key sites of infection. Our Tn-Seq screen identified 548 genes

required for respiratory melioidosis and of those ~512 were not associated with the capsular polysaccharide operon, the type 3 secretion system cluster 3 or the type 6 secretion system cluster 5. The identified genes comprised 33 genetic loci, or gene clusters with significant negative fold-changes (>15) located no more than a 4-gene distance from adjacent hits, required for respiratory melioidosis. Numerous loci identified possess functions related to metabolic processes during host infection, and experienced significant negative fold-changes, suggesting that genes in these loci are critical for bacterial survival in mammalian hosts. Specifically, genes encoding for proteins that function in histidine, purine, amino sugars, secondary metabolites, fatty acid and glycan biosynthesis among other cell wall components, experienced significant negative fold-changes (>150), demonstrating a compelling requirement of these genes for intracellular *B. pseudomallei* growth. Importantly, the histidine biosynthetic pathway is only present in bacteria, archaea, fungi and plants [142], making this genetic cluster an attractive virulence determinant for attenuation and therapeutic studies. Furthermore, amino sugars generated in the histidine biosynthetic pathway, may also constitute potential targets for aminoglycosides, inhibiting downstream metabolic pathways that utilize these amino sugars and are critical for *B. pseudomallei in vivo* growth. Other potential virulence determinants that may represent suitable targets for attenuation studies include clusters involved in purine and secondary metabolite biosynthesis, loci almost completely made up of hypothetical proteins and those that encode for surface expressed proteins, which may be induced during various stress conditions such as early stages of cell growth. Given the heterogeneity of host-pathogen interactions of *B. pseudomallei* in the host lung, it is likely that numerous virulence systems contribute to the bacterium's

pathogenesis at this key site, thus validating those virulence determinants involved in bacterial biosynthetic process that may hinder the growth of *B. pseudomallei in vivo*, may confer great advantages for prevention against *B. pseudomallei* morbidity and mortality.

6.3 Potential role of BopE in apoptosis inhibition through activation of the RAB45 GTPase

BopE is a T3SS3 effector protein with a guanine nucleotide exchange factor (GEF) domain [48] and is required for full virulence of *B. pseudomallei* in cultured macrophages. The BopE homologues and T3SS *Salmonella* effectors, SopE and SopE2, also exhibit GEF activity and target the mammalian Rho GTPases Rac1 and Cdc42, facilitating *Salmonella* invasion of epithelial cells [130]. BopE also exhibits GEF activity for Rac1 and Cdc42 but to a lower extent and notably, *B. pseudomallei* is not an invasive pathogen. Accordingly, we hypothesize that BopE may target other host GTPases involved in cellular pathways, such as RAB proteins involved in vesicular trafficking, which are exploited by numerous intracellular pathogens [143]. Although our initial hypothesis was that BopE directly contributes to the rapid escape of *B. pseudomallei* from endocytic vesicles by targeting yet known host proteins located in the *Burkholderia*-containing vacuolar membrane, a recent *B. mallei* yeast two-hybrid screen identified the RAB45 GTPase among other murine proteins, as a potential host cell target for BopE [132]. RAB45 is a newly identified small GTPase of the Ras superfamily of small GTPases [144] and its expression results in the activation of apoptosis in a human chronic myelogenous leukemia cell line by inducing phosphorylation of the mitogen-activated kinase p38, which leads to enhanced processing of caspase-3 and caspase-9, and

subsequent induction of apoptosis during cellular stress [145]. The RAB45 GTPase fits the profile of a potential BopE target, as this T3SS3 effector exhibits guanine nucleotide exchange factor activity [48] and the potential interaction of BopE and RAB45 may inhibit activation of the GTPase by blocking guanine nucleotide exchange, which may result in decreased phosphorylation of p38 and ultimate inhibition of apoptosis (Figure 26). Accordingly, inhibition of programmed cell death by BopE may be a significant benefit for *B. pseudomallei* as it provides the bacteria with time to establish a replicative niche inside host cells. This hypothesis is supported by the growth kinetics of the *bopE* mutant in infected macrophages, which showed a peak in intracellular numbers for this strain at approximately 9 hours post-infection, about 2 hours before the *bopA* mutant numbers reached a peak, suggesting that programmed cell death may be inhibited or delayed in the presence of BopE. Accordingly, validating RAB45-BopE interaction and evaluating the guanine nucleotide turnover kinetics of BopE would elucidate a potential role for this effector to *B. pseudomallei* infection. Importantly, assessing the role of RAB45 during *B. pseudomallei* colonization would elucidate a novel mechanism of apoptosis inhibition by a bacterial pathogen.

6.4 BapC may modify the *Burkholderia pseudomallei* cell wall during infection of host cells facilitating T3SS3 apparatus assembly

The T3SS3 effector BapC is a small 187-amino acid residue protein with predicted amino-terminal transmembrane and lytic transglycosylase domains, and is required for intracellular fitness of *B. pseudomallei*. Lytic transglycosylases are bacterial enzymes characterized as “space-making” autolysins that cleave the β -1,4 glycosidic

bonds between *N*-acetylmuramic acid and *N*-acetylglucosamine resulting in non-reducing 1,6-anhydro bonds in *N*-acetylmuramic acid peptides [146]. Lytic transglycosylases have been shown to be involved in insertion of bacterial cell-wall spanning structures such as pili, flagella and secretion systems; peptidoglycan biosynthesis and recycling; cell division and maintenance of bacterial morphology [147]. These autolysins have been implicated in the pathogenicity of several Gram-negative bacteria such as enterohemorrhagic *E. coli* (EHEC) and *Neisseria gonorrhoeae* [148, 149] and have been found in the T3SS and type 4 secretion system (T4SS) locus of *Burkholderia cepacia*, enteropathogenic and enterohemorrhagic *E. coli*, *S. enterica*, *S. flexneri*, *Yersinia enterocolitica*, *Brucella suis*, *Agrobacterium tumefaciens* and other bacterial pathogens [146]. Accordingly, BapC may function as a lytic transglycosylase in the bacterial periplasmic space during *B. pseudomallei* infection of host cells. Thus, we hypothesize that BapC may modify the bacterial cell wall, creating a pore for rapid T3SS3 apparatus assembly and passage through both bacterial membranes (Figure 26). Yet, inactivation of *bapC* results in a moderate defect in *B. pseudomallei* survival, suggesting that other *B. pseudomallei* lytic transglycosylases may complement the loss of *bapC*. BapC was recently shown to be secreted *in vitro* in a T3SS3-dependent manner [55], yet this finding contradicts a T3SS3 secretome screen, which did not identify BapC as a T3SS3-secreted effector [54]. To date, the potential mechanisms of delivery of T3SS-associated lytic transglycosylases to the periplasmic space remain relatively unknown, although some lytic transglycosylases have been shown to encode an amino-terminal periplasmic signal peptide sequence and are transported into the periplasmic space in a *sec*-dependent manner [148, 150]. Further, the *Brucella suis* and *A. tumefaciens* T4SS-associated lytic

transglycosylase VirB1 has been shown to transiently associate with T4SS apparatus components, potentially providing chaperone activity for apparatus components and traversing the bacterial inner membrane into the periplasm where it may mediate apparatus assembly [150, 151]. Thus, it may be possible that BapC is transported into the periplasm of *B. pseudomallei* through the general secretory pathway or by associating with apparatus components permitting transport of the effector to the periplasm. Therefore, identifying a potential periplasmic signal peptide sequence at the protein's amino terminal is of pressing concern. The predicted peptidoglycan pore size allows for diffusion of globular proteins with a molecular weight of ~55 kDa or less [151] and BapC, with a predicted 20.2 kDa molecular weight would easily diffuse through the periplasmic space allowing the potential docking of BapC to either the inner or outer membrane. Accordingly, identifying the subcellular distribution of BapC in the bacterium and importantly, validating BapC transglycosylase activity with the *B. pseudomallei* sacculus would provide great insight into BapC functions during infection and its modulation of *B. pseudomallei* peptidoglycan dynamics *in vivo*.

6.5 Induction of pyroptotic and/or apoptotic cell death during *Burkholderia pseudomallei* infection of host cells

The growth profile of the parental *B. pseudomallei* strain JW280 illustrates that early in the course of infection, bacterial numbers are significantly reduced (Figure 18). This decrease can be partially attributed to extracellular bacterial killing of gentamicin added to the culture medium, but in our hands, synchronized infection of macrophages by centrifugation leads to ~60% of bacterial inoculum internalization by 15 minutes post

infection, which implies that infected macrophages also contribute to the decline in bacterial numbers by killing intracellular *B. pseudomallei*. Yet, early killing of *B. pseudomallei* by infected macrophages is not 100% effective in eradicating the bacterium, suggesting that infected cells must resort to other methods of controlling intracellular *B. pseudomallei* numbers. Cell autonomous immune responses of macrophages against *B. pseudomallei* includes the induction of pyroptotic cell death through activation of caspase-1, which takes place early during the course of infection and seems to be dependent on bacterial strain and intracellular bacterial burden [152]. Yet *B. pseudomallei* can also induce apoptotic cell death in host cells [153] by mechanisms yet unknown. We previously hypothesized that potential induction of apoptosis may take place through activation of the MAP kinase p38 as a result of BopE-RAB45 interaction. Yet, activation of p38 and the outcome of this activation has been shown to be cell type and stimulus dependent [154]. Our Tn-Seq findings showed that *B. pseudomallei* colonizes and replicates in the lungs of mice as early as 6 hours post infection, but bacterial numbers in the liver remain relatively the same by 24 hours post infection [155], suggestive of altered immune responses associated with different cell types. Accordingly, we hypothesize that several mammalian cell types may harbor *B. pseudomallei* infection *in vivo* and these host cells may undergo pyroptotic or apoptotic cell death depending on the bacterial stimuli encountered. To address this hypothesis, first we would need to define the repertoire of mammalian cells that may harbor *B. pseudomallei* infection *in vivo* using our lung-specific mouse model of infection and analyze single cell suspensions from infected lungs, liver and spleen labeled with distinct cell surface markers using flow cytometry. Once the *B. pseudomallei* host cell repertoire

is defined, we have the ability to assess the role of specific caspases in inducing pyroptotic and/or apoptotic cell death at early or late time points in infection using our real time high throughput assay and *in vivo* optical diagnostic imaging. Results from these assays will further our knowledge of the pathogenesis of *B. pseudomallei in vivo*, would elucidate appropriate cell-autonomous immune responses against various *B. pseudomallei* stimuli and provide potential cell targets for therapeutics against infection with the pathogen.

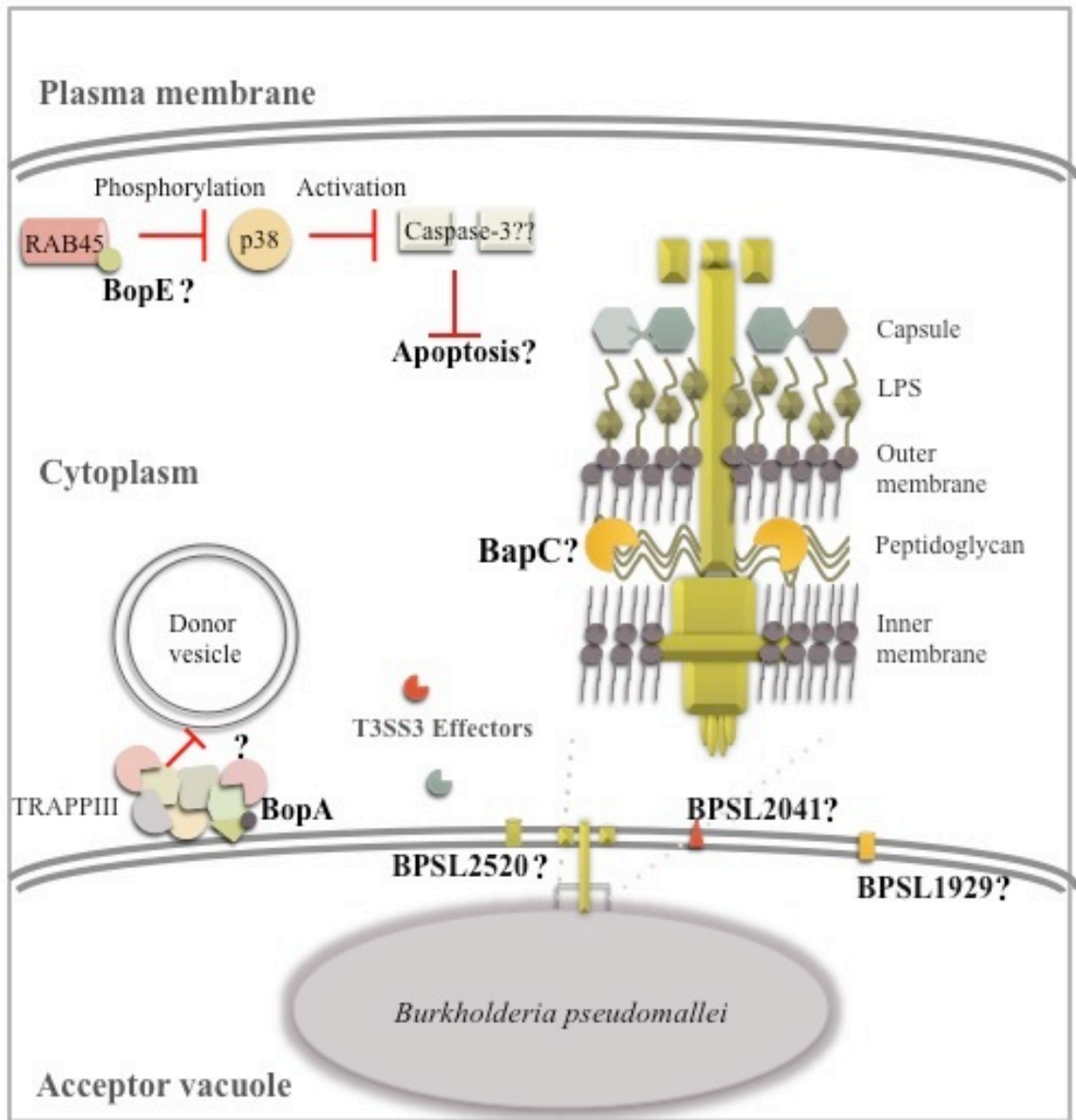


Figure 26. Model of the potential functions of T3SS3 effectors BopA, BopE and BapC during *Burkholderia pseudomallei* infection of host cells. Modification of the bacterial cell wall by BapC may facilitate passage of the T3SS3 needle through both bacterial membranes and peptidoglycan. BopA binding to TRAPPC8 may inhibit vesicle expansion also leading to vacuolar destabilization and the rapid escape of *B. pseudomallei* from the vacuole. Potential BopE interaction with the GTPase RAB45 may lead to inhibition of apoptotic cell death, providing *B. pseudomallei* the time required to establish a replicative niche in the cytoplasm of the host cell. Other T3SS3 translocated effector proteins likely carry out functions within the cell that promote *B. pseudomallei* intracellular survival.

REFERENCES

1. Whitmore A. An Account of a Glanders-like Disease occurring in Rangoon. *J Hyg (Lond)*. 1913;13(1):1-34 1. PubMed PMID: 20474526; PubMed Central PMCID: PMC2167219.
2. Stanton AT, Fletcher W. Melioidosis, A Disease of Rodents Communicable to Man. *Lancet*. 1925.
3. Cheng AC, Currie BJ. Melioidosis: epidemiology, pathophysiology, and management. *Clinical microbiology reviews*. 2005;18(2):383-416. Epub 2005/04/16. doi: 10.1128/CMR.18.2.383-416.2005. PubMed PMID: 15831829; PubMed Central PMCID: PMC1082802.
4. Miller WR, Pannell L, Cravitz L, Tanner WA, Ingalls MS. Studies on Certain Biological Characteristics of *Malleomyces mallei* and *Malleomyces pseudomallei*: I. Morphology, Cultivation, Viability, and Isolation from Contaminated Specimens. *Journal of bacteriology*. 1948;55(1):115-26. PubMed PMID: 16561426; PubMed Central PMCID: PMC518415.
5. Biegeleisen JZ, Jr., Mosquera R, Cherry WB. [Case of Human Melioidosis; Clinical, Epidemiological and Laboratory Findings]. *Rev Ecuat Hig Med Trop*. 1964;21:23-37. PubMed PMID: 14233520.
6. Yabuuchi E, Kosako Y, Oyaizu H, Yano I, Hotta H, Hashimoto Y, et al. Proposal of *Burkholderia* gen. nov. and transfer of seven species of the genus *Pseudomonas* homology group II to the new genus, with the type species *Burkholderia cepacia*

(Palleroni and Holmes 1981) comb. nov. *Microbiol Immunol*. 1992;36(12):1251-75.
PubMed PMID: 1283774.

7. Galyov EE, Brett PJ, DeShazer D. Molecular insights into *Burkholderia pseudomallei* and *Burkholderia mallei* pathogenesis. *Annual review of microbiology*. 2010;64:495-517. Epub 2010/06/10. doi: 10.1146/annurev.micro.112408.134030.
PubMed PMID: 20528691.

8. Dance DA. Melioidosis: the tip of the iceberg? *Clinical microbiology reviews*. 1991;4(1):52-60. PubMed PMID: 2004347; PubMed Central PMCID: PMC358178.

9. Howe C, Sampath A, Spotnitz M. The pseudomallei group: a review. *The Journal of infectious diseases*. 1971;124(6):598-606. PubMed PMID: 5001752.

10. Currie BJ, Ward L, Cheng AC. The epidemiology and clinical spectrum of melioidosis: 540 cases from the 20 year Darwin prospective study. *PLoS neglected tropical diseases*. 2010;4(11):e900. Epub 2010/12/15. doi: 10.1371/journal.pntd.0000900.
PubMed PMID: 21152057; PubMed Central PMCID: PMC2994918.

11. Holden MT, Titball RW, Peacock SJ, Cerdeno-Tarraga AM, Atkins T, Crossman LC, et al. Genomic plasticity of the causative agent of melioidosis, *Burkholderia pseudomallei*. *Proceedings of the National Academy of Sciences of the United States of America*. 2004;101(39):14240-5. doi: 10.1073/pnas.0403302101. PubMed PMID: 15377794; PubMed Central PMCID: PMC521101.

12. Sim SH, Yu Y, Lin CH, Karuturi RK, Wuthiekanun V, Tuanyok A, et al. The core and accessory genomes of *Burkholderia pseudomallei*: implications for human melioidosis. *PLoS pathogens*. 2008;4(10):e1000178. doi: 10.1371/journal.ppat.1000178.
PubMed PMID: 18927621; PubMed Central PMCID: PMC2564834.

13. Woods DE, DeShazer D, Moore RA, Brett PJ, Burtnick MN, Reckseidler SL, et al. Current studies on the pathogenesis of melioidosis. *Microbes and infection / Institut Pasteur*. 1999;1(2):157-62. PubMed PMID: 10594980.
14. Inglis TJ, Rolim DB, Sousa Ade Q. Melioidosis in the Americas. *The American journal of tropical medicine and hygiene*. 2006;75(5):947-54. PubMed PMID: 17123994.
15. Dance DA. Melioidosis as an emerging global problem. *Acta Trop*. 2000;74(2-3):115-9. PubMed PMID: 10674638.
16. Currie BJ. Melioidosis: evolving concepts in epidemiology, pathogenesis, and treatment. *Semin Respir Crit Care Med*. 2015;36(1):111-25. doi: 10.1055/s-0034-1398389. PubMed PMID: 25643275.
17. Zehnder AM, Hawkins MG, Koski MA, Lifland B, Byrne BA, Swanson AA, et al. *Burkholderia pseudomallei* isolates in 2 pet iguanas, California, USA. *Emerging infectious diseases*. 2014;20(2):304-6. doi: 10.3201/eid2002.131314. PubMed PMID: 24447394; PubMed Central PMCID: PMC3901496.
18. Lazar Adler NR, Govan B, Cullinane M, Harper M, Adler B, Boyce JD. The molecular and cellular basis of pathogenesis in melioidosis: how does *Burkholderia pseudomallei* cause disease? *FEMS microbiology reviews*. 2009;33(6):1079-99. Epub 2009/09/08. doi: 10.1111/j.1574-6976.2009.00189.x. PubMed PMID: 19732156.
19. Warawa J, Woods DE. Type III secretion system cluster 3 is required for maximal virulence of *Burkholderia pseudomallei* in a hamster infection model. *FEMS microbiology letters*. 2005;242(1):101-8. Epub 2004/12/29. doi: 10.1016/j.femsle.2004.10.045. PubMed PMID: 15621426.

20. Piggott JA, Hochholzer L. Human melioidosis. A histopathologic study of acute and chronic melioidosis. *Arch Pathol.* 1970;90(2):101-11. PubMed PMID: 5433595.
21. Lim C, Peacock SJ, Limmathurotsakul D. Association between activities related to routes of infection and clinical manifestations of melioidosis. *Clin Microbiol Infect.* 2015. doi: 10.1016/j.cmi.2015.09.016. PubMed PMID: 26417852.
22. Mu JJ, Cheng PY, Chen YS, Chen PS, Chen YL. The occurrence of melioidosis is related to different climatic conditions in distinct topographical areas of Taiwan. *Epidemiol Infect.* 2014;142(2):415-23. doi: 10.1017/S0950268813001271. PubMed PMID: 23714119.
23. Cheng AC, Jacups SP, Gal D, Mayo M, Currie BJ. Extreme weather events and environmental contamination are associated with case-clusters of melioidosis in the Northern Territory of Australia. *International journal of epidemiology.* 2006;35(2):323-9. doi: 10.1093/ije/dyi271. PubMed PMID: 16326823.
24. Dance D. Treatment and prophylaxis of melioidosis. *Int J Antimicrob Agents.* 2014;43(4):310-8. doi: 10.1016/j.ijantimicag.2014.01.005. PubMed PMID: 24613038; PubMed Central PMCID: PMC4236584.
25. White NJ, Dance DA, Chaowagul W, Wattanagoon Y, Wuthiekanun V, Pitakwatchara N. Halving of mortality of severe melioidosis by ceftazidime. *Lancet.* 1989;2(8665):697-701. PubMed PMID: 2570956.
26. Cheng AC, Fisher DA, Anstey NM, Stephens DP, Jacups SP, Currie BJ. Outcomes of patients with melioidosis treated with meropenem. *Antimicrobial agents and chemotherapy.* 2004;48(5):1763-5. PubMed PMID: 15105132; PubMed Central PMCID: PMC400582.

27. Chetchotisakd P, Chierakul W, Chaowagul W, Anunnatsiri S, Phimda K, Mootsikapun P, et al. Trimethoprim-sulfamethoxazole versus trimethoprim-sulfamethoxazole plus doxycycline as oral eradication treatment for melioidosis (MERTH): a multicentre, double-blind, non-inferiority, randomised controlled trial. *Lancet*. 2014;383(9919):807-14. doi: 10.1016/S0140-6736(13)61951-0. PubMed PMID: 24284287; PubMed Central PMCID: PMC3939931.
28. Maharjan B, Chantratita N, Vesaratchavee M, Cheng A, Wuthiekanun V, Chierakul W, et al. Recurrent melioidosis in patients in northeast Thailand is frequently due to reinfection rather than relapse. *Journal of clinical microbiology*. 2005;43(12):6032-4. doi: 10.1128/JCM.43.12.6032-6034.2005. PubMed PMID: 16333094; PubMed Central PMCID: PMC1317219.
29. Peacock SJ, Schweizer HP, Dance DA, Smith TL, Gee JE, Wuthiekanun V, et al. Management of accidental laboratory exposure to *Burkholderia pseudomallei* and *B. mallei*. *Emerging infectious diseases*. 2008;14(7):e2. doi: 10.3201/eid1407.071501. PubMed PMID: 18598617; PubMed Central PMCID: PMC2600349.
30. Wiersinga WJ, Currie BJ, Peacock SJ. Melioidosis. *The New England journal of medicine*. 2012;367(11):1035-44. doi: 10.1056/NEJMra1204699. PubMed PMID: 22970946.
31. Ussery DW, Kiil K, Lagesen K, Sicheritz-Ponten T, Bohlin J, Wassenaar TM. The genus *Burkholderia*: analysis of 56 genomic sequences. *Genome Dyn*. 2009;6:140-57. doi: 10.1159/000235768. PubMed PMID: 19696499.
32. Nandi T, Ong C, Singh AP, Boddey J, Atkins T, Sarkar-Tyson M, et al. A genomic survey of positive selection in *Burkholderia pseudomallei* provides insights into

- the evolution of accidental virulence. *PLoS pathogens*. 2010;6(4):e1000845. doi: 10.1371/journal.ppat.1000845. PubMed PMID: 20368977; PubMed Central PMCID: PMC2848565.
33. Moule MG, Hemsley CM, Seet Q, Guerra-Assuncao JA, Lim J, Sarkar-Tyson M, et al. Genome-wide saturation mutagenesis of *Burkholderia pseudomallei* K96243 predicts essential genes and novel targets for antimicrobial development. *mBio*. 2014;5(1):e00926-13. doi: 10.1128/mBio.00926-13. PubMed PMID: 24520057; PubMed Central PMCID: PMC3950516.
34. Schmidt H, Hensel M. Pathogenicity islands in bacterial pathogenesis. *Clinical microbiology reviews*. 2004;17(1):14-56. PubMed PMID: 14726454; PubMed Central PMCID: PMC321463.
35. Ray K, Marteyn B, Sansonetti PJ, Tang CM. Life on the inside: the intracellular lifestyle of cytosolic bacteria. *Nat Rev Microbiol*. 2009;7(5):333-40. doi: 10.1038/nrmicro2112. PubMed PMID: 19369949.
36. Gong L, Cullinane M, Treerat P, Ramm G, Prescott M, Adler B, et al. The *Burkholderia pseudomallei* type III secretion system and BopA are required for evasion of LC3-associated phagocytosis. *PloS one*. 2011;6(3):e17852. Epub 2011/03/18. doi: 10.1371/journal.pone.0017852. PubMed PMID: 21412437; PubMed Central PMCID: PMC3055895.
37. Devenish RJ, Lai SC. Autophagy and burkholderia. *Immunology and cell biology*. 2015;93(1):18-24. doi: 10.1038/icb.2014.87. PubMed PMID: 25331551.
38. Stevens MP, Wood MW, Taylor LA, Monaghan P, Hawes P, Jones PW, et al. An Inv/Mxi-Spa-like type III protein secretion system in *Burkholderia pseudomallei*

- modulates intracellular behaviour of the pathogen. *Molecular microbiology*. 2002;46(3):649-59. Epub 2002/11/02. PubMed PMID: 12410823.
39. Jones AL, Beveridge TJ, Woods DE. Intracellular survival of *Burkholderia pseudomallei*. *Infection and immunity*. 1996;64(3):782-90. Epub 1996/03/01. PubMed PMID: 8641782; PubMed Central PMCID: PMC173838.
40. Pruksachartvuthi S, Aswapokee N, Thankerngpol K. Survival of *Pseudomonas pseudomallei* in human phagocytes. *Journal of medical microbiology*. 1990;31(2):109-14. Epub 1990/02/01. PubMed PMID: 2304065.
41. Kingston CW. Chronic or latent melioidosis. *Med J Aust*. 1971;2(12):618-21. PubMed PMID: 5114173.
42. Blocker A, Holden D, Cornelis G. Type III secretion systems: what is the translocator and what is translocated? *Cellular microbiology*. 2000;2(5):387-90. Epub 2001/02/24. PubMed PMID: 11207594.
43. Cornelis GR. Type III secretion: a bacterial device for close combat with cells of their eukaryotic host. *Philosophical transactions of the Royal Society of London Series B, Biological sciences*. 2000;355(1397):681-93. Epub 2000/06/30. doi: 10.1098/rstb.2000.0608. PubMed PMID: 10874740; PubMed Central PMCID: PMC1692769.
44. Sun GW, Gan YH. Unraveling type III secretion systems in the highly versatile *Burkholderia pseudomallei*. *Trends in microbiology*. 2010;18(12):561-8. Epub 2010/10/19. doi: 10.1016/j.tim.2010.09.002. PubMed PMID: 20951592.

45. Rainbow L, Hart CA, Winstanley C. Distribution of type III secretion gene clusters in *Burkholderia pseudomallei*, *B. thailandensis* and *B. mallei*. *Journal of medical microbiology*. 2002;51(5):374-84. Epub 2002/05/07. PubMed PMID: 11990489.
46. Attree O, Attree I. A second type III secretion system in *Burkholderia pseudomallei*: who is the real culprit? *Microbiology*. 2001;147(Pt 12):3197-9. doi: 10.1099/00221287-147-12-3197. PubMed PMID: 11739751.
47. Geddes K, Cruz F, Heffron F. Analysis of cells targeted by *Salmonella* type III secretion in vivo. *PLoS pathogens*. 2007;3(12):e196. Epub 2007/12/28. doi: 10.1371/journal.ppat.0030196. PubMed PMID: 18159943; PubMed Central PMCID: PMC2151088.
48. Stevens MP, Friebel A, Taylor LA, Wood MW, Brown PJ, Hardt WD, et al. A *Burkholderia pseudomallei* type III secreted protein, BopE, facilitates bacterial invasion of epithelial cells and exhibits guanine nucleotide exchange factor activity. *Journal of bacteriology*. 2003;185(16):4992-6. Epub 2003/08/05. PubMed PMID: 12897019; PubMed Central PMCID: PMC166480.
49. Suparak S, Kespichayawattana W, Haque A, Easton A, Damnin S, Lertmemongkolchai G, et al. Multinucleated giant cell formation and apoptosis in infected host cells is mediated by *Burkholderia pseudomallei* type III secretion protein BipB. *Journal of bacteriology*. 2005;187(18):6556-60. doi: 10.1128/JB.187.18.6556-6560.2005. PubMed PMID: 16159789; PubMed Central PMCID: PMC1236626.
50. Kang WT, Vellasamy KM, Chua EG, Vadivelu J. Functional characterizations of effector protein BipC, a type III secretion system protein, in *Burkholderia pseudomallei*

- pathogenesis. *The Journal of infectious diseases*. 2015;211(5):827-34. doi: 10.1093/infdis/jiu492. PubMed PMID: 25165162.
51. Erskine PT, Knight MJ, Ruaux A, Mikolajek H, Wong Fat Sang N, Withers J, et al. High resolution structure of BipD: an invasion protein associated with the type III secretion system of *Burkholderia pseudomallei*. *Journal of molecular biology*. 2006;363(1):125-36. Epub 2006/09/05. doi: 10.1016/j.jmb.2006.07.069. PubMed PMID: 16950399.
52. Johnson S, Roversi P, Espina M, Olive A, Deane JE, Birket S, et al. Self-chaperoning of the type III secretion system needle tip proteins IpaD and BipD. *The Journal of biological chemistry*. 2007;282(6):4035-44. Epub 2006/11/02. doi: 10.1074/jbc.M607945200. PubMed PMID: 17077085; PubMed Central PMCID: PMC1894746.
53. Druar C, Yu F, Barnes JL, Okinaka RT, Chantratita N, Beg S, et al. Evaluating *Burkholderia pseudomallei* Bip proteins as vaccines and Bip antibodies as detection agents. *FEMS Immunol Med Microbiol*. 2008;52(1):78-87. doi: 10.1111/j.1574-695X.2007.00345.x. PubMed PMID: 17995960.
54. Vander Broek CW, Chalmers KJ, Stevens MP, Stevens JM. Quantitative proteomic analysis of *Burkholderia pseudomallei* Bsa type III secretion system effectors using hypersecreting mutants. *Molecular & cellular proteomics : MCP*. 2015;14(4):905-16. doi: 10.1074/mcp.M114.044875. PubMed PMID: 25635268; PubMed Central PMCID: PMCPMC4390269.
55. Treerat P, Alwis P, D'Cruze T, Cullinane M, Vadivelu J, Devenish RJ, et al. The *Burkholderia pseudomallei* Proteins BapA and BapC Are Secreted TTSS3 Effectors and

- BapB Levels Modulate Expression of BopE. *PloS one*. 2015;10(12):e0143916. doi: 10.1371/journal.pone.0143916. PubMed PMID: 26624293.
56. Muangman S, Korbsrisate S, Muangsombut V, Srinon V, Adler NL, Schroeder GN, et al. BopC is a type III secreted effector protein of *Burkholderia pseudomallei*. *FEMS microbiology letters*. 2011;323(1):75-82. Epub 2011/11/19. doi: 10.1111/j.1574-6968.2011.02359.x. PubMed PMID: 22092682.
57. Roberts IS. The biochemistry and genetics of capsular polysaccharide production in bacteria. *Annual review of microbiology*. 1996;50:285-315. doi: 10.1146/annurev.micro.50.1.285. PubMed PMID: 8905082.
58. Reckseidler-Zenteno S. Capsular Polysaccharides Produced by the Bacterial Pathogen *Burkholderia pseudomallei*. 2012. Available from: <http://cdn.intechopen.com/pdfs-wm/40582.pdf>.
59. Reckseidler-Zenteno SL, DeVinney R, Woods DE. The capsular polysaccharide of *Burkholderia pseudomallei* contributes to survival in serum by reducing complement factor C3b deposition. *Infection and immunity*. 2005;73(2):1106-15. doi: 10.1128/IAI.73.2.1106-1115.2005. PubMed PMID: 15664954; PubMed Central PMCID: PMC547107.
60. Warawa JM, Long D, Rosenke R, Gardner D, Gherardini FC. Role for the *Burkholderia pseudomallei* capsular polysaccharide encoded by the wcb operon in acute disseminated melioidosis. *Infection and immunity*. 2009;77(12):5252-61. doi: 10.1128/IAI.00824-09. PubMed PMID: 19752033; PubMed Central PMCID: PMC2786491.

61. Reckseidler SL, DeShazer D, Sokol PA, Woods DE. Detection of bacterial virulence genes by subtractive hybridization: identification of capsular polysaccharide of *Burkholderia pseudomallei* as a major virulence determinant. *Infection and immunity*. 2001;69(1):34-44. doi: 10.1128/IAI.69.1.34-44.2001. PubMed PMID: 11119486; PubMed Central PMCID: PMC97852.
62. Atkins T, Prior R, Mack K, Russell P, Nelson M, Prior J, et al. Characterisation of an acapsular mutant of *Burkholderia pseudomallei* identified by signature tagged mutagenesis. *Journal of medical microbiology*. 2002;51(7):539-47. PubMed PMID: 12132769.
63. Howard CJ, Glynn AA. The virulence for mice of strains of *Escherichia coli* related to the effects of K antigens on their resistance to phagocytosis and killing by complement. *Immunology*. 1971;20(5):767-77. PubMed PMID: 4950867; PubMed Central PMCID: PMC1455862.
64. Warawa JM, Long D, Rosenke R, Gardner D, Gherardini FC. Bioluminescent diagnostic imaging to characterize altered respiratory tract colonization by the *Burkholderia pseudomallei* capsule mutant. *Frontiers in microbiology*. 2011;2:133. Epub 2011/07/02. doi: 10.3389/fmicb.2011.00133. PubMed PMID: 21720539; PubMed Central PMCID: PMC3118415.
65. Basler M, Pilhofer M, Henderson GP, Jensen GJ, Mekalanos JJ. Type VI secretion requires a dynamic contractile phage tail-like structure. *Nature*. 2012;483(7388):182-6. doi: 10.1038/nature10846. PubMed PMID: 22367545; PubMed Central PMCID: PMC3527127.

66. Schwarz S, West TE, Boyer F, Chiang WC, Carl MA, Hood RD, et al. Burkholderia type VI secretion systems have distinct roles in eukaryotic and bacterial cell interactions. *PLoS pathogens*. 2010;6(8):e1001068. doi: 10.1371/journal.ppat.1001068. PubMed PMID: 20865170; PubMed Central PMCID: PMCPMC2928800.
67. Basler M, Mekalanos JJ. Type 6 secretion dynamics within and between bacterial cells. *Science*. 2012;337(6096):815. doi: 10.1126/science.1222901. PubMed PMID: 22767897; PubMed Central PMCID: PMCPMC3557511.
68. Leiman PG, Basler M, Ramagopal UA, Bonanno JB, Sauder JM, Pukatzki S, et al. Type VI secretion apparatus and phage tail-associated protein complexes share a common evolutionary origin. *Proceedings of the National Academy of Sciences of the United States of America*. 2009;106(11):4154-9. doi: 10.1073/pnas.0813360106. PubMed PMID: 19251641; PubMed Central PMCID: PMCPMC2657435.
69. Shalom G, Shaw JG, Thomas MS. In vivo expression technology identifies a type VI secretion system locus in *Burkholderia pseudomallei* that is induced upon invasion of macrophages. *Microbiology*. 2007;153(Pt 8):2689-99. doi: 10.1099/mic.0.2007/006585-0. PubMed PMID: 17660433.
70. Burtnick MN, Brett PJ, Harding SV, Ngugi SA, Ribot WJ, Chantratita N, et al. The cluster 1 type VI secretion system is a major virulence determinant in *Burkholderia pseudomallei*. *Infection and immunity*. 2011;79(4):1512-25. doi: 10.1128/IAI.01218-10. PubMed PMID: 21300775; PubMed Central PMCID: PMC3067527.
71. Hopf V, Gohler A, Eske-Pogodda K, Bast A, Steinmetz I, Breitbach K. BPSS1504, a cluster 1 type VI secretion gene, is involved in intracellular survival and virulence of *Burkholderia pseudomallei*. *Infection and immunity*. 2014;82(5):2006-15.

doi: 10.1128/IAI.01544-14. PubMed PMID: 24595140; PubMed Central PMCID: PMC3993457.

72. Brett PJ, Deshazer D, Woods DE. Characterization of *Burkholderia pseudomallei* and *Burkholderia pseudomallei*-like strains. *Epidemiol Infect.* 1997;118(2):137-48. PubMed PMID: 9129590.

73. Warawa JM, Long D, Rosenke R, Gardner D, Gherardini FC. Bioluminescent diagnostic imaging to characterize altered respiratory tract colonization by the *Burkholderia pseudomallei* capsule mutant. *Front Microbiol.* 2011;2:133. Epub 2011/07/02. doi: 10.3389/fmicb.2011.00133. PubMed PMID: 21720539; PubMed Central PMCID: PMC3118415.

74. Fodah RA, Scott JB, Tam HH, Yan P, Pfeffer TL, Bundschuh R, et al. Correlation of *Klebsiella pneumoniae* comparative genetic analyses with virulence profiles in a murine respiratory disease model. *PloS one.* 2014;9(9):e107394. doi: 10.1371/journal.pone.0107394. PubMed PMID: 25203254; PubMed Central PMCID: PMC4159340.

75. Lawrenz MB, Fodah RA, Gutierrez MG, Warawa J. Intubation-mediated intratracheal (IMIT) instillation: a noninvasive, lung-specific delivery system. *J Vis Exp.* 2014;(93):e52261. doi: 10.3791/52261. PubMed PMID: 25490457; PubMed Central PMCID: PMC4354010.

76. Warawa JM, Lawrenz MB. Bioluminescent imaging of bacteria during mouse infection. *Methods Mol Biol.* 2014;1098:169-81. Epub 2013/10/30. doi: 10.1007/978-1-62703-718-1_14. PubMed PMID: 24166377.

77. Lawrenz MB, Fodah RA, Gutierrez MG, Warawa J. Intubation-mediated Intratracheal (IMIT) Instillation: A Noninvasive, Lung-specific Delivery System. *J Vis Exp.* 2014;(93). Epub 2014/12/10. doi: 10.3791/52261. PubMed PMID: 25490457.
78. Gutierrez MG, Pfeffer TL, Warawa JM. Type 3 Secretion System Cluster 3 Is a Critical Virulence Determinant for Lung-Specific Melioidosis. *PLoS neglected tropical diseases.* 2015;9(1):e3441. Epub 2015/01/09. doi: 10.1371/journal.pntd.0003441. PubMed PMID: 25569630.
79. Beji A, Izard D, Gavini F, Leclerc H, Leseine-Delstanche M, Krembel J. A rapid chemical procedure for isolation and purification of chromosomal DNA from gram-negative bacilli. *Analytical biochemistry.* 1987;162(1):18-23. Epub 1987/04/01. PubMed PMID: 3605586.
80. Goodman AL, McNulty NP, Zhao Y, Leip D, Mitra RD, Lozupone CA, et al. Identifying genetic determinants needed to establish a human gut symbiont in its habitat. *Cell host & microbe.* 2009;6(3):279-89. doi: 10.1016/j.chom.2009.08.003. PubMed PMID: 19748469; PubMed Central PMCID: PMC2895552.
81. Simon R, Priefer U, Pühler A. A broad range mobilization system for in vivo genetic engineering: transposon mutagenesis in gram-negative bacteria. *Bio/Technology.* 1983;1:784-91.
82. Moore RA, DeShazer D, Reckseidler S, Weissman A, Woods DE. Efflux-mediated aminoglycoside and macrolide resistance in *Burkholderia pseudomallei*. *Antimicrobial agents and chemotherapy.* 1999;43(3):465-70. PubMed PMID: 10049252; PubMed Central PMCID: PMC89145.

83. Goodman AL, Kulasekara B, Rietsch A, Boyd D, Smith RS, Lory S. A signaling network reciprocally regulates genes associated with acute infection and chronic persistence in *Pseudomonas aeruginosa*. *Dev Cell*. 2004;7(5):745-54. Epub 2004/11/05. doi: 10.1016/j.devcel.2004.08.020. PubMed PMID: 15525535.
84. Goodman AL, McNulty NP, Zhao Y, Leip D, Mitra RD, Lozupone CA, et al. Identifying genetic determinants needed to establish a human gut symbiont in its habitat. *Cell host & microbe*. 2009;6(3):279-89. Epub 2009/09/15. doi: 10.1016/j.chom.2009.08.003. PubMed PMID: 19748469; PubMed Central PMCID: PMC2895552.
85. Skurnik D, Roux D, Aschard H, Cattoir V, Yoder-Himes D, Lory S, et al. A comprehensive analysis of in vitro and in vivo genetic fitness of *Pseudomonas aeruginosa* using high-throughput sequencing of transposon libraries. *PLoS pathogens*. 2013;9(9):e1003582. Epub 2013/09/17. doi: 10.1371/journal.ppat.1003582. PubMed PMID: 24039572; PubMed Central PMCID: PMC3764216.
86. Lopez CM, Rholl DA, Trunck LA, Schweizer HP. Versatile dual-technology system for markerless allele replacement in *Burkholderia pseudomallei*. *Applied and environmental microbiology*. 2009;75(20):6496-503. Epub 2009/08/25. doi: 10.1128/AEM.01669-09. PubMed PMID: 19700544; PubMed Central PMCID: PMC2765137.
87. Skorupski K, Taylor RK. Positive selection vectors for allelic exchange. *Gene*. 1996;169(1):47-52. PubMed PMID: 8635748.

88. Currie BJ, Fisher DA, Howard DM, Burrow JN, Selvanayagam S, Snelling PL, et al. The epidemiology of melioidosis in Australia and Papua New Guinea. *Acta Trop.* 2000;74(2-3):121-7. PubMed PMID: 10674639.
89. Allworth AM. Tsunami lung: a necrotising pneumonia in survivors of the Asian tsunami. *Med J Aust.* 2005;182(7):364. PubMed PMID: 15804231.
90. Chierakul W, Winothai W, Wattanawaitunechai C, Wuthiekanun V, Rugtaengan T, Rattanalertnavee J, et al. Melioidosis in 6 Tsunami Survivors in Southern Thailand. *Clin Infect Dis.* 2005;41(7):982-90. PubMed PMID: 16142663.
91. Svensson E, Welinder-Olsson C, Claesson BA, Studahl M. Cutaneous melioidosis in a Swedish tourist after the tsunami in 2004. *Scand J Infect Dis.* 2006;38(1):71-4. PubMed PMID: 16338844.
92. Athan E, Allworth AM, Engler C, Bastian I, Cheng AC. Melioidosis in tsunami survivors. *Emerg Infect Dis.* 2005;11(10):1638-9. PubMed PMID: 16355505.
93. Owen SJ, Batzloff M, Chehrehasa F, Meedeniya A, Casart Y, Logue CA, et al. Nasal-associated lymphoid tissue and olfactory epithelium as portals of entry for *Burkholderia pseudomallei* in murine melioidosis. *The Journal of infectious diseases.* 2009;199(12):1761-70. doi: 10.1086/599210. PubMed PMID: 19456230.
94. Lim WK, Gurdeep GS, Norain K. Melioidosis of the head and neck. *Med J Malaysia.* 2001;56(4):471-7. Epub 2002/05/17. PubMed PMID: 12014768.
95. Tan NG, Sethi DS. An unusual case of sorethroat: nasopharyngeal melioidosis. *Singapore medical journal.* 1997;38(5):223-5. Epub 1997/05/01. PubMed PMID: 9259605.

96. Wuthiekanun V, Suputtamongkol Y, Simpson AJ, Kanaphun P, White NJ. Value of throat swab in diagnosis of melioidosis. *Journal of clinical microbiology*. 2001;39(10):3801-2. Epub 2001/09/28. doi: 10.1128/JCM.39.10.3801-3802.2001. PubMed PMID: 11574624; PubMed Central PMCID: PMC88440.
97. Dance DA. Melioidosis. *Curr Opin Infect Dis*. 2002;15(2):127-32. PubMed PMID: 11964912.
98. Currie BJ, Fisher DA, Howard DM, Burrow JN. Neurological melioidosis. *Acta Trop*. 2000;74(2-3):145-51. PubMed PMID: 10674643.
99. Revelli DA, Boylan JA, Gherardini FC. A non-invasive intratracheal inoculation method for the study of pulmonary melioidosis. *Front Cell Infect Microbiol*. 2012;2:164. Epub 2012/12/26. doi: 10.3389/fcimb.2012.00164. PubMed PMID: 23267442; PubMed Central PMCID: PMC3526731.
100. St John JA, Ekberg JA, Dando SJ, Meedeniya AC, Horton RE, Batzloff M, et al. *Burkholderia pseudomallei* penetrates the brain via destruction of the olfactory and trigeminal nerves: implications for the pathogenesis of neurological melioidosis. *MBio*. 2014;5(2):e00025. Epub 2014/04/17. doi: 10.1128/mBio.00025-14. PubMed PMID: 24736221; PubMed Central PMCID: PMC3993850.
101. Lever MS, Nelson M, Stagg AJ, Beedham RJ, Simpson AJ. Experimental acute respiratory *Burkholderia pseudomallei* infection in BALB/c mice. *Int J Exp Pathol*. 2009;90(1):16-25. PubMed PMID: 19200247.
102. Lathem WW, Crosby SD, Miller VL, Goldman WE. Progression of primary pneumonic plague: a mouse model of infection, pathology, and bacterial transcriptional activity. *Proceedings of the National Academy of Sciences of the United States of*

- America. 2005;102(49):17786-91. Epub 2005/11/25. doi: 10.1073/pnas.0506840102. PubMed PMID: 16306265; PubMed Central PMCID: PMC1308902.
103. Clayton JA, Collins FS. Policy: NIH to balance sex in cell and animal studies. *Nature*. 2014;509(7500):282-3. Epub 2014/05/17. PubMed PMID: 24834516.
104. Stevens MP, Haque A, Atkins T, Hill J, Wood MW, Easton A, et al. Attenuated virulence and protective efficacy of a *Burkholderia pseudomallei* bsa type III secretion mutant in murine models of melioidosis. *Microbiology*. 2004;150(Pt 8):2669-76. Epub 2004/08/04. doi: 10.1099/mic.0.27146-0. PubMed PMID: 15289563.
105. Warawa JM, Gherardini FC. Modeling of acute respiratory melioidosis and glanders. In: Georgiev VS, editor. National Institute of Allergy and Infectious Diseases, NIH Volume 3, Intramural Research. New York, NY: Humana Press; 2010. p. 117-21.
106. Lawrenz MB, Fodah RA, Gutierrez M, Warawa J. Intubation-mediated intratracheal (IMIT) instillation: A non-invasive, lung-specific delivery system *JoVE*. 2014;in press.
107. Warawa JM. Evaluation of surrogate animal models of melioidosis. *Front Microbio*. 2010;1(141). Epub Dec 29, 2010.
108. Winstanley C, Hales BA, Hart CA. Evidence for the presence in *Burkholderia pseudomallei* of a type III secretion system-associated gene cluster. *Journal of medical microbiology*. 1999;48(7):649-56. doi: 10.1099/00222615-48-7-649. PubMed PMID: 10403415.
109. Burtnick MN, Brett PJ, Nair V, Warawa JM, Woods DE, Gherardini FC. *Burkholderia pseudomallei* Type III Secretion System Mutants Exhibit Delayed Vacuolar

- Escape Phenotypes in RAW 264.7 Murine Macrophages. *Infect Immun*. 2008. PubMed PMID: 18443088.
110. van Opijnen T, Bodi KL, Camilli A. Tn-seq: high-throughput parallel sequencing for fitness and genetic interaction studies in microorganisms. *Nature methods*. 2009;6(10):767-72. Epub 2009/09/22. doi: 10.1038/nmeth.1377. PubMed PMID: 19767758; PubMed Central PMCID: PMC2957483.
111. Baugh L, Gallagher LA, Patrapuvich R, Clifton MC, Gardberg AS, Edwards TE, et al. Combining functional and structural genomics to sample the essential Burkholderia structome. *PloS one*. 2013;8(1):e53851. doi: 10.1371/journal.pone.0053851. PubMed PMID: 23382856; PubMed Central PMCID: PMC3561365.
112. Gallagher LA, Ramage E, Patrapuvich R, Weiss E, Brittnacher M, Manoil C. Sequence-defined transposon mutant library of Burkholderia thailandensis. *mBio*. 2013;4(6):e00604-13. doi: 10.1128/mBio.00604-13. PubMed PMID: 24194535; PubMed Central PMCID: PMC3870259.
113. Wiles TJ, Norton JP, Russell CW, Dalley BK, Fischer KF, Mulvey MA. Combining quantitative genetic footprinting and trait enrichment analysis to identify fitness determinants of a bacterial pathogen. *PLoS genetics*. 2013;9(8):e1003716. Epub 2013/08/31. doi: 10.1371/journal.pgen.1003716. PubMed PMID: 23990803; PubMed Central PMCID: PMC3749937.
114. Skurnik D, Roux D, Cattoir V, Danilchanka O, Lu X, Yoder-Himes DR, et al. Enhanced *in vivo* fitness of carbapenem-resistant *oprD* mutants of *Pseudomonas aeruginosa* revealed through high-throughput sequencing. *Proceedings of the National Academy of Sciences of the United States of America*. 2013;110(51):20747-52. Epub

2013/11/20. doi: 10.1073/pnas.1221552110. PubMed PMID: 24248354; PubMed Central PMCID: PMC3870709.

115. Reckseidler-Zenteno SL, Moore R, Woods DE. Genetics and function of the capsules of *Burkholderia pseudomallei* and their potential as therapeutic targets. *Mini Rev Med Chem*. 2009;9(2):265-71. PubMed PMID: 19200030.

116. Schell MA, Ulrich RL, Ribot WJ, Brueggemann EE, Hines HB, Chen D, et al. Type VI secretion is a major virulence determinant in *Burkholderia mallei*. *Molecular microbiology*. 2007;64(6):1466-85. doi: 10.1111/j.1365-2958.2007.05734.x. PubMed PMID: 17555434.

117. Tan GY, Liu Y, Sivalingam SP, Sim SH, Wang D, Paucod JC, et al. *Burkholderia pseudomallei* aerosol infection results in differential inflammatory responses in BALB/c and C57Bl/6 mice. *Journal of medical microbiology*. 2008;57(Pt 4):508-15. doi: 10.1099/jmm.0.47596-0. PubMed PMID: 18349373.

118. Burtnick MN, Brett PJ, Harding SV, Ngugi SA, Ribot WJ, Chantratita N, et al. The Cluster 1 Type VI Secretion System Is a Major Virulence Determinant in *Burkholderia pseudomallei*. *Infection and immunity*. 2011;79(4):1512-25. Epub 2011/02/09. doi: 10.1128/IAI.01218-10. PubMed PMID: 21300775; PubMed Central PMCID: PMC3067527.

119. Pilatz S, Breitbach K, Hein N, Fehlhaber B, Schulze J, Brenneke B, et al. Identification of *Burkholderia pseudomallei* genes required for the intracellular life cycle and in vivo virulence. *Infection and immunity*. 2006;74(6):3576-86. Epub 2006/05/23. doi: 10.1128/IAI.01262-05. PubMed PMID: 16714590; PubMed Central PMCID: PMC1479254.

120. Hopf V, Gohler A, Eske-Pogodda K, Bast A, Steinmetz I, Breitbach K. BPSS1504, a cluster 1 type VI secretion gene, is involved in intracellular survival and virulence of *Burkholderia pseudomallei*. *Infection and immunity*. 2014;82(5):2006-15. Epub 2014/03/07. doi: 10.1128/IAI.01544-14. PubMed PMID: 24595140; PubMed Central PMCID: PMC3993457.
121. Yang M, Lv Y, Xiao J, Wu H, Zheng H, Liu Q, et al. *Edwardsiella* comparative phylogenomics reveal the new intra/inter-species taxonomic relationships, virulence evolution and niche adaptation mechanisms. *PLoS ONE*. 2012;7(5):e36987. Epub 2012/05/17. doi: 10.1371/journal.pone.0036987. PubMed PMID: 22590641; PubMed Central PMCID: PMC3349661.
122. Logsdon LK, Meccas J. Requirement of the *Yersinia pseudotuberculosis* effectors YopH and YopE in colonization and persistence in intestinal and lymph tissues. *Infection and immunity*. 2003;71(8):4595-607. Epub 2003/07/23. PubMed PMID: 12874339; PubMed Central PMCID: PMC166012.
123. Auerbuch V, Lenz LL, Portnoy DA. Development of a competitive index assay to evaluate the virulence of *Listeria monocytogenes actA* mutants during primary and secondary infection of mice. *Infection and immunity*. 2001;69(9):5953-7. Epub 2001/08/14. PubMed PMID: 11500481; PubMed Central PMCID: PMC98721.
124. Ogawa M, Yoshimori T, Suzuki T, Sagara H, Mizushima N, Sasakawa C. Escape of intracellular *Shigella* from autophagy. *Science*. 2005;307(5710):727-31. Epub 2004/12/04. doi: 10.1126/science.1106036. PubMed PMID: 15576571.

125. Zhou D, Galan J. Salmonella entry into host cells: the work in concert of type III secreted effector proteins. *Microbes and infection / Institut Pasteur*. 2001;3(14-15):1293-8. PubMed PMID: 11755417.
126. Howell HA, Logan LK, Hauser AR. Type III Secretion of ExoU Is Critical during Early *Pseudomonas aeruginosa* Pneumonia. *mBio*. 2013;4(2). Epub 2013/03/14. doi: 10.1128/mBio.00032-13. PubMed PMID: 23481600; PubMed Central PMCID: PMC3604777.
127. Burtnick MN, Brett PJ, Nair V, Warawa JM, Woods DE, Gherardini FC. *Burkholderia pseudomallei* type III secretion system mutants exhibit delayed vacuolar escape phenotypes in RAW 264.7 murine macrophages. *Infection and immunity*. 2008;76(7):2991-3000. Epub 2008/04/30. doi: 10.1128/IAI.00263-08. PubMed PMID: 18443088; PubMed Central PMCID: PMC2446725.
128. Yates RM, Hermetter A, Russell DG. The kinetics of phagosome maturation as a function of phagosome/lysosome fusion and acquisition of hydrolytic activity. *Traffic*. 2005;6(5):413-20. doi: 10.1111/j.1600-0854.2005.00284.x. PubMed PMID: 15813751.
129. Ray K, Bobard A, Danckaert A, Paz-Haftel I, Clair C, Ehsani S, et al. Tracking the dynamic interplay between bacterial and host factors during pathogen-induced vacuole rupture in real time. *Cellular microbiology*. 2010;12(4):545-56. doi: 10.1111/j.1462-5822.2010.01428.x. PubMed PMID: 20070313.
130. Hardt WD, Chen LM, Schuebel KE, Bustelo XR, Galan JE. *S. typhimurium* encodes an activator of Rho GTPases that induces membrane ruffling and nuclear responses in host cells. *Cell*. 1998;93(5):815-26. PubMed PMID: 9630225.

131. Gutierrez MG, Warawa JM. Attenuation of a select agent-excluded *Burkholderia pseudomallei* capsule mutant in hamsters. *Acta Trop.* 2016. doi: 10.1016/j.actatropica.2015.12.006. PubMed PMID: 26836271.
132. Memisevic V, Zavaljevski N, Pieper R, Rajagopala SV, Kwon K, Townsend K, et al. Novel *Burkholderia mallei* Virulence Factors Linked to Specific Host-Pathogen Protein Interactions. *Molecular & cellular proteomics : MCP.* 2013;12(11):3036-51. Epub 2013/06/27. doi: 10.1074/mcp.M113.029041. PubMed PMID: 23800426; PubMed Central PMCID: PMC3820922.
133. Barrowman J, Bhandari D, Reinisch K, Ferro-Novick S. TRAPP complexes in membrane traffic: convergence through a common Rab. *Nature reviews Molecular cell biology.* 2010;11(11):759-63. doi: 10.1038/nrm2999. PubMed PMID: 20966969.
134. Ishii Y, Nakahara T, Kataoka M, Kusumoto-Matsuo R, Mori S, Takeuchi T, et al. Identification of TRAPPC8 as a host factor required for human papillomavirus cell entry. *PloS one.* 2013;8(11):e80297. doi: 10.1371/journal.pone.0080297. PubMed PMID: 24244674; PubMed Central PMCID: PMC3828182.
135. Scrivens PJ, Noueihed B, Shahrzad N, Hul S, Brunet S, Sacher M. C4orf41 and TTC-15 are mammalian TRAPP components with a role at an early stage in ER-to-Golgi trafficking. *Molecular biology of the cell.* 2011;22(12):2083-93. doi: 10.1091/mbc.E10-11-0873. PubMed PMID: 21525244; PubMed Central PMCID: PMC3113772.
136. Lynch-Day MA, Bhandari D, Menon S, Huang J, Cai H, Bartholomew CR, et al. Trs85 directs a Ypt1 GEF, TRAPPIII, to the phagophore to promote autophagy. *Proceedings of the National Academy of Sciences of the United States of America.*

2010;107(17):7811-6. doi: 10.1073/pnas.1000063107. PubMed PMID: 20375281;
PubMed Central PMCID: PMCPMC2867920.

137. Cai Y, Chin HF, Lazarova D, Menon S, Fu C, Cai H, et al. The structural basis for activation of the Rab Ypt1p by the TRAPP membrane-tethering complexes. *Cell*. 2008;133(7):1202-13. doi: 10.1016/j.cell.2008.04.049. PubMed PMID: 18585354; PubMed Central PMCID: PMCPMC2465810.

138. Gutierrez MG, Pfeffer TL, Warawa JM. Type 3 secretion system cluster 3 is a critical virulence determinant for lung-specific melioidosis. *PLoS neglected tropical diseases*. 2015;9(1):e3441. doi: 10.1371/journal.pntd.0003441. PubMed PMID: 25569630; PubMed Central PMCID: PMCPMC4287560.

139. Revelli DA, Boylan JA, Gherardini FC. A non-invasive intratracheal inoculation method for the study of pulmonary melioidosis. *Frontiers in cellular and infection microbiology*. 2012;2:164. doi: 10.3389/fcimb.2012.00164. PubMed PMID: 23267442; PubMed Central PMCID: PMCPMC3526731.

140. Lever MS, Nelson M, Stagg AJ, Beedham RJ, Simpson AJ. Experimental acute respiratory *Burkholderia pseudomallei* infection in BALB/c mice. *Int J Exp Path*. 2009;90(1):16-25. doi: 10.1111/j.1365-2613.2008.00619.x.

141. Silva EB, Dow SW. Development of *Burkholderia mallei* and *pseudomallei* vaccines. *Frontiers in cellular and infection microbiology*. 2013;3:10. Epub 2013/03/20. doi: 10.3389/fcimb.2013.00010. PubMed PMID: 23508691; PubMed Central PMCID: PMC3598006.

142. Kulis-Horn RK, Persicke M, Kalinowski J. Histidine biosynthesis, its regulation and biotechnological application in *Corynebacterium glutamicum*. *Microb Biotechnol*.

2014;7(1):5-25. doi: 10.1111/1751-7915.12055. PubMed PMID: 23617600; PubMed Central PMCID: PMC3896937.

143. Brumell JH, Scidmore MA. Manipulation of rab GTPase function by intracellular bacterial pathogens. *Microbiol Mol Biol Rev.* 2007;71(4):636-52. doi: 10.1128/MMBR.00023-07. PubMed PMID: 18063721; PubMed Central PMCID: PMC2168649.

144. Shintani M, Tada M, Kobayashi T, Kajiho H, Kontani K, Katada T. Characterization of Rab45/RASEF containing EF-hand domain and a coiled-coil motif as a self-associating GTPase. *Biochem Biophys Res Commun.* 2007;357(3):661-7. doi: 10.1016/j.bbrc.2007.03.206. PubMed PMID: 17448446.

145. Nakamura S, Takemura T, Tan L, Nagata Y, Yokota D, Hirano I, et al. Small GTPase RAB45-mediated p38 activation in apoptosis of chronic myeloid leukemia progenitor cells. *Carcinogenesis.* 2011;32(12):1758-72. doi: 10.1093/carcin/bgr205. PubMed PMID: 21890458.

146. Koraimann G. Lytic transglycosylases in macromolecular transport systems of Gram-negative bacteria. *Cell Mol Life Sci.* 2003;60(11):2371-88. doi: 10.1007/s00018-003-3056-1. PubMed PMID: 14625683.

147. Scheurwater E, Reid CW, Clarke AJ. Lytic transglycosylases: bacterial space-making autolysins. *Int J Biochem Cell Biol.* 2008;40(4):586-91. doi: 10.1016/j.biocel.2007.03.018. PubMed PMID: 17468031.

148. Yu YC, Lin CN, Wang SH, Ng SC, Hu WS, Syu WJ. A putative lytic transglycosylase tightly regulated and critical for the EHEC type three secretion. *J*

Biomed Sci. 2010;17:52. doi: 10.1186/1423-0127-17-52. PubMed PMID: 20587027; PubMed Central PMCID: PMCPMC2912269.

149. Chan YA, Hackett KT, Dillard JP. The lytic transglycosylases of *Neisseria gonorrhoeae*. *Microb Drug Resist.* 2012;18(3):271-9. doi: 10.1089/mdr.2012.0001. PubMed PMID: 22432703; PubMed Central PMCID: PMCPMC3412582.

150. Llosa M, Zupan J, Baron C, Zambryski P. The N- and C-terminal portions of the *Agrobacterium* VirB1 protein independently enhance tumorigenesis. *Journal of bacteriology.* 2000;182(12):3437-45. PubMed PMID: 10852875; PubMed Central PMCID: PMCPMC101919.

151. Hoppner C, Carle A, Sivanesan D, Hoepfner S, Baron C. The putative lytic transglycosylase VirB1 from *Brucella suis* interacts with the type IV secretion system core components VirB8, VirB9 and VirB11. *Microbiology.* 2005;151(Pt 11):3469-82. doi: 10.1099/mic.0.28326-0. PubMed PMID: 16272371.

152. Bast A, Krause K, Schmidt IH, Pudla M, Brakopp S, Hopf V, et al. Caspase-1-dependent and -independent cell death pathways in *Burkholderia pseudomallei* infection of macrophages. *PLoS pathogens.* 2014;10(3):e1003986. doi: 10.1371/journal.ppat.1003986. PubMed PMID: 24626296; PubMed Central PMCID: PMCPMC3953413.

153. Kespichayawattana W, Rattanachetkul S, Wanun T, Utaisincharoen P, Sirisinha S. *Burkholderia pseudomallei* induces cell fusion and actin-associated membrane protrusion: a possible mechanism for cell-to-cell spreading. *Infection and immunity.* 2000;68(9):5377-84. Epub 2000/08/19. PubMed PMID: 10948167; PubMed Central PMCID: PMC101801.

154. Zarubin T, Han J. Activation and signaling of the p38 MAP kinase pathway. *Cell Res.* 2005;15(1):11-8. doi: 10.1038/sj.cr.7290257. PubMed PMID: 15686620.
155. Gutierrez MG, Yoder-Himes DR, Warawa JM. Comprehensive identification of virulence factors required for respiratory melioidosis using Tn-seq mutagenesis. *Frontiers in cellular and infection microbiology.* 2015;5:78. doi: 10.3389/fcimb.2015.00078. PubMed PMID: 26583079.

CURRICULUM VITAE

Maria Gutierrez

EDUCATION

- Ph.D., Microbiology and Immunology, University of Louisville, KY 2016
- M.S., Microbiology and Immunology, University of Louisville, KY 2013
- B.S., Chemistry with Emphasis in Biochemistry, San Diego State University, CA 2011

RESEARCH EXPERIENCE

Graduate Research Assistant 2012 – Present

Department of Microbiology and Immunology, University of Louisville

Dissertation Chair: Jonathan M. Warawa, Ph.D.

Project: Characterize the role of the Tier 1 Select Agent *Burkholderia pseudomallei* Type 3 Secretion System effector proteins in mediating viability of the bacterium in a lung-specific mouse model of disease and in macrophage cell culture models.

- Planned, carried out and analyzed experimental results to determine attenuation level, differential phenotype and trafficking pattern associated with distinct *B. pseudomallei* mutant strains in *in vitro* and *in vivo* disease models.

- Maintained *B. mallei* and *B. pseudomallei* Select Agent inventories and BSL-3 and ABSL-3 laboratory spaces in compliance with CDC and APHIS Biological Select Agent And Toxins regulations.
- Resolved technical problems associated with *in vitro* and *in vivo* scientific protocols, procedures and equipment.
- Prepared study protocols, spreadsheets, charts, graphs, presentations and manuscripts to communicate experimental work flow and results to both scientists and the general public.

Graduate Research Assistant

Spring 2012 - Fall 2012

Department of Microbiology and Immunology, University of Louisville

Mentor: Silvia M. Uriarte, Ph.D.

Project: Investigate the effects of fusion proteins of the HIV-1 cell penetrating TAT peptide and the synaptobrevin domain of the mammalian Vesicle-Associated Membrane Proteins (VAMP) -3 and -8 on human neutrophil degranulation.

- Planned, carried out and analyzed experimental results to determine the inhibitory effects of TAT-VAMP-3 and TAT-VAMP-8 fusion proteins on human neutrophil degranulation using flow cytometry.
- Prepared presentations, spreadsheets and graphs to communicate weekly experimental results related to on-going experiments.
- Trained and assisted graduate and undergraduate students in on-going laboratory research projects.

Undergraduate Research Assistant

Summer 2010 Lung

Biology Center, University of California San Francisco

Mentor: David Erle, M.D.

- Investigated expression of the secreted polymeric mucin MUC5AC and the protein disulfide isomerase AGR2 in airway epithelial cells of allergen-challenged mice.
- Prepared both oral and written presentations to communicate weekly experimental findings.

Undergraduate Research Assistant

2009 – 2011

Department of Chemistry and Biochemistry, San Diego State University

Mentor: Tom Huxford, Ph.D.

- Assisted graduate students on research projects by performing literature searches and conducting experiments to confirm expression of proteins in cultured cells in preparation for protein purification and crystallization.
- Prepared both oral and written presentations to communicate weekly experimental findings and important scientific findings related to the NF κ B signaling pathway.

TECHNICAL EXPERTISE

Select Agent and BSL-3 training

Flow cytometry Histology

Mouse model of respiratory disease

Cell transfection

Agarose gel electrophoresis

Polyacrylamide gel electrophoresis

Polymerase chain reaction	Immunohistochemistry	Cell culture
Antibiotic protection assays	Adenylyl cyclase assays	ELISA
<i>In vivo</i> imaging	Tissue sectioning	Immunohistochemistry
High-throughput screening	Confocal microscopy	Western blotting

PUBLICATIONS

Gutierrez MG, Warawa JM. Attenuation of a select agent-excluded *Burkholderia pseudomallei* capsule mutant in hamsters. *Acta Trop.* 2016. doi: 10.1016/j.actatropica.2015.12.006.

Gutierrez MG, Yoder-Himes DR, Warawa JM. Comprehensive identification of virulence factors required for respiratory melioidosis using Tn-seq mutagenesis. *Front. Cell. Infect. Microbiol.* 2015; 5:78. doi:10.3389/fcimb.2015.00078.

Gutierrez MG, Pfeffer TL, Warawa JM. Type 3 secretion system cluster 3 is a critical virulence determinant for lung-specific melioidosis. *PLoS Neglected Tropical Diseases.* 2015;9(1):e3441. doi: 10.1371/journal.pntd.0003441.

Lawrenz MB, Fodah RA, Gutierrez MG, Warawa JM. Intubation-mediated intratracheal (IMIT) instillation: a noninvasive, lung-specific delivery system. *J Vis Exp.* 2014;(93):e52261. doi: 10.3791/52261.

PRESENTATIONS

Gutierrez MG, Pfeffer TL, Warawa JM. *Burkholderia pseudomallei* Type III Secretion System Cluster 3: An Exploration Into Bacterial Pathogenesis. Research!Louisville, 2013. Poster presentation

Gutierrez MG, Pfeffer TL, Warawa JM. Identification of Genetic Factors Required for Initial Host Colonization by the Bacterium *Burkholderia pseudomallei*. Midwest Microbial Pathogenesis Conference, 2013. Poster presentation

Gutierrez MG, Le J, Rodriguez-Hernandez L, McNeil K, Uriarte SM. Revamping Neutrophil Degranulation: Inhibition Studies Using TAT-VAMP-Fusion Proteins. Research! Louisville, 2012. Poster Presentation

Gutierrez MG, Schroeder B, Erle D. AGR2 and MUC5AC: Changes in airway epithelium in mucous metaplasia. San Diego State University Student Research Symposium, 2011. Oral Presentation

Gutierrez MG, Schroeder B, and Erle D. AGR2 and MUC5AC: Changes in airway epithelium in mucous metaplasia. Annual Biomedical Research Conference for Minority Students, 2010. Poster Presentation

Gutierrez MG, Schroeder B, Erle D. AGR2 and MUC5AC: Changes in airway epithelium in mucous metaplasia. Amgen Scholars Symposium, University of California, Los Angeles, 2010. Oral Presentation

Gutierrez MG, Huxford T. Phosphate Dependency in Interfacial Metal Bridging of an Antibody and its Antigen. San Diego State University Student Research Symposium, 2010. Oral Presentation

HONORS AND AWARDS

- Letter of Commendation, Department of Microbiology and Immunology, University of Louisville 2015
- Midwest Microbial Pathogenesis Conference Travel Award Recipient 2013
- Undergraduate Research Excellence Award, San Diego State University 2011
- Amgen Scholars Program, University of California, San Francisco 2010
- CSU Louis Stokes Alliance for Minority Participation Scholars Program 2010
- NIH-Minority Biomedical Research Support/IMSD Program Scholar 2008-2011

LEADERSHIP/COMMUNITY ENGAGEMENT

- DuPont Manual High School Fair Judge 2014-2016
- Louisville Regional Science and Engineering Fair Judge 2015-2016
- Kentucky Junior Academy of Sciences Judge 2015-2016
- Science mentor for High School student 2013-2014
- Treasurer, Microbiology and Immunology Student Organization 2012-2013
- Student tutor for Elementary School student 2011-2013